AN ABSTRACT OF THE THESIS OF

Leila Kelly Barker for the degree of Master of Science in Environmental Engineering presented on September 16, 2014.

Title: Effects of Silver Ions and Nanoparticles on Suspended Cells and Biofilms of *Nitrosomonas europaea*

Abstract approved: _____

Lewis Semprini

Silver nanoparticles are increasingly being incorporated into consumer products due to their broad-spectrum antimicrobial properties. The resulting influx of silver nanoparticles into wastewater may pose a threat to bacteria involved in biological wastewater treatment. Ammonia-oxidizing bacteria, which convert ammonia to nitrite in the first step of nitrification, are highly sensitive to contamination, and inhibition of these bacteria by silver nanoparticles may complicate the removal of nitrogen from wastewater. This study examined the effects of silver ions and silver nanoparticles on biofilms, suspended cells, and resuspended biofilms of *Nitrosomonas europaea*, a model ammonia-oxidizing bacterium. Intact biofilms were exposed to varying concentrations of silver ions and nanoparticles. Nitrite production, bound silver, protein content, and effluent silver concentrations were monitored. Suspended batch cells were exposed to silver ions or nanoparticles to study nitrification inhibition and cell death resulting from ion or nanoparticle exposure. Resuspended biofilms were exposed to silver ion in batch tests to compare inhibition and cell death to suspended cells and intact biofilms. Experiments confirmed that silver ions inhibit nitrification in both *N. europaea* biofilms and suspended cells to a greater degree than silver nanoparticles. Intact biofilms were found to be more resistant to silver ion inhibition than suspended

cells, but resuspended biofilms were no more resistant than suspended cells. Silver sorption tests on both suspended cells and resuspended biofilms confirmed that both adsorb silver on a similar protein basis, indicating that extracellular polymeric substances in biofilms do not bind silver ions. The combination of inhibition and sorption results suggests that the increased resistance of *N. europaea* biofilms compared to suspended cells is not attributable to interference from EPS, but rather to mass-transfer limitations resulting from the structure of the biofilm. Cell lysis was found to be responsible for some but not all observed nitrification inhibition in suspended cells and biofilms. Results suggest that loss of nitrifying activity in biofilms may result from a combination of enzyme-specific inhibition, cell death, and sloughing of biofilm cells. The slow recovery of nitrification activity in biofilms after exposure to silver ions supports these observations. Toxicity of silver nanoparticles was found to stem from silver ion release, which occurred slowly in the presence of high-ionic-strength media. Findings from this study suggest that silver nanoparticles are unlikely to impact ammonia oxidation in wastewater treatment plants.

Effects of Silver Ions and Nanoparticles on Suspended Cells and Biofilms of *Nitrosomonas europaea*

by

Leila Kelly Barker

A THESIS

submitted to

Oregon State University

in partial fulfillment of

the requirements for the

degree of

Master of Science

Presented September 16, 2014

Commencement June 2015

Master of Science thesis of Leila Kelly Barker presented on September 16, 2014

APPROVED:

Major Professor, representing Environmental Engineering

Head of the School of Chemical, Biological, and Environmental Engineering

---

Dean of the Graduate School

I understand that my thesis will become part of the permanent collection of Oregon State University libraries. My signature below authorizes release of my thesis to any reader upon request.

Leila Kelly Barker, Author

ACKNOWLEDGEMENTS

I would like to express my sincere appreciation to Jonathan Giska for introducing me to this project. Many thanks to Dr. Lewis Semprini and Dr. Tyler Radniecki for their guidance and feedback. Dr. Ellen Lauchnor kindly helped with questions about biofilms, and Dr. Mohammad Azizian provided invaluable assistance on many occasions with lab equipment and techniques. Andy Ungerer is an ICP wizard. Dr. Adam Higgins and Dr. Mark Dolan allowed me to use their lab space and helped with fluorescence microscopy. Thanks to the Stacey Harper lab for use of their flow cytometer, and to Fan Wu in particular for his patience in training and troubleshooting. Matthew Palmer, Alyssa Deline, and Raha Kannan provided an extra set of hands in some experiments. I would also like to express my gratitude to fellow students Stephanie Rich, Courtney Fisher, Kevin McKeage, and Dan Pike for participating in the Biofilm Survival Team, enabling me to spend some weekends away from the drip flow reactors. Alf shukur to Nora, Paul, Eve, Joseph, and Jeff for their support.

This research was funded by NSF Grant #1067572 (Division of Chemical, Bioengineering, Environmental and Transport Systems – Environmental Health and Safety of Nanotechnology program).

TABLE OF CONTENTS

TABLE OF CONTENTS (Continued)

LIST OF FIGURES

LIST OF FIGURES (Continued)

Figure Page

LIST OF FIGURES (Continued)

Figure Page

LIST OF TABLES

1. Introduction

The manufacture and use of nanomaterials has increased dramatically in recent years as new industrial and commercial applications are discovered. New techniques for nanomaterial synthesis have led to an increase in the variety of sizes, shapes and coatings of engineered nanomaterials. Many questions exist about the toxicity of nanomaterials and their fate and transport in environmental systems (Luoma, 2008).

Silver nanoparticles (AgNP) are among the most abundant nanomaterials currently produced. Silver has been used for millennia to treat water and prevent bacterial infection due to its strong antimicrobial activity and low toxicity to humans and other animals. AgNP, with their high surface area to volume ratio and potential for persistence, have been incorporated into water filters, wound dressings, clothing, toothpaste, and sundry other products (Project on Emerging Nanotechnologies, 2014). Studies have shown that AgNP can leach into water from consumer products and accumulate in wastewater. AgNP have been detected both in the influent of wastewater treatment plants (WWTP) and in sludge produced at WWTP (Luoma, 2008). The potential for AgNP to adversely affect biological treatment processes in WWTP is a significant economic and environmental concern (Sheng & Liu, 2011).

The removal of nitrogen from wastewater in WWTP is important for preventing eutrophication in water released to the environment (Metcalf & Eddy, 1979). Nitrogen removal begins with nitrification, a two-step biologically-mediated process in which ammonia (NH_3) is oxidized to nitrite (NO_2^-) and then to nitrate (NO_3^-) (Arp, Sayavedra-Soto, & Hommes, 2002). Ammonia-oxidizing bacteria (AOB), which oxidize NH_3 to NO_2^-, are sensitive to a wide range of contaminants, including Ag^+ and AgNP (Choi & Hu, 2008; U.S.EPA, 1993). This study looks at the effects of silver ions (Ag^+) and AgNP on pure cultures of *Nitrosomonas europaea*, a model AOB. Previous

studies have examined effects of Ag^+ and AgNP on bacteria in suspended cells and biofilms (J. W. Anderson, Semprini, & Radniecki, 2014; C. L. Arnaout & Gunsch, 2012; Radniecki, Stankus, Neigh, Nason, & Semprini, 2011). This study builds on work by Giska (2013) examining silver-induced nitrification inhibition in intact biofilms, while also looking into inhibition and silver sorption in resuspended biofilms and cell death resulting from Ag^+ and AgNP.

The goals of this study are to:

- Compare nitrification inhibition of suspended *N. europaea* cells, intact biofilms, and resuspended biofilms in the presence of Ag^+ and AgNP
- Examine the relationship between cell-bound silver and nitrification inhibition in *N. europaea* biofilms
- Study the recovery of biofilms following exposure to Ag^+
- Determine whether suspended cells and biofilms of *N. europaea* bind silver in similar silver-to-protein ratios
- Examine the extent to which cell death is responsible for decreased nitrification rates in suspended cells and biofilms exposed to Ag^+

2. Literature Review

2.1 Silver nanoparticles

Silver has been used for medicinal purposes since the time of Hippocrates. Beginning in the late nineteenth century, silver compounds came into wide use as a means of treating and preventing infections (Alexander, 2009). Although ionic silver (Ag^+) is harmless to humans, except at very high concentrations, it is toxic to microbes (Luoma, 2008). Silver is persistent and bioaccumulative, and can be highly toxic to aquatic organisms (Eisler, 1996; Luoma, 2008). As such, silver has been classified by the U.S. EPA as a priority pollutant since 1977 (U.S.EPA, 1977).

Nanoparticles are generally defined as engineered materials smaller than 100 nanometers (nm) in all three dimensions. The production and use of silver nanoparticles (AgNP) predates the widespread use of the term "nano" (Nowack, Krug, & Height, 2011). M. Carey Lea reported synthesis of a nanoscale citrate-stabilized silver colloid in 1889 (Lea, 1889). Collargol, a nanosilver product with a mean diameter of 10 nm, was first commercially produced in 1897 (Nowack et al., 2011). Since then, a range of techniques have been developed to produce AgNP of different sizes, shapes, and physical-chemical properties (Frattini, Pellegri, Nicastro, & Sanctis, 2005; Manes, 1968; Moudry, 1960). The Woodrow Wilson Institute's Project on Emerging Nanotechnologies (http://www.nanotechproject.org) lists 1,854 consumer products containing nanoparticles as of February 2014, 410 of which contain AgNP. Among these products are wound dressings, bedsheets, toothpastes, soaps, toilet seats, curling irons, air purifiers, clothing, and children's toys (Project on Emerging Nanotechnologies, 2014).

Metal nanoparticles, including AgNP, exhibit physical, chemical, and biological properties that differ from both the ion and the bulk material (Luoma, 2008; Nowack et al., 2011). One key characteristic of nanoparticles is their high surface

area to volume ratio. In the smallest nanoparticles, up to 40-50% of atoms are found on the surface (Farré, Gajda-Schrantz, Kantiani, & Barceló, 2009). This percentage is lower in larger nanoparticles, but still far exceeds that of the bulk material. 20 nm AgNP have a surface area:volume ratio of 0.30 (nanoComposix, 2014). In contrast, in particles larger than 1 micrometer, surface atoms account for fewer than 1% of all atoms (Guo & Tan, 2009). The drastically higher surface area to volume ratio of AgNP compared to bulk silver contributes to greater antimicrobial activity (Royal Society, 2004; Luoma, 2008; Morones et al., 2005). A further consequence of the high surface area:volume ratio of AgNP is that many physical properties, such as solubility and stability, are strongly affected by the nature of the nanoparticle surface (nanoComposix, 2014).

At least part of AgNP toxicity comes from the release of Ag^+ (Blaser, Scheringer, Mcleod, & Hungerbuhler, 2008; Kittler, Greulich, Diendorf, Koller, & Epple, 2010; Lubick, 2008). Ag^+ is susceptible to uptake by ion transporters because it shares properties with Na^+ and Cu^+ (Luoma, 2008). Liu and Hurt's kinetic analysis of Ag^+ release from citrate-stabilized nanoparticles found that release of Ag^+ from AgNP is a two-step oxidation process in which dissolved oxygen and protons interact with AgNP and produce peroxide intermediates (H_2O_2), which oxidize Ag^0 to Ag^+ (Liu & Hurt, 2010). AgNP were thus seen to be more stable at higher pH and lower dissolved oxygen concentrations. The study also found reduced AgNP dissolution in the presence of natural organic matter (NOM); both humic and fulvic acids reduced dissolution in a dose-dependent manner. Nanoparticle stability has been found to be partially a function of the type of capping agent used, and AgNP toxicity varies with the nature of the capping agent (C. L. Arnaout & Gunsch, 2012; Lin, Lin, Dong, & Hsu, 2012).

Silver has a high affinity for complexation with sulfur and phosphorus compounds (Ahrland, Chatt, Davies, & Williams, 1958a, 1958b). Especially strong complexes are formed between silver and sulfide (-SH) ligands (Adams & Kramer, 1999).

Interactions between Ag^+ and the thiol (R-SH) groups of membrane-bound enzymes and proteins cause cell death as a consequence of membrane instability and decreases in nutrient uptake (McDonnell & Russell, 1999). Additionally, Ag^+ has been shown to disrupt the respiratory chain of *E. coli,* possibly by binding to thiol groups of NADH dehydrogenase (Holt & Bard, 2005).

Specific particle-based mechanisms of toxicity are still a matter of debate (Liu, Sonshine, Shervani, & Hurt, 2010). Lok et al. (2007) found that bacterial strains that are resistant to Ag^+ are able to tolerate exposure to AgNP, suggesting that antibacterial activities of AgNP are due to Ag^+ release in the presence of oxygen. Kostigen Mumper, Ostermeyer, Semprini, & Radniecki (2013) found that AgNP dissolution increased rapidly in the presence of ammonia (NH_3), with a corresponding increase in AgNP toxicity. However, Ag^+ toxicity was unaffected by NH_3 concentration. This supports the theory that increased AgNP toxicity is due to Ag^+ release.

AgNP have been found to alter membrane morphology in *E. coli*, increasing permeability (Sondi & Salopek-Sondi, 2004). This may be due to the oxidation of membrane lipids by peroxides produced in the first stage of AgNP dissolution (Liu et al., 2010; Stark, 2005). Some researchers have hypothesized that AgNP may act as a "Trojan horse," able to enter a bacterial cell via endocytosis and subsequently release Ag^+ (Liu & Hurt, 2010; Liu et al., 2010; Lubick, 2008). Smaller AgNP have been found to have more bactericidal effects due to their higher surface area to volume ratio, and toxicity of AgNP has also been linked to shape (Pal, Tak, & Song, 2007).

An optical characteristic found in AgNP, but not in bulk silver, is localized surface plasmon resonance (LSPR). AgNP display a peak absorbance at approximately 400 nm for stable nanoparticles, shifting to longer wavelengths for aggregated particles (MacCuspie, 2011). UV-Vis spectroscopy has been shown to be a useful method for quantifying aggregation of AgNP (Kostigen Mumper, Ostermeyer, Semprini, &

Radniecki, 2013). The intensity of the peak absorbance and width of the peak can provide information about the concentration of AgNP in solution and the extent to which aggregation has occurred (Zook, Long, Cleveland, Geronimo, & MacCuspie, 2011). This can help researchers understand how AgNP react in a variety of experimental and environmental conditions.

Fate and transport of AgNP

At present, silver concentrations range from 0.03-500 ng/L in natural waters (Luoma, 2008). Silver, per se, is not a new contaminant in water systems. Conventional film photography, in particular, produced high Ag^+ emissions due to the use of silver nitrate in developing chemicals (Purcell & Peters, 1998), and total silver emissions peaked during the late 1970s and early 1980s in Europe and North America (Luoma, 2008). However, the increase in AgNP manufacturing and use has resulted in a higher proportion of silver loading resulting from AgNP, whose fate, transport, and toxicity are less well understood. The increased use of AgNP has raised the likelihood of release into the environment, though it is not predicted to result in concentrations exceeding the ng/L range (Luoma, 2008).

Biotic and abiotic environmental factors can have powerful influences on the fate and transport of Ag^+ and AgNP. Silver has a strong tendency to adsorb to surfaces (Russell & Hugo, 1994). Additionally, Ag^+ have a tendency to bind to NOM, creating complexes of reduced toxicity and bioavailability (Luoma, 2008). Experiments with bovine serum albumin (BSA), a model protein, have shown that BSA binds AgNP, slowing NH_3-dependent dissolution as well as chelating free Ag^+ (Ostermeyer, Kostigen Mumper, Semprini, & Radniecki, 2013). NOM has been found to increase stability of AgNP, slowing the rate at which they release Ag^+ while simultaneously binding free Ag^+ to reduce toxicity (Wirth, Lowry, & Tilton, 2012). Previous studies suggest Ag^+ may be reduced to form Ag^o clusters or may reattach to AgNP (Liu & Hurt, 2010; Morones et al., 2005). However, thermodynamic and experimental data suggest that all AgNP will be converted to Ag^+ under environmentally relevant

conditions where sufficient dissolved oxygen is present (Liu & Hurt, 2010). Complexation of Ag^+ with free sulfides and sulfide ligands in NOM can result in very low free Ag^+ concentrations in most freshwater environments (Adams & Kramer, 1999). This limits the bioavailability and therefore the toxicity of silver. The abundance of ligands in particulate matter means that Ag^+ concentrations in sediment can be 10,000 times higher than in water (Luoma, 2008).

At present, there are no known examples of adverse effects of AgNP in natural environmental settings (Luoma, 2008). However, a particular concern is the potential impact of AgNP on wastewater treatment processes. Biological wastewater treatment, which removes nutrients from wastewater prior to discharge, relies on microorganisms that are highly sensitive to perturbation (U.S.EPA, 1993). AOB carry out the first step in the removal of nitrogen from wastewater: the oxidation of NH_3 to NO_2^- (Arp et al., 2002). AOB are considered to be among the most sensitive microbes in wastewater treatment plants, and are known to be inhibited by silver (U.S.EPA, 1993). Preserving the health of organisms involved in this stage of biological wastewater treatment is key to managing the nitrogen cycle and avoiding failure in wastewater treatment.

2.2 Nitrification and *Nitrosomonas europaea*

The transformation of reduced nitrogen in the form of ammonia (NH_3) or ammonium (NH_4^+) to oxidized nitrogen in the form of NO_2^-, NO_3^-, or gases (nitric oxide [NO] and nitrous oxide [N_2O]) is known as nitrification (Chain et al., 2003). Wastewater is rich in ammonia, and nitrification is a critical part of wastewater reclamation (Arp et al., 2002; Metcalf & Eddy, 1979). AOB perform the first step in nitrification, namely the conversion of NH_3 to NO_2^-. NO_2^- is subsequently converted to NO_3^- by nitrite-oxidizing bacteria of the genus *Nitrobacter* (Arp et al., 2002).

Nitrosomonas europaea is model AOB that has been the focus of many studies due to the ease with which it can be cultured compared to other AOB (Arp et al., 2002). The United States Department of Energy selected *N. europaea* for whole-genome sequencing due to its importance in research. Sequencing was managed by the Joint Genome Institute and performed at the Lawrence Livermore National Laboratory (Chain et al., 2003).

Oxidation of NH_3 to NO_2^- by *N. europaea* takes place in two steps. In the first step, the enzyme ammonia monooxygenase (AMO) catalyzes the oxidation of NH_3 to hydroxylamine (NH_2OH), with molecular oxygen (O_2) serving as the electron donor (Equation 2-1). In the second step, the enzyme hydroxylamine oxidoreductase (HAO) catalyzes the oxidation of NH_2OH to NO_2^-, with a water molecule serving as the oxidizing agent (Arp et al., 2002).

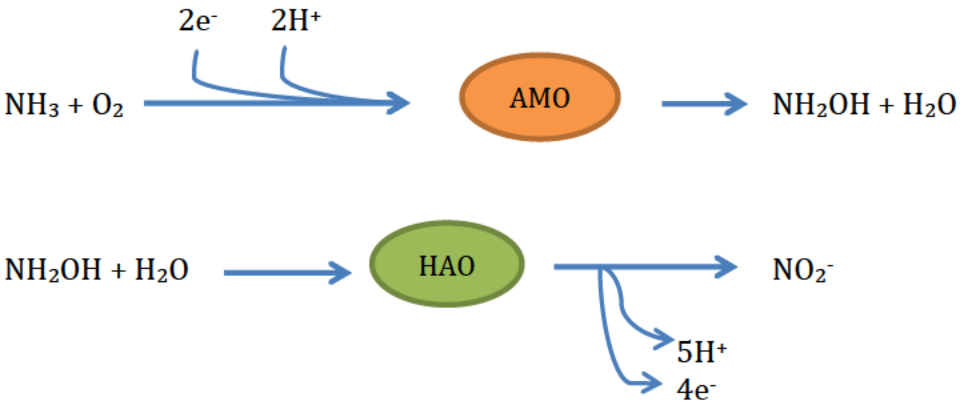

(2-1)

AMO is a membrane-bound enzyme composed of three polypeptides (Arp et al., 2002). In addition to ammonia, AMO can oxidize a wide range of substrates, included halogenated organic compounds and aromatic molecules, suggesting applications for bioremediation of contaminated sites (Arp et al., 2002; Chain et al., 2003; Ensign, Hyman, & Arp, 1993). AMO quickly loses activity upon cell lysis,

partially as a result of the loss of copper (believed to be a cofactor) from the enzyme (Ensign et al., 1993).

An obligate chemolithoautotroph, *N. europaea* can derive all its energy and reductant for growth from the oxidation of NH_3 to NO_2^-, and acquires nearly all carbon for growth from carbon dioxide fixation (Arp et al., 2002; Chain et al., 2003). The oxidation of NH_3 to NO_2^- is an energetically poor process; consequently, *N. europaea* has slow rates of growth and yield, with a generation time of 8-12 hours under ideal conditions (Watson, Valois, & Waterbury, 1981).

Because *N. europaea* must convert NH_3 to NO_2^- in order to acquire energy, measuring NO_2^- production provides information on the overall metabolic activity of cells. The colorimetric assay for quantifying NO_2^-, developed by Hageman and Hucklesby, is a simple method for monitoring NO_2^- production (Hageman & Hucklesby, 1971). Specific Oxygen Uptake Rates (SOURs) for both the AMO and HAO enzymes can be measured separately to explore enzyme-specific inhibition (Ely, Williamson, Guenther, Hyman, & Arp, 1995).

2.3 Biofilms

Bacteria in natural environments are frequently found growing in multicellular, surface-adhered communities called biofilms (Berne, Kysela, & Brun, 2010; Lopez, Vlamakis, & Kolter, 2010; Whitchurch, Tolker-Nielsen, Ragas, & Mattick, 2002). Biofilms are architecturally complex aggregates with highly variable compositions (Berne et al., 2010). Bacterial cells in biofilms grow encased in an extracellular matrix they produce themselves (Lopez et al., 2010). In biological wastewater treatment, bacteria in trickling filters adhere to rocks or engineered packing material and form biofilms.

Biofilms are known to be more resistant than planktonic cells to contaminants, including antimicrobials (G. G. Anderson & O'Toole, 2008; Lewis, 2005; Lopez et al., 2010). Biofilm resistance to antimicrobials can result in cells surviving 100 to 1000 times the minimal lethal dose for suspended cells, a finding that holds across a wide range of both antimicrobials and bacterial species (G. G. Anderson & O'Toole, 2008; Giska, 2013; Lauchnor, Radniecki, & Semprini, 2011; Lewis, 2005). One posited explanation for biofilm resistance to environmental stress is the higher proportion of so-called "persisters," nongrowing and nondividing cells that are resistant to many bactericidal agents and can ensure survival of their genetically-identical kin cells when microbicides are present (Lewis, 2005).

Biofilms also benefit from the presence of the extracellular matrix, which slows diffusion of small molecules, including contaminants (G. G. Anderson & O'Toole, 2008; Hall-Stoodley & Stoodley, 2009). Space constraints and the diffusion barrier result in a lower rate of bacterial growth (G. G. Anderson & O'Toole, 2008). In addition to slower overall growth, limitations in the diffusion of nutrients can create dormant zones within the biofilm, contributing to resistance (Hall-Stoodley & Stoodley, 2009). In some species, two-thirds of biofilm cells have been found to be metabolically inactive (Rani et al., 2007).

Heterogeneity in biofilm cells is a result of gene expression, not gene composition, and results from "microenvironments" created by gradients of nutrients, oxygen, and electron receptors (Lopez et al., 2010). The overall state of biofilms resembles the stationary phase of batch-grown suspended bacterial cells. This is reflected in both the rate of metabolism and the different set of metabolites produced during stationary versus exponential phases (Lopez et al., 2010).

Several studies have investigated the ability of the biofilm extracellular matrix to limit penetration of toxins. The composition of the extracellular matrix varies widely across species and environmental conditions, but typically includes exopolysaccharides, proteins (both secreted proteins and cell-surface adhesins),

lipids, glycolipids, and nucleic acids (Berne et al., 2010; Montanaro et al., 2011). Alginate, an extracellular polymer produced by *Pseudomonas aeruginosa*, is able to trap some antimicrobial agents. This is believed to be due to its anionic nature and ability to retain cations. Adsorption of positively-charged antimicrobial agents by anionic extracellular polymers may therefore be a means of protection for some bacteria (G. G. Anderson & O'Toole, 2008). However, measurements of Ag^+ sorption by alginate have found that it does not adsorb Ag^+ effectively (Ostermeyer et al., 2013). Additionally, numerous studies have shown that antibiotics can diffuse throughout biofilms without severely impacting viability, indicating that in some cases mechanisms other than decreased antimicrobial diffusion must account for biofilm survival (G. G. Anderson & O'Toole, 2008).

Molecular mechanisms regulating biofilm formation vary widely across species and within the same species, depending on environmental conditions. In many Gram-negative organisms, including *N. europaea*, quorum-sensing systems triggered by acyl homoserine lactones promote biofilm formation (Burton, Read, Pellitteri, & Hickey, 2005). Non-quorum-sensing molecules, including antibiotics and secondary metabolites, can also induce biofilm formation (Lopez et al., 2010). Biofilm adhesion to growth surfaces depends on a number of factors, including bacterial hydrophobicity and surface charge, surface porosity, surface roughness, and the physical configuration of the surface (An, 2000).

As a regular part of their growth cycle, bacterial biofilms disperse in order to colonize new habitat (McDougald, Rice, Barraud, Steinberg, & Kjelleberg, 2011). Dispersal may also occur as a survival strategy (Karatan & Watnick, 2009). Drivers of dispersal include overcrowding, changes in the physical environment, lowered nutrient availability, or presence of contaminants (Berne et al., 2010; McDougald et al., 2011). Dispersal may be associated with a significant loss of biofilm biomass (McDougald et al., 2011).

Biofilms of *N. europaea* have been successfully grown in a drip-flow reactor system that allows for studies of inhibition on intact biofilms. Lauchnor et al. (2011) showed that *N. europaea* biofilms were more resistant than suspended cells to phenol and toluene, two known nitrification inhibitors. The study also found that average specific NH_3 oxidation rates of *N. europaea* biofilms were a full order of magnitude lower than those of suspended cells in the same growth medium. Biofilms that were resuspended in batch reactors increased their specific activity fivefold, but were inhibited to the same degree as suspended cells. Results suggested that some degree of biofilm protection from inhibition was due to the presence of low-activity stationary cells in biofilms (Lauchnor et al., 2011).

2.4 Silver Toxicity Studies

Studies of Ag^+ and AgNP toxicity have been carried out using a range of nanoparticle sizes and capping agents, and with a variety of bacterial species, growth environments, and analytical techniques (C. L. Arnaout & Gunsch, 2012; Bjarnsholt et al., 2007; Fabrega, Renshaw, & Lead, 2009; Kalishwaralal, BarathManiKanth, Pandian, Deepak, & Gurunathan, 2010; Radniecki et al., 2011; Wirth et al., 2012). The wide variety of testing conditions and research questions has resulted in little overlap.

Studies of AgNP exposure in *N. europaea* have primarily dealt with suspended cells growing in batch cultures. Ag^+ has consistently been found to result in higher toxicity than AgNP at equivalent concentrations of total silver (Christina Lee Arnaout, 2012; Giska, 2013; Radniecki et al., 2011). Arnaout (2012) showed that nitrification inhibition in *N. europaea* varies strongly with AgNP characteristics such as zeta potential and capping agents, which affect the rate of Ag^+ release. In these studies, citrate-capped AgNP were found to cause higher nitrification inhibition than polyvinylpyrrolidone (PVP)-capped AgNP, and greater cell membrane lysis than

both gum arabic (GA)-capped AgNP and PVP-capped AgNP. Citrate-capped AgNP were also found to have more rapid Ag^+ dissolution than GA-capped and PVP-capped AgNP. In a study using citrate-capped AgNP, Radniecki et al. (2011) found that *N. europaea* were more sensitive to 20 nm AgNP than 80 nm AgNP, owing to increased Ag^+ release from smaller nanoparticles. Nanoparticle-specific toxicity was found to be negligible. The study also showed that Ag^+ and AgNP both act via similar inhibition mechanisms in *N. europaea*, lowering AMO activity and destabilizing the cell membrane (Radniecki et al., 2011). Arnaout (2012) used Live/Dead staining to study cell membrane integrity and found that high concentrations of Ag^+ or AgNP result in cell lysis and death.

Environmental factors including pH and ionic strength have been shown to affect AgNP toxicity in *N. europaea*. Kostigen Mumper et al. (2013) found that dissolution rates and toxicity of citrate-capped AgNP increased with higher pH and higher concentrations of NH_3. Ag^+ toxicity was unaffected by NH_3 concentrations, suggesting that heightened AgNP toxicity is due to increased Ag^+ release. Anderson et al. (2014) found that water hardness (Mg^{2+} and Ca^{2+}) affects Ag^+ and AgNP toxicity. Mg^{2+} and Ca^{2+} cause rapid aggregation of citrate-capped AgNP, which lowers Ag^+ dissolution rates and results in decreased nitrification inhibition. Increased concentrations of Mg^{2+} were also found to reduce adsorption of Ag^+ to cells. Experiments can be dependent on the order of addition of AgNP and test media, which may complicate comparisons of results from different studies. Dilution of AgNP in deionized water prior to addition of media has been found to reduce aggregation, resulting in more stable AgNP suspensions and dose-dependent inhibition (Radniecki et al., 2011).

Several studies have examined the inhibitory and toxic effects of Ag^+ and AgNP on biofilms. Bjarnsholt et al. found that the concentration of Ag^+ required to eradicate biofilms of *Pseudomonas aeruginosa* was 10-100 times higher than that needed to eradicate planktonic cells (Bjarnsholt et al., 2007). Fabrega, Renshaw, & Lead found

that cell viability of *P. putida* biofilm cells was unaffected by AgNP concentration, but that sloughing of biofilm sometimes increased in a dose-dependent manner (Fabrega et al., 2009).

Organic matter in the environment can affect AgNP toxicity by interacting with AgNP and released Ag^+. Wirth, Lowry, & Tilton (2012) found that humic acids stabilized AgNP and bound Ag^+, significantly reducing toxicity in biofilms of *Pseudomonas fluorescens*. Fabrega et al. (2009) found that the presence of Suwannee River fulvic acid reduced AgNP-induced sloughing of *P. putida* biofilm into suspension while increasing bioaccumulation of AgNP to biofilms.

Few biofilm-specific Ag^+ and AgNP toxicity studies have been carried out on *N. europaea*. Results of experiments on biofilms and suspended cells have shown that *N. europaea* biofilms can withstand higher levels of both Ag^+ and AgNP than suspended cells (Giska, 2013). Tests of AgNP toxicity on suspended cells of *N. europaea* in the presence of alginate, a model extracellular polysaccharide, found that alginate was able to bind to AgNP and slow dissolution, but provided no protection against Ag^+ (Ostermeyer et al., 2013). This suggests that *N. europaea* biofilm cells may not be protected from contact with Ag^+ via binding of EPS to Ag^+, but that resistance to Ag^+- and AgNP-induced inhibition is due to other causes.

This study aims to build on research into AgNP-induced nitrification inhibition in *N. europaea*, with a particular focus on the impacts of Ag^+ and AgNP on biofilms. In addition to investigating inhibition of intact biofilms over a longer exposure period than has been previously performed, this work studied Ag^+-induced nitrification inhibition of biofilms that were detached from their growth surfaces and resuspended in test media. Cell membrane integrity of suspended cells, intact biofilms, and resuspended biofilms was also measured over a range of Ag^+ concentrations, and sorption of silver to biomass was studied via titration of cells into Ag^+ solution and quantification of silver bound to intact biofilms.

3. Materials and Methods

The work performed in this study can be broadly broken down into classes of experiments on intact biofilms, resuspended biofilms, and suspended cells. Nitrification inhibition tests and cell membrane integrity testing were performed on all three classes. Ag^+ sorption was studied in intact biofilms via harvesting and inductively coupled plasma optical emission spectrometry (ICP-OES), and in suspended cells and resuspended biofilms via titration and a silver ion-specific electrode. For the reader's convenience, a diagram outlining the steps performed and data obtained for all tests is provided in the Appendix (Figure 26-Figure 27).

3.1 Chemicals

For purposes of clarification and reproducibility, several of the chemicals used in this study are detailed below, along with their manufacturers.

- Silver ion (Ag^+) as silver nitrate: 1,000 ppm Ag in dilute nitric acid (RICCA Chemical Company, Arlington, TX)
- Silver nanoparticles: 20 nm citrate-stabilized BioPure AgNP, 1,000 ppm (nanoComposix, San Diego, CA)
- HEPES buffer: HEPES Free Acid, High Purity Grade , MW 238.30 (EMD Millipore, Billerica, CA)
- EDTA: EDTA Free Acid, Electrophoresis Grade, FW 292.25 (Fisher Scientific, Waltham, MA)
- Sulfanilamide, FW 172.21 (J.T. Baker Chemical Co., Phillipsburg, NJ)
- N-1-Napthylethylenediamine Dihydrochloride, J.T. Baker Brand, FW 259.18 (Avantor Performance Materials, Inc., Center Valley, PA)

3.2 *N. europaea* growth and cultivation

Nitrosomonas europaea cells (strain ATCC 19718) were provided by Luis Sayavedra-Soto (Oregon State University). Cells were cultured in batch at 30°C, as previously described (Radniecki, Dolan, & Semprini, 2008). Biofilms were grown in DFR media, as previously described in Lauchnor et al. (2011), with the exception of the use of a lower concentration of Mg^{2+} (200 μM rather than 730 μM). This modification was introduced in order to minimize nanoparticle aggregation in tests using AgNP. Media consisted of 15 mM HEPES; 2.5 mM $(NH_4)_2SO_4$; 10 μM KH_2PO_4; 3.77 mM Na_2CO_3; 200 μM $MgSO_4$; 200 μM $CaCl_2$; 9.9 μM $FeSO_4$; 16.5 μM EDTA free acid; and 0.65 μM $CuSO_4$. All inhibition experiments, both in DFR and batch, were carried out using this low ionic strength DFR media.

3.3 Batch experiments on suspended cells

Nitrification inhibition experiments were conducted on suspended cells using low ionic strength DFR media containing 200 μM Mg^{2+}, as previously described (Giska, 2013), in order to compare to results from previous studies and to results obtained from intact and resuspended biofilms in this study. Three-hour batch nitrification inhibition tests were performed on batch-grown suspended cells of *N. europaea* over a range of Ag^+ and AgNP concentrations. Batch-grown cells were harvested in late-exponential growth phase. Cells were centrifuged at 9,000 rpm for 30 minutes and then washed and resuspended in 30 mM HEPES buffer (pH 7.8). Test bottles were inoculated with the resuspended *N. europaea* cells to achieve an optical density of ~0.072 at 600 nm.

For both Ag^+ and AgNP tests, Ag^+ or AgNP were added to ~31 mL Nanopure water (dependent on harvested cell density), followed by addition of 3.5 mL 10x

concentrated media and then inoculation of cells to achieve a final volume of 35 mL. In treatments using AgNP, the two steps of addition of AgNP to nanopure water and addition of 10x concentrated media were both followed by shaking at 250 rpm for 15 minutes to help prevent AgNP aggregation prior to cell inoculation (Radniecki et al., 2011). Treatments, containing Ag^+ or AgNP, were run in triplicate alongside controls containing only test media and cells for 3 h, and NO_2^- levels were monitored every 45 min. NO_2^- production was normalized by cell protein mass. Percent nitrification inhibition relative to control samples was calculated for each sample using Equation 3-1:

$$\% \text{ Inhibition} = \left(1 - \frac{\text{treatment } NO_2^- / \text{ mg protein}}{\text{control } NO_2^- / \text{ mg protein}}\right) \times 100\% \qquad (3\text{-}1)$$

At the end of the 3-hour batch experiments, samples were taken from batch bottles for cell viability (Live/Dead) analysis. This procedure is described in detail in Analytical Methods (Section 3.7).

3.4 Drip flow reactor experiments on intact biofilms

Inoculation

Biofilms were inoculated and grown on frosted glass slides in four-channel Model DFR 110 Drip Flow Reactors (DFR) (BioSurface Technologies Inc., Bozeman, MT, USA), as previously described (Lauchnor et al., 2011). *N. europaea* cells grown in batch were aseptically harvested in late-exponential phase. Cells were concentrated approximately six-fold under aseptic conditions via centrifugation for 20 minutes at 9,000 g, followed by partial decanting of the supernatant and resuspension of cells. 12 mL of concentrated cells were added via syringe to each channel of the autoclaved DFR. The DFR was incubated for 3-4 days at 30°C to promote attachment of cells to the glass slides, prior to starting fluid flow.

Growth

Following incubation, autoclaved influent tubing and effluent tubing were attached to the DFR. The DFR was set up at a downward angle of 9 degrees and growth media was continuously pumped using a peristaltic pump at a rate of 0.8 mL min^{-1} (0.2 mL min^{-1} per channel). DFR effluent was sampled aseptically, as described previously (Lauchnor et al., 2011), and monitored for flowrate and NO_2^- levels. Experiments were run after the biofilms achieved steady state NO_2^- production (defined as leveling off for at least 3 days at a production level of 0.025-0.035 mmol $NO_2^- h^{-1}$). Biofilms typically required 4-5 weeks of growth to reach steady state. One experiment was also performed on "mature" biofilms, which were grown for a further 4 weeks after achieving steady-state NO_2^- production.

DFR media

DFR media was prepared as previously described (Lauchnor et al., 2011), with the exception of the use of a lower magnesium concentration. The media consisted of 15 mM HEPES, 2.5 mM $(NH_4)_2SO_4$, 10 µM KH_2PO_4, 3.77 mM Na_2CO_3, 200 µM $MgSO_4$, 200 µM $CaCl_2$, 9.9 µM $FeSO_4$, 16.5 µM EDTA (free acid), and 0.65 µM $CuSO_4$. The use of 200 µM $MgSO_4$ (as opposed to the 730 µM described in Lauchnor *et al.*) was intended to reduce nanoparticle aggregation as previously reported (Giska, 2013). On several occasions, media containing 730 µM $MgSO_4$ was used for the first week of biofilm growth to test whether the standard magnesium concentration enhanced biofilm survival; no difference was observed compared to low-magnesium growth conditions. All media used in experiments for this study (both for batch and DFR experiments) was of the low-magnesium DFR formulation.

DFR Experiments

48-hour inhibition experiments were performed by injecting Ag^+ or AgNP continuously for 48 hours. A concentrated feed of Ag^+ or AgNP was delivered at a rate of 0.1 mL h^{-1} using a syringe pump equipped with 3 syringes. Ag^+ and AgNP

concentrations in the syringe solution were determined from each channel's measured peristaltic flow rate, which typically ranged from 0.18-0.22 mL min^{-1}. The syringe solution and regular media from the peristaltic pump were mixed via a three-way valve prior to reaching the DFR channels to achieve the calculated dilution. Influent concentrations achieved via this method were 0.5 ppm or 1.5 ppm for both Ag^+ and AgNP. In each experiment, two channels were exposed to Ag^+ or AgNP and one channel received a control solution identical to that of the treatment channels, but lacking Ag^+ or AgNP. A second control channel received no syringe solution, and received only regular growth media from the peristaltic pump.

The syringe solution consisted of autoclaved Nanopure water. This differed from previous Ag^+/AgNP DFR experiments (Giska, 2013), which used low ionic strength DFR media or 30 mM HEPES as the syringe solution. This decision to use Nanopure water was made with two considerations in mind. Firstly, it was important to minimize AgNP aggregation and dissolution. The risk of AgNP aggregation in HEPES over the course of 48 hours was deemed to be much higher than over 3 hours (the length of previous experiments), and this risk would be minimized by suspending AgNP in ultrapure water. Previous research has also shown that Ag^+ release from citrate-capped AgNP in ultrapure water was minimal after 48 hours at 37°C (Kittler et al., 2010). Thus, the AgNP syringe solution was unlikely to become substantially more or less toxic during the course of 48 hours at 30°C. Secondly, the much lower flow rate from the syringe in the 48-hour experiments meant a lower likelihood of the syringe solution diluting the DFR media or altering the pH to any appreciable degree, thus permitting the use of Nanopure water for the current tests.

Effluent from each channel was collected aseptically at 30-minute intervals for the first three hours of the experiment and at regular intervals thereafter for 48 hours. Flow rates were determined by weighing effluent collected in vials of known weight. NO_2^- concentrations were determined via colorimetric assay, and NO_2^- production rates (in mmol h^{-1}) were calculated from concentrations and flow rates. Nitrification

inhibition was calculated relative to the initial NO_2^- production rate of each lane prior to addition of Ag^+ or AgNP using Equation 3-2:

$$\% \text{ Inhibition} = \left(1 - \frac{\text{sample nitrite production rate}(\text{mmol h}^{-1})}{\text{nitrite production rate prior to start of experiment}(\text{mmol h}^{-1})}\right) \times 100\% \quad (3\text{-}2)$$

To account for system-wide variations resulting from external factors such as temperature fluctuations, percent inhibition of the treated biofilms was calculated by subtracting percent inhibition of the biofilm receiving the control syringe solution.

Effluent samples collected during the experiment were also used to study the concentration of silver in DFR effluent over time. The effluent of all experiments was acidified and silver was quantified via ICP-OES to determine if a breakthrough curve existed and to perform a mass balance of silver into and out of the DFR system. Details of sample preparation and ICP-OES analysis are provided in Analytical Methods (Section 3.7). An attempt was also made to analyze effluent from AgNP experiments via UV-Vis spectroscopy to determine whether aggregation or dissolution of AgNP had occurred (details are provided in Section 3.7).

At the end of the exposure period, the DFR was disconnected and the biofilms were harvested from the frosted glass slides via scraping with a sterile razor blade and repeated rinsing with 2 mL of 30 mM HEPES (pH 7.8). In some experiments, biofilms were divided horizontally into two portions (upper and lower biofilm, corresponding to the upper third and lower two-thirds of the frosted glass slide, respectively), and each of these portions was harvested individually for separate analysis. Suspended cells in the DFR wells downstream of each glass slide were harvested via pipetting and suspended in 2 mL 30 mM HEPES (pH 7.8). The harvested biofilms and suspended well cells were vortexed for two minutes, placed in a sonication bath for five minutes, and vortexed for two more minutes to disperse and homogenize the biological content for protein quantification and ICP-OES silver

analysis. Details of protein quantification and ICP-OES analysis are discussed in Analytical Methods (Section 3.7).

Specific oxygen uptake rates (SOURs) were measured for some biofilms. Samples from both the slide (upper and lower portions) and well of each lane were taken, and both AMO- and HAO-SOURs were measured. Details of the SOUR measurement procedure are found in Section 3.7. Oxygen uptake rates were compared to final biofilm nitrification rates and normalized by protein content to examine how well SOURs and NO_2^- production were correlated.

Biofilms from one experiment were analyzed for cell membrane integrity using Live/Dead staining and flow cytometry (details of the procedure are provided in the Analytical Methods section).

One aim of this research was to explore the degree to which biofilms are able to recover activity following silver exposure. To study this, some biofilms were left growing after the conclusion of Ag^+ exposure tests, and their nitrification activity was monitored after influent Ag^+ was shut off. These were termed "recovery experiments." Two recovery experiments (0.5 ppm Ag^+ and 1.5 ppm Ag^+) were performed with a recovery period of 7-10 days following 48-hour Ag^+ exposures to determine the rate at which biofilms would return to pre-exposure nitrification levels. Following the recovery period, the biofilms were harvested and tested for protein and silver content in the same manner as described above.

3.5 Resuspended biofilm experiments

One of the questions in this study was whether the protection from Ag^+-induced inhibition seen in biofilms results from the chemical makeup of the biofilm, the physical structure of the intact biofilm, or some combination of factors. In this work,

Ag^+-induced nitrification inhibition was studied in resuspended biofilms (biofilms detached from their growth surface and resuspended in liquid media). Results were compared with results from intact biofilms and suspended cells with the goal of understanding the nature of biofilm resistance.

Nitrification inhibition was studied via 3-hour batch experiments, as with suspended cells. Biofilms that had achieved steady-state NO_2^- production were detached from glass slides via scraping with a sterile razor blade and suspended in 30 mM HEPES. Harvested biofilms were then vortexed to homogenize cell concentrations. Bottles containing test media were inoculated with cells to an OD_{600} of ~0.072. Treatments and controls were done in triplicate. 3-hour batch inhibition experiments were then performed using the same steps as batch suspended cell experiments (described above in Section 3.3 Batch experiments). In several tests, samples were analyzed for cell membrane integrity via Live/Dead staining and flow cytometry (details are provided below in Analytical Methods).

3.6 Ag^+ sorption experiments

The quantity of suspended cells or biofilms required to adsorb a given quantity of Ag^+ was studied by titrating suspended cells or resuspended biofilms into a 25-mL solution of 2.5 mM $(NH_4)_2SO_4$ in 30 M HEPES containing 10 ppm Ag^+. Suspended cells were first concentrated via centrifugation and resuspension in 30 mM HEPES, as previously described. Resuspended biofilms were harvested as described above and directly suspended in 30 mM HEPES without centrifugation in order to prevent loss of EPS. Cell concentrations in each vial prior to titration were determined via OD_{600} and biuret assay. The concentration of silver in solution was measured using a Cole-Parmer silver/sulfide ion selective electrode (more details are provided in the Analytical Methods section). The total amount of silver remaining in solution (in mg) was then graphed against the quantity of cells added (in mg protein).

3.7 Analytical methods

NO_2^- concentrations were determined using a colorimetric assay (absorbance at 540nm) as previously described (Hyman & Arp, 1995). Protein content was determined using the biuret test, measuring absorbance at 540nm. Protein samples were digested in 3 M NaOH for 30 minutes (Hyman & Arp, 1995). OD_{600} measurements were used to estimate protein concentrations for batch experiments. NO_2^- and protein spectrophotometer measurements were made using a Beckman Coulter DU530 Life Science UV-Vis spectrophotometer (Brea, CA, USA).

Total silver in DFR effluent and harvested biofilms was measured via ICP-OES. DFR effluent samples (0.5 mL) were acidified with 50 µL of concentrated sulfuric acid and 4.45 mL of 3% nitric acid (for a final dilution of 1:10) to keep Ag^+ in solution and diminish interference from HEPES (Giska, 2013). Prior to overnight digestion at 60˚C, harvested biofilm suspensions were acidified in glass screw cap test tubes with concentrated phosphoric acid and concentrated nitric acid in a ratio of 1:2:3 (cells:H_3PO_4:HNO_3). Silver concentrations were measured with a Teledyne Leeman Labs Prodigy ICP-OES (Hudson, NH, USA) in axial mode using the 328.068 nm wavelength with triplicate peak integrations. Biofilms were harvested in the evening and samples were typically run the following morning. Standards used to prepare the standard curve were 0 ppb, 50 ppb, 100 ppb, 250 ppb, 500 ppb, 1 ppm, 2.5 ppm, 5.0 ppm, and 10.0 ppm, with a QC concentration of 1.0 ppm.

The initial aggregation/dissolution state of AgNP was studied via DLS using a NanoBrook 90Plus Particle Size Analyzer (Brookhaven Instruments Corporation, Holtsville, NY). AgNP aggregation and dissolution data from DFR effluent and batch media containing AgNP was monitored using a Beckman Coulter DU530 Life Science UV-Vis spectrophotometer (Brea, CA) and a Hewlett –Packard 8453 UV-Vis spectrophotometer (Paolo Alto, CA) on a wavelength scan of 300-700nm.

Aggregation and dissolution were inferred by examining spectra, as demonstrated by Zook et al. (2011).

SOURs were measured using a Clark-type oxygen electrode (YSI, Inc., Yellow Springs, OH) in a water-jacketed reaction cell (Gilson, Inc., Middleton, WI) at 30˚C. A stir bar in the 1.8-mL cell mixed the samples. After addition of the sample, 2.5 mM $(NH_4)_2SO_4$ was added to the reaction cell to provide an excess of substrate. Changes in dissolved oxygen content were measured as a function of time. After the AMO-SOUR was measured, 100 µM allylthiourea (ATU) was added to halt AMO activity. 750 µM NH_2OH was then added to measure the HAO-SOUR. The oxygen electrode was calibrated with an oxygen saturation value of 0.235 mM (7.54 mg/L) at 30°C.

Cell viability (defined as cells with intact membranes) was quantified via fluorescent staining followed by flow cytometry. For batch suspended cell and resuspended biofilm tests, 50 µL samples were taken from each batch bottle at the end of the 3-hour inhibition test. Each sample was diluted with 50 µL 30 mM HEPES to a final OD_{600} of ~0.036; this dilution was found to improve the quality of flow cytometer output. The diluted samples were then combined in a 1:1 ratio with with SYTO 9 and propidium iodide (Live/Dead® *Bac*Light™ Bacterial Viability Kit, Molecular Probes/ThermoFisher Scientific, Waltham, MA) in a U-bottom 96-well plate and incubated for 15 minutes in darkness. Samples were then analyzed using a BD Accuri™ C6 flow cytometer (BD Biosciences, San Jose, CA) to determine the percentage of cells in each sample with compromised membranes (the percentage that failed to exclude propidium iodide). For intact biofilm tests, 50 µL samples were taken via pipetting from each slide and well before the remainder of the biofilm was harvested. Each sample was then diluted with 50 µL 30 mM HEPES. Staining and plate reading were performed as described above for suspended cells.

The gating and standard curve for Live/Dead analysis was established prior to these tests using batch-grown *N. europaea* cells harvested during late-exponential phase. Live cells were combined with dead cells (killed by exposure to 78% ethanol) at

different ratios to produce standards of 0% dead, 25% dead, 50% dead, 75% dead, and 100% dead cells. A gate was manually fit to the frequency plot produced by the flow cytometer, and a standard curve was generated from the five dilutions. Gating data and examples of raw experimental results are shown in Figure 31-Figure 32 in the Appendix.

A Cole-Parmer® silver/sulfide ion-selective electrode (EW-27502-41, Cole-Parmer, Vernon Hills, IL) attached to a VWR SympHony SB70P meter (VWR International, Radnor, PA) was used to measure dissolved Ag^+ remaining in solution during cell titration experiments. The test solution consisted of 25 mL 2.5 mM $(NH_4)_2SO_4$ in 30 mM HEPES with 0.5 mL 5 M $NaNO_3$ (ionic strength adjuster). The raw output generated by the electrode was in mV with 0.1 mV resolution; a new standard curve ($R^2 > 0.99$) was generated immediately prior to each titration experiment using standard concentrations of 0.1 ppm Ag^+, 1 ppm Ag^+, 5 ppm Ag^+, and 10 ppm Ag^+.

The ion-selective electrode was also used to examine AgNP dissolution in some batch bottles containing test media. For measurements of Ag^+ released by AgNP in batch bottles, the test solution consisted of 35 mL DFR solution (prepared as above with 3.5 mL 10x DFR media and 31.5 mL Nanopure H_2O). 2 ppm AgNP were added to the test media, and bottles were shaken as described above in the method for batch experiments. 0.7 mL $NaNO_3$ was added to the solution prior to measuring Ag^+ concentrations.

4. Results and Discussion

The first section (4.1) deals with inhibition experiments on intact biofilms. These were 48-hour exposures of either Ag^+ or AgNP, followed in some cases by recovery periods of 7-10 days when Ag^+ or AgNP were not added in order to study the rate at which nitrifying activity was recovered following inhibition by silver. Data include NO_2^- production rates, effluent silver concentrations, and quantities of biomass and bound silver in biofilms harvested at the end of each experiment. SOURs were performed in order to determine whether loss of nitrifying activity was the result of selective inhibition of the AMO enzyme. Results of this study (including nitrification inhibition and effluent concentrations) are compared with those previously obtained (Giska, 2013). Experiments in the current study were run on a considerably longer timescale than previous tests (48 hours vs. 3 hours).

The second section (4.2) covers results of 3-hour batch nitrification inhibition experiments on suspended cells and resuspended biofilms exposed to a range of Ag^+ concentrations. Activity levels and inhibition of resuspended biofilms are compared to suspended cells and intact biofilms.

The third section (4.3) deals with quantification of live and dead cells (suspended cells, resuspended biofilms, and intact biofilms) following exposure to Ag^+. Live/Dead staining and flow cytometry were used to determine the percentage of cells with compromised membranes. Live/Dead results are compared to nitrification inhibition data and SOURs to gain a clearer picture of the nature of Ag^+-induced inhibition.

The fourth section (4.4) includes results of experiments in which known quantities of suspended cells or biofilms were titrated into a solution containing 10 ppm Ag^+ to study sorption of Ag^+ to biomass.

4.1 Intact biofilms

4.1.1 48-hour Ag^+ exposure and recovery

Results of Ag^+ inhibition tests on nitrification rates of intact biofilms are shown in Figure 1. Figure 1a presents nitrite production rates over the course of 48 hours for each influent Ag^+ concentration and illustrates how biofilms exposed to Ag^+ experienced decreases in nitrification over time. Initial nitrite production rates ranged from 0.025 – 0.035 mmol NO_2^-/hr for standard biofilms and 0.031-0.035 mmol NO_2^-/hr for mature biofilms (Figure 1a). As described above, these production rates were maintained for at least 3 days prior to the start of each experiment. This range of initial nitrite production rates is in keeping with prior observations from the same DFR system (Giska, 2013; Lauchnor et al., 2011).

A total of five experiments were conducted using Ag^+: two each at 0.5 ppm and 1.5 ppm on standard biofilms, and one experiment on mature biofilms (those grown for an additional 4 weeks) at 0.5 ppm. Nitrification inhibition over time for each experiment is presented in Figure 1b. Standard biofilms exposed to Ag^+ at 0.5 and 1.5 ppm were inhibited to a similar extent throughout the 48-hour exposures. Percent nitrification inhibition after 3 hours of exposure was similar for both concentrations, and later measurements showed little difference in inhibition (Figure 1b). The similar inhibition levels for 0.5 ppm and 1.5 ppm Ag^+ at 3 hours are in agreement with previous observations that found inhibition levels at 0.5 and 1.0 ppm Ag^+ were not significantly different (Giska, 2013). It should be noted that Giska's measurements of approximately 50% nitrification inhibition at 3 hours for both 0.5 and 1.0 ppm Ag^+ are higher than this study's results (approximately 30% inhibition at 3 hours). This may be due to a slightly longer stationary phase being maintained in this study prior to experimentation. The additional two days of steady-state NO_2^- production may have resulted in a slightly more mature

"standard" biofilm. Giska's study found that more mature biofilms (those cultured for an additional four weeks after achieving steady-state NO_2^- production) demonstrated significantly higher resistance to inhibition than standard biofilms.

Nitrite production rates of biofilms exposed to 0.5 ppm and 1.5 ppm Ag^+ decreased throughout the 48-hour exposures. Nitrification rates decreased most markedly in the first hours of exposure and leveled off considerably during the last 24 hours. This sharp initial decrease may be explained by several phenomena. The first of these is sloughing of the biofilm upon initial exposure. Biomass was occasionally visible in the effluent of biofilms exposed to Ag^+, particularly in the earliest hours of experiments. Biofilm sloughing is a known survival mechanism (McDougald et al., 2011), and loss of biomass could clearly account for lower overall nitrification activity in the remaining biofilm. Fabrega et al. observed a dose-dependent increase in biomass sloughing with *Pseudomonas putida* biofilms, with the greatest sloughing occurring upon initial exposure (Fabrega et al., 2009).

A second possible explanation for the rapid decrease in nitrification during the first hours of exposure is that cells near the surface of the biofilm become saturated with silver during the first hours of Ag^+ exposure, and that the most accessible binding sites for silver are unavailable after this initial stage. In this case, subsequent addition of silver would result in little binding, with most Ag^+ exiting in the effluent. Effluent measurements showing breakthrough of silver after several hours (Figure 9) seem to support this latter explanation (effluent measurements are discussed in more detail below).

In this study, sloughed biomass was not quantified; only biomass present in the DFR at the end of the experiment was measured. Table 1 provides final biomass measurements and nitrification rates of some biofilms in this study (including biofilms exposed to AgNP, which are discussed in the next section). Figure 2 shows final nitrification rates graphed against biomass of harvested biofilms. T-tests were performed to determine if significant differences existed between control and

treated biofilms (mature biofilms were excluded). There was a significant difference in nitrification activity of control (M=0.0278 mmol NO_2^-/hr, SD = 0.0055) and treated (M=0.0161 mmol NO_2^-/hr, SD= 0.0062) biofilms (p=0.002). No significant difference was found between the protein content of control (M=1125 μg, SD=708) and treated (M=911 μg, SD=393) biofilms (p=0.44). NO_2^- production was significantly higher among control biofilms than treated biofilms. The average protein content of control biofilms is slightly higher than that of treated biofilms, but the difference is not significant. This complicates a sloughing-based analysis. However, it should be noted that only one set of control biomass measurements exists for a standard-biofilm Ag^+ exposure test (Test 3 – 1.5 ppm Ag^+ followed by recovery). Looking at data points from this test alone, the difference between average biomasses of control and treated biofilms is greater than that seen in other tests. This may indicate that sloughing plays a role during Ag^+ exposure in standard biofilms. The absence of control data for other Ag^+ tests makes it impossible to verify a trend.

Figure 3a plots specific nitrification rates (normalized by cell protein) against influent Ag^+ concentrations. Because some control biofilms were later used in resuspended biofilm experiments, cell protein was not measured for those controls. Control data are only available for one standard biofilm experiment (Test 3 – 1.5 ppm Ag^+ with recovery). In this experiment, specific nitrification rates of treated biofilms are on average lower than those of controls. Treated biofilms from a second 1.5 ppm Ag^+ test (no control data available) also had low specific nitrification rates. These data indicate a decrease in biomass-normalized activity with increasing influent Ag^+. This would support a model in which enzymatic inactivation or cell death accounts for some loss of activity in treated biofilms.

Mature biofilms

Mature biofilms exposed to 0.5 ppm Ag^+ maintained significantly higher nitrification activity levels than standard biofilms exposed to 0.5 ppm and 1.5 ppm Ag^+ (Figure

1). This difference was observed as early as 3 hours into the exposure and was maintained over the entire course of the experiment. Percent inhibition of mature biofilms was approximately 30% after 48 hours, as opposed to 50-60% for standard biofilms exposed to the same Ag^+ concentration. It should be noted that while mature biofilms contained more biomass than standard biofilms (Table 1), their initial nitrite production was not significantly higher (Figure 1a; $P > 0.05$ for all t-tests comparing initial nitrification rates of mature biofilms to initial nitrification rates of standard biofilms). Higher final nitrite production in mature biofilms compared to standard biofilms was therefore a result of lower inhibition, not higher initial activity.

Biomass and nitrification rates of mature biofilms are included in Figure 2. As with standard biofilms, final nitrification activity of treated mature biofilms is lower than that of controls. There is no difference between the average biomass of control and treated mature biofilms. This suggests sloughing of biomass did not play a significant role in loss of nitrifying activity in mature biofilms. Figure 3a illustrates the lower specific nitrification rates of treated mature biofilms versus control mature biofilms; these data are in line with those of standard biofilms from Test 3. This suggests that nitrifying activity in mature biofilms is inhibited by Ag^+ via enzymatic inactivation, cell death, or another nonspecific inhibition mechanism.

Recovery

Two recovery experiments were performed on biofilms exposed to Ag^+. The inhibition data for these experiments during their 48-hour Ag^+ exposures are shown in Figure 1b (where the experiments are labeled "0.5 ppm Ag^+ [B]" and "1.5 ppm Ag^+ [A]"). Influent Ag^+ was switched off after 48 hours, and results from the recovery stage are shown in Figure 4. Biofilms exposed to 1.5 ppm Ag^+ did not achieve any significant recovery after 7 days, at which point the experiment was stopped. Biofilms exposed to 0.5 ppm Ag^+ showed some recovery after 7 days, and the experiment was extended. The results show recovery to approximately 80% of

initial activity after 10 days for biofilms exposed to 0.5 ppm Ag^+. After the 10-day measurement was taken, a media change resulted in the sudden death of all biofilms, and the experiment could not continue.

Figure 5 plots nitrification activity in 0.5 ppm Ag^+-exposed biofilms during their recovery phase alongside nitrification activity of normal growing biofilms. The 8 "typical" biofilms averaged in this graph had been grown in the drip-flow reactor for 168 hours before reaching nitrification activity of ~0.01 mmol NO_2^-/hr (the starting point for this graph). The graph demonstrates that the recovering biofilms increased their nitrification activity slower than regular growing biofilms. This suggests that Ag^+ still present in the DFR continued to inhibit or kill biofilms even after influent Ag^+ was stopped.

The results of these experiments show a slower recovery than was observed in previous experiments following 3-hour exposures to 2.0 ppm Ag^+ (Giska, 2013). Giska found that mature biofilms exposed to 2.0 ppm Ag^+ recovered to 100% of initial activity (up from 25%) 9 days after influent Ag^+ was switched off. In this study, only biofilms exposed to 0.5 ppm Ag^+ demonstrated recovery, and only to 80% of initial activity (up from 40%) after 10 days. Given that Giska's recovery experiments were performed on mature biofilms, the results cannot be directly compared to the standard biofilms in this study. The significantly greater biomass typical of mature biofilms may allow for more rapid growth and accelerate the rate of recovery.

A sudden and near-total loss of activity occurred immediately following a media change after the 240th hour of recovery in the 0.5 ppm Ag^+ recovery experiment (Test 7). This was assumed to be the result of media contamination. Protein and silver content for Test 7 were quantified after harvesting, but only the 1.5 ppm Ag^+ test (Test 3) is plotted in Figure 2 and Figure 3a. Biomass measurements of "post-recovery" exposed biofilms (Test 3) are similar to those of biofilms harvested immediately following 1.5 ppm Ag^+ exposure (Test 2). Final nitrification rates are

not significantly different between the two tests. As noted previously, the Ag^+-exposed biofilms from Test 3 had lower protein content than the control biofilms, which may indicate that sloughing occurred during Ag^+ exposure. The similarity of protein content between biofilms harvested immediately after exposure (Test 2) and those harvested a week later (Test 3) suggests that no growth took place during the "recovery" week. The absence of protein data from the 0.5 ppm Ag^+ recovery experiment is particularly unfortunate in this instance, as some recovery did occur and valid protein measurements might have been helpful in determining the role of biomass growth in recovery. (Protein measurements were made for biofilms in the 0.5 ppm Ag^+ recovery test [Test 7]; they are presented in Table 3. The measurements are far lower than any others in this study. This is presumably due to sloughing from contaminated media.)

Summary

Several findings emerge from the results of these Ag^+ exposure experiments. Inhibition continues to increase for the full 48 hours of exposure, although the rate of increase in inhibition is highest in the first hours. Inhibition stops increasing after Ag^+ is removed from the influent, suggesting that increases in Ag^+-induced inhibition are the result of continuous exposure and not the lingering effects of earlier exposure. Biofilms exposed to 1.5 ppm Ag^+ did not experience significantly greater inhibition than those exposed to 0.5 ppm Ag^+, in spite of receiving a threefold higher dose over an extended period. Sloughing may account for some loss of nitrifying activity in exposed biofilms.

Biofilms exposed to 0.5 ppm Ag^+ took a week to recover to a statistically significant degree. The lack of an immediate increase in nitrification activity suggests that recovery is not due to a quick reversal of enzyme-specific inhibition but rather to growth of new biomass or slow reactivation of previously dormant cells. Recovery was slower than typical biofilm growth, suggesting that residual Ag^+ present in the DFR continued to inhibit biofilm cells.

4.1.2 48-hour AgNP exposure

Nitrification rates of biofilms exposed to AgNP are shown in Figure 6a, with corresponding percent inhibition shown in Figure 6b. Experiments were performed on biofilms exposed to 0.5 ppm AgNP and 1.5 ppm AgNP. Biofilms exposed to either concentration exhibited statistically significant decreases in nitrite production after 48 hours compared to control biofilms (Figure 6b; see Appendix Table 5, Table 6, and Figure 35 for further details on statistical analysis).

When comparing nitrification rates prior to and after 48 hours of exposure, nitrification inhibition did not differ significantly between biofilms exposed to 0.5 ppm AgNP (~27%) and those exposed to 1.5 ppm AgNP (~32%) (Figure 6b). However, an equipment failure four hours into the 1.5 ppm AgNP experiment resulted in a brief interruption of flow for the media and syringe solutions. Additionally, abnormally cold weather in the latter 24 hours of the experiment caused the temperature in the room housing the DFR to drop to 25°C for several hours. Both of these events may have had negative impacts on nitrite production in all lanes. In addition to the two lanes exposed to 1.5 ppm AgNP, both control lanes exhibited some decreased nitrification after 48 hours with respect to initial nitrification rates (Appendix, Table 6 and Figure 35). Inhibition of both treated biofilms was normalized against the control receiving the blank syringe solution in order to calculate values for Figure 6b. Had the equipment and weather events not occurred, the normalized inhibition of biofilms exposed to 1.5 ppm AgNP may have been higher, and could have been significantly greater than inhibition of biofilms exposed to 0.5 ppm AgNP.

Initial nitrite production rates ranged from 0.031 to 0.036 mmol NO_2^-/hr (Figure 6a), which agrees with Lauchnor (2011) and Giska's (2013) previous work on *N. europaea* biofilms. Inhibition was much lower for biofilms exposed to AgNP (Figure 6b) than for biofilms exposed to the same concentration of Ag^+ (Figure 1b); this

finding agreed with results of previous 3-hour Ag^+ and AgNP inhibition experiments (Giska, 2013). While Giska's results found only approximately 5% inhibition after 3 hours of exposure to 20 ppm AgNP, this study (Figure 6b) found 32% inhibition after 48 hours of exposure to 1.5 ppm AgNP (an approximately equal mass loading of AgNP). This may be due to the longer exposure, which allowed more time for Ag^+ to be released from AgNP embedded in the biofilms; alternatively, increased aggregation at higher AgNP concentrations may have contributed to less dissolution in Giska's study. Contrary to in the Ag^+ experiments, biofilms exposed to AgNP did not show dramatically higher rates of increasing inhibition in the first three hours of exposure compared to later on.

The final protein content of biofilms exposed to AgNP (589-1311 μg protein, mean = 955 μg) did not differ significantly from control biofilms in the same tests (291-1237 μg protein, mean = 829 μg) (Table 1 and Figure 2). This suggests that exposure to AgNP did not cause significant sloughing in these tests. Results from Test 5 (1.5 ppm AgNP influent) may indicate that specific nitrite production in biofilms is affected by AgNP exposure (Figure 3b). Test 4 (0.5 ppm AgNP) shows no such correlation.

No recovery experiments were run on AgNP-exposed biofilms.

4.1.3 Silver binding to biomass

One of the questions in this research was whether a correlation existed between nitrification inhibition and the concentration of silver bound to biofilm biomass. An overall correlation between bound silver and nitrification activity is not seen in Figure 7a, which presents nitrification activity of biofilms after 48 hours of Ag^+ exposure graphed against the concentration of sorbed silver (in micrograms of silver per milligram of protein). However, a few interesting observations can be

made. For all treatments, duplicates tend to be in good agreement. Biofilms exposed to the same treatment (Ag^+ at a given concentration) had similar silver-to-protein ratios when harvested. Identical treatments also yielded similar nitrification activity after 48 hours (as a percentage of initial activity).

Biofilms exposed to 1.5 ppm Ag^+ had lower concentrations of bound silver than those exposed to 0.5 ppm Ag^+ (Figure 7a). This is opposite the trend that would be expected. It is interesting to note that both treatments showed similar levels of inhibition when harvested (Figure 1b). This may have been a result of biofilms sloughing off cells that were more heavily exposed. Dose-dependent AgNP-induced sloughing has been previously documented in *P. aeruginosa* and *S. epidermidis* biofilms (Kalishwaralal et al., 2010). However, sloughed biomass was not quantified in this study.

While no overall correlation in silver binding is seen among Ag^+-exposed biofilms (Figure 7a), biofilms exposed to 1.5 ppm AgNP had higher concentrations of bound silver than biofilms exposed to 0.5 ppm AgNP (Figure 7b). This follows the trend that would be expected based on silver mass loadings.

The concentration of bound silver in biofilms exposed to 1.5 ppm AgNP was 4-5 times that of biofilms exposed to 1.5 ppm Ag^+ (Figure 7a, Figure 7b). In spite of this, inhibition in the AgNP-exposed biofilms was significantly lower. This suggests that AgNP were largely stabilized and did not experience significant dissolution. Biofilms exposed to 0.5 ppm AgNP had lower bound silver concentrations than biofilms exposed to 0.5 ppm Ag^+ (including mature biofilms and recovered biofilms). This may indicate that AgNP in this test largely passed through the DFR without adsorbing to biomass, in contrast to the 1.5 ppm AgNP test. 0.5 ppm AgNP-exposed biofilms exhibited less inhibition than biofilms exposed to 0.5 ppm Ag^+, with the exception of Ag^+-exposed biofilms that were allowed to recover for 10 days.

The silver-to-protein ratio in biofilms that were exposed to 0.5 ppm Ag^+ and harvested after a 10-day recovery period (mean value: 61 μg Ag/mg protein) was the same as biofilms harvested immediately after exposure to 0.5 ppm Ag^+ (mean: 60 μg Ag/mg protein) (Figure 7a). This indicates that silver does not leach from biofilms during recovery. It could also indicate that recovery is possible without a decrease in the silver-to-protein ratio (such as might be seen if there were significant new cell growth during recovery). Recovered biofilms were also marginally less inhibited (19.8%) than biofilms exposed to 0.5 ppm AgNP (26.7%) (Figure 7a, Figure 7b), despite having more bound silver (61 μg Ag/mg protein vs. 21 μg Ag/mg protein). However, it must be noted that the biofilms in the recovery experiment died suddenly following the addition of new media just prior to harvesting. (See Appendix for notes on biofilm death following addition of new media.) This likely resulted in sloughing of some biomass before it could be quantified; as seen in Table 3, protein measurements for these biofilms were significantly lower than for all other harvested biofilms. (Table 3 is discussed in more detail in Section 4.1.5.) It is unclear whether sloughing would affect the silver-to-protein ratio in the remaining biofilm.

Mature biofilms exposed to 0.5 ppm Ag^+ had higher silver-to-protein ratios (88.6 μg Ag/mg protein) than standard biofilms (60 μg Ag/mg protein) (Figure 7a), as well as higher rates of nitrification activity (~0.02 mmol NO_2^-/hr vs. ~0.01 mmol NO_2^-/hr) (Figure 1a). This may be related to biofilm thickness; more mature biofilms may be able to adsorb greater quantities of silver in upper layers, while cells farther from the surface remain protected and maintain their activity.

Figure 8 presents biomass-normalized nitrification rates (specific nitrification rates) graphed against bound silver for both Ag^+ and AgNP exposures. While no correlation is shown between specific nitrite production rates and silver bound to biomass, some interesting results are indicated. Biofilms exposed to 1.5 ppm AgNP have much higher silver-to-protein ratios (97-121 μg Ag/mg protein) than biofilms

exposed to 1.5 ppm Ag^+(23-27 μg Ag/mg protein), indicating that Ag^+ causes more inhibition of specific nitrification despite the presence of less bound silver. As noted previously, this is likely due to lack of AgNP dissolution. Biofilms exposed to 1.5 ppm AgNP had silver concentrations approximately six times higher than those exposed to 0.5 ppm AgNP (97-121 μg Ag/mg protein vs. 15-28 μg Ag/mg protein) . Final specific nitrification rates were not significantly different between the two treatments, indicating that the silver was in the form of AgNP. This is consistent with Ag^+ and not AgNP being the primary inhibitor. The results also indicate the biofilms captured more AgNP as their concentration increased. Mature biofilms exposed to 0.5 ppm Ag^+ had lower specific nitrification rates (0.0108-0.0137 mmol NO_2^-/mg protein/hr) than standard biofilms exposed to the same concentration (0.0279-0.0344 mmol NO_2^-/mg protein/hr). The specific nitrification rates of mature biofilms exposed to 0.5 ppm Ag^+ were similar to those of standard biofilms exposed to 1.5 ppm Ag^+ (Figure 8). However, mature biofilms were less inhibited than standard biofilms despite having higher concentrations of bound silver (Figure 7a). The lower biomass-normalized activity of mature biofilms may contribute to their protection from Ag^+-induced inhibition. It is also likely that the presence of more biomass (particularly inactive biomass) in mature biofilms enables biofilms to adsorb greater quantities of Ag^+ without experiencing high inhibition.

4.1.4 Silver in effluent samples

Silver content in effluent samples was measured to determine whether a breakthrough curve existed during the course of Ag^+ or AgNP exposure, and to compare effluent silver concentrations with influent concentrations and with bound silver. Concentrations of silver in DFR effluent are shown in Figure 9. Results for both Ag^+ and AgNP tests are shown in the same graph.

Effluent from Ag^+ exposure experiments

Effluent silver concentrations did not differ significantly between standard biofilms exposed to 0.5 ppm Ag^+ and 1.5 ppm Ag^+ (Figure 9). Insufficient replicates are available to determine if effluent silver concentrations from mature biofilms exposed to 0.5 ppm Ag^+ differed from those of standard biofilms. These effluent silver concentrations are in the same range as those measured by Giska (2013) for standard and mature biofilms exposed to 0.5 ppm Ag^+ – 2.0 ppm Ag^+. None of the effluent silver concentrations exceed approximately 0.1 ppm; in many cases, effluent measurements were a full order of magnitude lower than influent concentrations. Sorption to the reactor, effluent tubes, collection vials, and ICP-OES sample tubes is likely the cause. Previous tests on the same DFR system found that when media containing 2 ppm Ag^+ was run through the reactor with no biofilm present, less than 10% of influent silver was detected in effluent measurements over the course of 3 hours (Giska, 2013).

Effluent collected from the first two experiments run with Ag^+ was found to have no detectable silver after being stored for more than 2 weeks, even when refrigerated or frozen. Thereafter, ICP-OES measurements were performed the day following conclusion of the experiment. Even with reduced storage time, it is impossible to eliminate silver loss due to sorption.

Because of the low effluent concentrations in Ag^+ experiments, it is hard to confidently identify a breakthrough curve. Effluent concentrations rise for approximately the first 5 hours in the 0.5 ppm Ag^+ experiments before approaching a steady state. In the 1.5 ppm Ag^+ experiment, this steady state is reached later (at around 24 hours). Given an overall flow rate of 12 mL h^{-1} per lane and a liquid volume of less than 10 mL, five hours is considerably longer than the amount of time required for the Ag^+ concentration in the biofilm lane to approach the influent concentration. Giska (2013) found that peak effluent concentrations were reached at 1 hour in lanes containing no biofilms. It seems likely that sorption of Ag^+ to

biofilms is responsible for the more gradual increase in effluent silver concentrations seen here.

Effluent from AgNP exposure experiments

Effluent concentrations from experiments run using AgNP were significantly higher than those from experiments using Ag^+ (Figure 9). It is interesting to note that the 0.5 ppm AgNP experiment was the only case in which the effluent silver concentration approached a breakthrough concentration near the influent concentration. This occurred after 16 hours, and effluent concentrations were relatively stable after that point. Silver concentrations rose much more rapidly in the 1.5 ppm AgNP measurements, but then leveled off for 24 hours (matching effluent concentrations from the 0.5 ppm AgNP biofilms) before rising once again. It is possible that the effluent silver measurements of the two experiments would have diverged farther given more time. More silver from AgNP experiments than from Ag^+ experiments can be accounted for in effluent (30-43% for 1.5 ppm AgNP, 80-100% for 0.5 ppm AgNP, and <22% for all Ag^+ tests after 24 hours). AgNP likely entered the effluent without significant dissolution, and were thus less prone to being lost via sorption to the reactor and to collection vials. This is supported by results from Giska (2013) showing that 80-90% of influent AgNP were recovered in effluent measurements after 1 hour when no biofilm was present.

4.1.5 Spatial distribution of biomass and silver

When biofilms were harvested at the end of each experiment, significant quantities of cells were visible in the fluid collection wells downstream of the slides on which the biofilms were grown. Cells were found in large clumps either adhered to the well or floating in it. Because these cells constituted part of the biomass in each lane and potentially contributed to NO_2^- production, their protein content and silver levels

were measured and added to those of the cells on the slide to comprise the overall biomass and bound silver levels discussed in 4.1.3.

Table 2 lists theoretical silver mass loadings and actual measurements of bound silver for all experiments in which bound silver was measured. In most cases, silver bound to biomass accounts for a small fraction of the silver used in the experiment. The exception is for mature biofilms, where approximately 50% of the silver was recovered from biofilms. The numbers in Table 2 refer to measurements taken from the entire lane (slide and well).

Table 3 presents biomass and silver harvested from slides and wells in most DFR experiments. Figure 10 shows the distribution of both biomass and silver in the DFR lanes. In both control and treated lanes, the majority of biomass was found on the slide, with approximately 10-30% in the well (Figure 10a). In treated lanes, a similar proportion of silver was located on the slide vs. in the well (Figure 10b), indicating that the bound silver content of cells in the well was similar to that of cells on the slide. Slightly higher proportions of both biomass and silver were measured on slides exposed to AgNP compared to those exposed to Ag^+ (Table 3). These results may indicate a slightly reduced degree of sloughing in biofilms exposed to AgNP versus those exposed to Ag^+. This may be correlated with the lower inhibition observed in AgNP-exposed biofilms.

Mature biofilms exposed to 0.5 ppm Ag^+ had a higher percentage of biomass on the slide than most "standard" Ag^+-exposed biofilms (mean = 84.2% for mature biofilms, 68.9% for standard biofilms; P = 0.050) (Table 3). Mature biofilms also had a slightly higher percentage of bound silver located on the slide than "standard" biofilms exposed to Ag^+ (mean = 97% vs. 70%, P = 0.056). Both of these comparisons exclude Test 7 for the reasons described previously.

Exposed mature biofilms had the highest biomass of any exposed biofilms at time of harvest (Table 3) while displaying the second-highest set of bound silver

concentrations (after 1.5 ppm AgNP) (Figure 7). These observations suggest that mature biofilms are able to adsorb high concentrations of Ag^+ with little sloughing. This may be due to the presence of more inactive biomass in mature biofilms.

4.1.6 Specific oxygen uptake rates (SOURs)

Specific oxygen uptake rates (SOURs) were measured to study whether Ag^+ affected *N. europaea* biofilm cells in an enzyme-specific manner. Cells used in SOUR tests were taken from a uniform mixture of harvested biofilm cells, and protein was measured from the remainder of the sample in order to calculate protein-normalized oxygen uptake rates. *N. europaea* cells were injected into the water-jacketed reaction cell and provided with an excess of substrate (2.5 mM $(NH_4)_2SO_4$) to measure the AMO-SOUR, after which 100 μM ATU was added to halt AMO activity. 750 μM NH_2OH was then added as a substrate for HAO, and the HAO-SOUR was measured. SOURs were performed for biofilms from the 1.5 ppm Ag^+ exposure + recovery experiment. AMO-SOURs and HAO-SOURs from slides and wells are presented in Table 4, along with protein measurements for each sample and final nitrification rates from each lane.

SOURs were performed on biofilms from Test 3 (1.5 ppm Ag^+ with recovery). As shown in Figure 4b, exposed biofilms from this test displayed ~55% inhibition at the time of harvest. AMO-SOURs and HAO-SOURs of control biofilms averaged 4.36 mmol O_2/hr and 1.32 mmol O_2/hr, respectively (Table 4). These averages were three times higher than the average AMO-SOURs and HAO-SOURs of biofilms exposed to 1.5 ppm Ag^+ (1.42 mmol O_2/hr and 0.375 mmol O_2/hr, respectively); if the difference in SOUR activity matched the difference in final nitrite production between control and treated DFR biofilms, SOURs of control samples would be expected to be only approximately twice as high as SOURs of exposed samples. The

ratio of AMO-SOURs to HAO-SOURs averaged around 3.3 for both treatments and controls. This AMO/HAO ratio is within the range of ratios for control *N. europaea* cells in previous studies (Radniecki et al., 2008; Radniecki et al., 2009).

It was noted that biomass of control samples was higher on average than that of treatments (Table 4). SOURs were normalized by protein content to compare to previous studies. Biomass-normalized SOURs were also analyzed to determine whether they correlated with biomass-normalized nitrite production rates and to determine if a difference existed between biomass-specific SOURs of control and exposed biofilms.

Biomass-normalized AMO-SOURs of control samples averaged 21.0 mmol O_2/mg protein/hr in this test (Table 4). Radniecki et al. (2009) reported AMO-SOURs of approximately 70 mmol O_2/mg protein/hr for suspended *N. europaea* cells. The average HAO-SOUR of control biofilms in this test was 6.34 mmol O_2/mg protein/hr (Table 4). This is approximately half of the value reported by Radniecki et al. for suspended cells (2009). Given that resuspended *N. europaea* biofilms have been found to have lower activity levels than suspended cells (Lauchnor, 2011; see also Section 4.2.1), an average of 21.0 mmol O_2/mg protein/hr seems reasonable for biofilm cells resuspended for SOUR tests.

No correlation was seen between either biomass-normalized AMO-SOURs or HAO-SOURs of harvested biofilms and biomass-normalized nitrite production rates of corresponding biofilms as measured prior to harvesting (Figure 11). This may be due to the much lower overall activity of intact biofilms compared to SOUR samples (which were resuspended and provided with excess NH_3).

Figure 12 presents biomass-normalized AMO-SOURs and HAO-SOURs from all samples. Average biomass-normalized SOURs (both AMO and HAO) were higher in controls than treatments by a factor of 1.6 (Table 4). An independent samples t-test found that the difference between control and exposed biofilms was significant for

HAO-SOURs ($p = 0.022$), but not for AMO-SOURs ($p = 0.092$). This indicates that HAO activity decreased in the presence of Ag^+. AMO activity may have decreased, but the statistical analysis finds that AMO is not significantly more inhibited than HAO, indicating that the observed nitrification inhibition is not due to AMO-specific inhibition. The difference in biomass-normalized SOURs is not sufficient to account for the difference in nitrite production between control and exposed biofilms.

SOURs of control and exposed samples were graphed together against measured biomass to explore whether oxygen uptake correlated with sample biomass (regardless of exposure). Positive correlations are seen between AMO-SOURs and protein content (Figure 13a) and between HAO-SOURs and protein content (Figure 13b). The ratio of the slopes of the trendlines (0.019/0.0055) is 3.45, approximately equal to the average AMO:HAO ratios of control and exposed biofilms (3.3, as mentioned above).

The results presented in Figure 12 and Figure 13 suggest that the mechanism by which nitrite production in biofilms is inhibited is a general one, rather than a specific mechanism that targets AMO. Radniecki et al. (2011) found that Ag^+ selectively inhibited AMO after 1 hour of exposure, particularly at higher Ag^+ concentrations. It is possible that the longer exposure in this test resulted in more general inhibition, including cell death, which would affect both AMO and HAO activity. Sloughing likely played a role in nitrification inhibition as well; samples exposed to 1.5 ppm Ag^+ had lower biomasses on average than controls (Table 1), though the difference was not enough in itself to account for the degree of nitrification inhibition observed.

4.1.7 Summary

Results from these experiments confirm earlier findings that AgNP inhibit nitrification in *N. europaea* biofilms to a lesser degree than Ag^+. Data for inhibition and effluent concentrations agree with trends seen in earlier work. Mature biofilms are more resistant than less mature (standard) biofilms to inhibition by Ag^+, possibly due to the presence of more inactive biomass. Even though influent concentrations (0.5 ppm and 1.5 ppm for both Ag^+ and AgNP) differed by a factor of 3, no significant difference in inhibition was observed between biofilms exposed to the two different concentrations. No clear correlation was found between bound silver and nitrification inhibition in DFR biofilms; this contrasts with previous findings by Giska.

Sloughing of biomass may account for some loss of nitrifying activity. Comparing final biomass measurements across experiments does not indicate a correlation between biomass and activity. However, the correlation between SOURs (both AMO and HAO) and the biomass of harvested biofilms demonstrates that specific oxygen uptake remains somewhat linear for biofilms, regardless of Ag^+ exposure. Control biofilms in the SOUR experiment had more biomass than exposed biofilms, suggesting that sloughing was likely responsible for some changes in activity in this instance. SOUR results suggest that Ag^+ toxicity in extended-exposure DFR biofilm tests does not take the form of selective AMO inhibition. Inhibition may result from Ag^+ killing cells and thereby halting all metabolic activity. Neither AMO/HAO inhibition nor loss of biomass alone can account for the difference in nitrite production between control and exposed biofilms; a combination of inhibition and sloughing is likely responsible.

4.2 Inhibition of suspended cells and resuspended biofilms

4.2.1 Ag^+ inhibition tests

Suspended cells

Experiments were conducted on batch-grown suspended cells in order to compare inhibition to previous studies (Christina Lee Arnaout, 2012; Giska, 2013; Radniecki et al., 2011) and to results obtained for intact and resuspended biofilms in this study. Figure 14a shows nitrification inhibition of suspended cells exposed to 0.05 – 0.25 ppm Ag^+. Inhibition was concentration dependent, ranging from ~20% to ~90%. Inhibition of ~20% at 0.05 ppm is in the range of that observed by Giska (2013) and Radniecki et al. (2011). Inhibition of ~90% at 0.25 ppm agrees with Giska (2013) and Arnaout (2012). Inhibition at 0.10 ppm (observed at ~75% in this study) was consistently higher than that observed by either Giska or Radniecki et al. (~40%). Nitrification rates of control cells were highly consistent during individual experiments but varied somewhat between experiments. Therefore, a graph of percent nitrification inhibition is displayed, without a corresponding overall graph of nitrification rates. Nitrification inhibition was consistent both across replicates and between experiments, as demonstrated by the error bars.

All 3-hour batch inhibition tests were performed using the same media as the biofilms (low-Mg^{2+} DFR media). This differs slightly from the regular-strength DFR media used by Giska (2013) and more significantly from the minimal 30 mM HEPES/2.5 mH $(NH_4)_2SO_4$ media (no Mg^{2+}) used by Radniecki et al. (2011). Previous work by Anderson et al. (2014) found decreased inhibition with increasing levels of Mg^{2+} when cells were exposed to 0.5 ppm Ag^+ for 3 hours. It is not clear why protection from Mg^{2+} was not observed in these tests compared to the observations of Anderson et al.

As observed by Giska (2013), suspended cells were more susceptible to Ag^+ inhibition than biofilms. Suspended cells exposed to 0.25 ppm Ag^+ were inhibited by approximately 90% after 3 hours (Figure 14a), compared with approximately 25% inhibition observed after 3 hours in biofilms exposed to twice the concentration (0.50 ppm Ag^+) (Figure 1b).

Resuspended biofilms

Resuspended biofilms were exposed to 0.05-0.25 ppm Ag^+ to compare nitrification inhibition to inhibition observed in suspended cells. Nitrification inhibition of these biofilms in 3-hour batch tests is shown in Figure 14b. One set of resuspended biofilm tests was performed first, with Ag^+ concentrations of 0.10-0.25 ppm. While inhibition of suspended cells in this range was 75-90% (Figure 14a), inhibition of resuspended biofilms was 90-97% (Figure 14b). Inhibition in resuspended biofilms was concentration dependent, and replicates were highly consistent. No protection from inhibition was observed when compared to suspended cells exposed to equal concentrations of Ag^+. In fact, somewhat higher percent inhibition was observed in the resuspended biofilm cells, and inhibition occurred more rapidly. This difference may have resulted from pipetting variations of Ag^+ at low concentrations. However, it was suspected that the centrifugation, concentration, and resuspension of the biofilms might have resulted in cell damage or shearing of EPS, making cells more vulnerable to Ag^+. Two further tests (denoted with asterisks) were performed with 0.05 ppm Ag^+ and 0.10 ppm Ag^+. Cell preparation for these tests was gentler and involved resuspension and brief vortexing (no centrifugation). Once again, inhibition was concentration dependent, but inhibition of cells exposed to 0.10 ppm Ag^+ was 65% as opposed to 90% in the previous test. This is close to (and within the margin of error of) the 75% inhibition of suspended cells exposed to 0.10 ppm Ag^+. Resuspended biofilms exposed to 0.05 ppm Ag^+ showed 35% inhibition, slightly higher than the 23% inhibition of suspended cells exposed to the same concentration. The results of the second set of tests suggest that resuspended

biofilms are inhibited by Ag^+ to the same degree as suspended cells. This would indicate that EPS provides no protective value against Ag^+.

The baseline nitrification activity of control resuspended biofilm cells was lower than that of control suspended *N. europaea* cells. The average nitrification rate of control suspended cells was 0.13 mmol NO_2^-/mg protein/hr, compared with 0.079 mmol NO_2^-/mg protein/hr for resuspended biofilm controls. This is likely a result of the large numbers of inactive or low-activity cells present in biofilms (Rani et al., 2007). The average nitrification rate of resuspended biofilms was greater than that of intact biofilms in this study (0.035 mmol NO_2^-/mg protein/hr) (Table 1), and higher than the nitrification rate of any individual intact biofilm. This agrees with prior observations of resuspended *N. europaea* biofilms (Lauchnor et al., 2011). It should be noted that while Lauchnor found a fivefold increase in activity when biofilm cells were resuspended, this study found only a twofold increase. The heightened activity of biofilm cells resuspended in media suggests that cells that were previously oxygen- and ammonia-limited are able to take advantage of access to nutrients and immediately increase their nitrification activity.

In addition to increased exposure to nutrients, biofilm cells that were previously shielded from the effects of Ag^+ by virtue of their location deeper in the biofilm are exposed to Ag^+ once the biofilm is dispersed and resuspended. The lack of protection from Ag^+-induced inhibition in resuspended *N. europaea* biofilms suggests that biofilm resistance to inhibition may be partially a result of mass-transfer limitations. If binding of Ag^+ to EPS throughout the biofilm were a significant cause of protection from inhibition, this would be expected to potentially remain a source of protection in resuspended biofilms. However, protection disappears when biofilms are resuspended, suggesting that an Ag^+ diffusion gradient or lower cell activity is responsible for protection in intact biofilms.

Lauchnor (2011) found that higher rates of initial nitrite production in both suspended cultures and biofilms of *N. europaea* corresponded to higher percent

nitrification inhibition during experiments when phenol was the inhibiting agent. In this study, the higher rates of nitrification in control resuspended biofilms compared to intact biofilms corresponded to higher percent nitrification inhibition, as observed in the phenol studies. The lower activity of intact biofilms may provide protection from Ag^+-induced inhibition. Sloughing can be discounted as a cause of lowered activity in resuspended biofilms, as all cells remain in the batch reactor for the duration of the experiment.

4.2.2 AgNP inhibition tests

In initial tests (not shown), no nitrification inhibition was observed in suspended cells exposed to up to 5 ppm AgNP for 3 hours. These results differ slightly from previous work using DFR media (Giska, 2013), which found 10% inhibition at 1 ppm AgNP and 20% inhibition at 10 ppm AgNP in the same low-Mg^{2+} medium.

Some AgNP batch inhibition tests were extended beyond 3 hours in order to determine whether inhibition would be seen with longer exposures. Figure 15 shows nitrification activity of cells exposed to 2 ppm and 5 ppm AgNP for 8 hours. Figure 16 shows corresponding percent inhibition. During the normal 3-hour exposure, little difference is seen compared to controls, while some difference occurs with longer exposures. After 5 hours, 3-4% inhibition was seen in suspended cells exposed to 2 ppm and 5 ppm AgNP. This might be due to slow release of Ag^+, potentially as a result of AgNP aggregation. The fact that inhibition is only seen after several hours seems to support the theory that Ag^+ release is the key cause of nitrification inhibition in this system.

A silver ion probe was used to study Ag^+ release by measuring free Ag^+ in bottles containing test media and 2 ppm AgNP (but no cells). Figure 17 displays free Ag^+ in solution over time. An increase from <0.01 ppm Ag^+ to 0.03 ppm is seen after 5

hours; this Ag^+ concentration would be consistent with the low level of inhibition observed in cells exposed to 2 ppm AgNP after 5 hours. This degree of dissolution is lower than that measured by Anderson (2014) in spite of the lower Mg^{2+} concentration in this media (which would theoretically allow for greater dissolution). The presence of trace ions such as Fe^{2+}, Ca^{2+}, and Cl^- in the DFR media may have contributed to increased aggregation and to the decreased Ag^+ release seen in this study.

The inhibition data can be compared with inhibition results from Ag^+ batch tests. As shown in Figure 14a, exposure to 0.05 ppm Ag^+ resulted in ~20% nitrification inhibition after 3 hours. This test's findings of 3-4% inhibition after 5 hours are consistent with those results, bearing in mind that cells in the AgNP bottles were exposed to less than 0.03 ppm Ag^+ for most of the experiment. It should be noted that nitrification rates in the extended batch tests were not linear after 3 hours. This is often associated with depletion of NH_3.

The lack of inhibition seen in 3-hour AgNP batch experiments does not differ from inhibition in DFR experiments after 3 hours. In the latter, only ~13% inhibition and ~2% inhibition (both with wide margins of error) were seen after 3 hours of 0.5 ppm and 1.5 ppm AgNP influent, respectively. This low level of inhibition indicates a significant degree of aggregation likely occurred during DFR tests. (Figure 28 [Appendix] displays UV-Vis scans of effluent from lanes exposed to 0.5 ppm AgNP, which were an attempt to visualize AgNP aggregation in the system. It is unclear from the results whether aggregation occurred prior to or after contact with the biofilm.)

4.2.3 Summary

These results confirm earlier findings that suspended cells are more susceptible to Ag^+ inhibition than intact biofilms. Results for Ag^+ exposure in suspended cells closely resemble previous work (Christina Lee Arnaout, 2012; Giska, 2013; Radniecki et al., 2011), with the exception of higher inhibition seen with some intermediate concentrations. This study also found that resuspended biofilms are inhibited by Ag^+ to approximately the same extent as suspended cells, indicating a complete loss of protection from inhibition once the biofilm is resuspended. Little inhibition was seen in suspended cells exposed to AgNP, even at concentrations exceeding those used in DFR experiments. This may be due to AgNP aggregation in the presence of divalent cations found in the media. Future experiments should include AgNP tests on resuspended biofilms (especially in minimal media, where aggregation is likely to be less of a factor) to compare inhibition with that of suspended cells.

4.3 Live/Dead results

Previous research has shown that silver inhibits the AMO enzyme of *N. europaea*; high concentrations of silver have also been shown to lead to cell death by disrupting membrane integrity (Christina Lee Arnaout, 2012; Radniecki et al., 2011). This study attempted to quantify the role of cell death in the inhibition of suspended cells, intact biofilms, and resuspended biofilms. Live/Dead analysis was performed on control cells and cells exposed to Ag^+. As mentioned above, the Live/Dead stain distinguishes cells with intact membranes (designated “live”) from those with compromised membranes (“dead”). No Live/Dead analysis was done for cells exposed to AgNP due to time constraints and the large quantities of AgNP and biofilms that would be required for replicates.

4.3.1 Suspended cells

Cell membrane integrity of batch-grown suspended cells subjected to 3-hour batch Ag^+ inhibition tests was quantified via fluorescent staining ("Live/Dead") followed by flow cytometry. Results of nitrification inhibition tests on these cells are presented in Figure 14a. Results of Live/Dead analysis are presented in Figure 18. Samples of raw flow cytometer output data are provided in the Appendix (Figure 32).

Samples exposed to up to 0.10 ppm Ag^+ experienced low or negligible increases in cell death (less than 10% above control samples) (Figure 18). At concentrations of 0.15 ppm and above, however, cell death was high. This study's findings of ~93% cell death at 0.20 ppm Ag^+ agree precisely with those of Arnaout (2012).

Figure 19 plots the percentage of dead cells after 3 hours (normalized against the percentage of dead cells in controls) against nitrification inhibition after 3 hours. The correlation is not linear, indicating that there is not a direct correspondence between cell death and observed nitrification inhibition. Of particular interest are suspended cells exposed to 0.10 ppm Ag^+. As noted in Figure 14a, at this concentration nitrification was 75% inhibited after 3 hours. However, cell death is only 5% higher than among control cells. This indicates that most of the inhibition observed at this concentration is of cells with still-intact membranes. A similar pattern of inhibition far exceeding cell death is seen for cells exposed to 0.075 and (less dramatically) 0.05 ppm Ag^+.

These results suggest that at low Ag^+ concentrations, nitrification is inhibited through a specific mechanism, most likely inhibition of the AMO enzyme. Radniecki et al. (2011) found that Ag^+ selectively inhibited AMO in batch tests of suspended cells, but that selectivity for AMO was far greater at 0.20 ppm than at 0.10 ppm. This inhibition was found to be irreversible, possibly due to the difficulty of removing Ag^+ from cells. In this study, SOUR tests of intact biofilms exposed to 1.5 ppm Ag^+

found no AMO-specific inhibition. At higher concentrations, cell death resulting in compromised membranes is responsible for a large fraction of nitrification inhibition.

4.3.2 Intact biofilms

Results of Live/Dead staining and flow cytometry on cells harvested from post-experiment DFR biofilms are shown in Figure 20. Raw flow cytometry output data are shown in Figure 33 (Appendix). As with SOURs, Live/Dead samples were divided into cells attached to the slide and cells in the DFR well.

Biofilms exposed to 1.5 ppm Ag^+ for 48 hours had significantly more dead cells than control biofilms, both in slide and well samples. Approximately 80% of Ag^+-exposed cells attached to slides were dead after 48 hours, compared to ~20% of control cells. This higher rate of cell death in control biofilms compared to control resuspended cells is reasonable, given the 4-week culturing period of the biofilms. Of cells sampled from wells, approximately 25% of exposed cells were dead, compared to ~15% of control cells. The margin of error was widest for control cells attached to slides.

Biofilm cells exposed to 1.5 ppm Ag^+ showed approximately 70% nitrification inhibition after 48 hours (Figure 21). This inhibition is comparable to suspended cells after 3 hours of exposure to 0.10 ppm Ag^+ (~75% inhibition [Figure 14a]). There are several likely reasons for the higher death observed in the biofilms following treatment with Ag^+. First, the period of exposure was much longer. More cell death would be expected in batch tests of suspended cells with longer exposures. Second, the concentration of Ag^+ used in the biofilm test was higher than that used in the batch suspended cell tests. Third, some death may be a result of post-experimental cell lysis resulting from preparation of cells for Live/Dead

staining; cells may have been exposed to Ag^+ after being pipetted from slides, resulting in death. Analysis of intact biofilms via confocal microscopy may be more helpful for analyzing live/dead percentages by visualizing lysed and unlysed cells in situ. DFR biofilm inhibition experiments could be run at both lower Ag^+ concentrations and shorter exposures to determine if live/dead results more closely resemble suspended cells under those conditions. Longer exposures of suspended cells to Ag^+ should also be performed.

As seen in Table 1, the biomass-normalized nitrification rates of these 1.5 ppm Ag^+-treated biofilms were among the lowest of all biofilms in this study, while the measured protein content was average to high compared to other biofilms, including controls. No measurements were made to determine the protein content of any sloughed biomass, but given the high biomass in the harvested biofilm it is not possible to draw conclusions about the role sloughing may have played in loss of nitrifying activity.

The high percentage of dead cells (Figure 20) may explain the results of the 1.5 ppm Ag^+ recovery test discussed above in Section 4.1.1. In that experiment, no recovery was observed after 7 days (Figure 4). The death of a large fraction of biofilm cells could account for the lack of recovery. Cell death in exposed biofilms could also explain the slow recovery of biofilms exposed to 0.5 ppm Ag^+, which took much longer to increase nitrite production than normal growing biofilms starting at the same activity level (Figure 5).

It is interesting to note that cell death in wells of exposed biofilms was lower than cell death in cells attached to slides. In both biofilms, the majority of silver (78% or 90%) was located on the slide (Table 3). However, in one biofilm, only 48% of biomass was on the slide (the proportion was 84% for the other biofilm). The lower silver-to-biomass ratio in the well of the first biofilm may have resulted in lower death, skewing the overall results.

The results of Live/Dead staining on biofilms echo the results of AMO-SOURs and HAO-SOURs in that both tests point toward a non-specific inhibition of nitrification activity. The results may support a model in which cell death is partially responsible for loss of activity in exposed biofilms. This is further backed up by recovery experiments (Figure 4 and Figure 5) that show long recovery times. However, cell death alone is insufficient to account for the loss of nitrification seen in exposed biofilms in this test.

4.3.3 Resuspended biofilms

Live/Dead results for resuspended biofilms exposed to Ag^+ in 3-hour batch experiments are shown in Figure 22. Corresponding inhibition data (excerpted from Figure 14b) are presented in Figure 23. The proportion of dead cells was high in all resuspended biofilm samples, ranging from 30-55% (Figure 22). These percentages are somewhat higher than the percentage of dead cells in intact control biofilms (15-20%), and far higher than control suspended cells (5-8%). While the overall percentage of dead cells is high in all resuspended biofilm samples, cells exposed to 0.05 ppm Ag^+ or 0.10 ppm Ag^+ do not show higher rates of cell death than controls in spite of experiencing 35% and 65% inhibition, respectively (Figure 23). This echoes trends seen with suspended cells and suggests that inhibition is enzyme-specific at these concentrations. Resuspended biofilms were exposed to much lower concentrations of Ag^+ than intact DFR biofilms, as well as shorter exposure times. It is possible that biofilm inhibition is initially enzyme-specific, leading to death with longer exposures or higher concentrations. Insufficient biofilm was available to test higher Ag^+ exposures on resuspended biofilms.

The Live/Dead results for intact and resuspended biofilms are less clearly delineated than those for suspended cells, as can be seen by comparing gating data from Figure 33 (DFR biofilms) and Figure 34 (resuspended biofilms) with data from

Figure 32 (suspended cells) (Appendix). Live/Dead staining for the intact and resuspended biofilm samples may have been complicated by interference from extracellular DNA or other macromolecules found in EPS.

4.3.4 Summary

Suspended cells of *N. europaea* can tolerate low concentrations (up to 0.10 ppm) of Ag^+ for up to 3 hours with minimal loss of cell membrane integrity, even as nitrification activity is severely inhibited. At higher concentrations, the percentage of dead cells rises rapidly. Cell death increases with increasing concentrations of Ag^+, exceeding 90% at 0.20 ppm. At low Ag^+ concentrations, nitrification inhibition of suspended cells is mostly due to factors other than cell death, most likely inhibition of the AMO enzyme. Intact DFR biofilms exposed to 1.5 ppm Ag^+ showed high rates of cell death corresponding with high inhibition, but comparisons to suspended cells are complicated by the significantly higher Ag^+ concentration and longer exposure period in the DFR biofilm experiment. Results indicate that cell death may have been partially responsible for the loss of nitrifying activity in intact biofilms. Like suspended cells, resuspended biofilms experienced no significant increase in cell death after 3 hours of exposure to low concentrations of Ag^+ (up to 0.10 ppm). This suggests that nitrification inhibition of both suspended cells and biofilms is initially due to enzymatic inhibition at low concentrations, leading to cell death with longer exposures; higher concentrations cause more rapid cell death.

4.4 Silver uptake/titration analysis

Suspended cells and resuspended biofilms were titrated into a solution containing Ag^+ in order to measure how much Ag^+ could be adsorbed by biomass, and to

determine whether a difference existed between suspended cell and biofilm sorption. Figure 24 shows the amount of silver remaining in a 25 mL solution of 10 ppm Ag^+ in 2.5 mM $(NH_4)_2SO_4$/30 mM HEPES as suspended cells or resuspended biofilms were titrated into solution. Biofilms and suspended cells of *N. europaea* appear to bind silver similarly on a protein basis. This procedure permitted independent calculation of silver-to-biomass binding.

A mass balance gives a maximum silver saturation of approximately 180 μg Ag/mg protein after approximately 0.83 mg of suspended cell protein is titrated, or ~160 μg Ag/mg protein after titration of ~1.4 mg of suspended cell protein. The concentration of bound silver in the resuspended biofilm (measured based on the final data point after titration of ~0.83 mg protein) is 180 μg Ag/mg protein. These numbers are 30-150% higher than the highest measurements for silver bound to intact DFR biofilms (~120 μg Ag/mg protein for 1.5 ppm AgNP treatments, ~100 μg Ag/mg protein for 0.5 ppm Ag^+ (mature biofilm) treatments, and ~70 μg Ag/mg protein for 0.5 ppm Ag^+ (standard biofilm) treatments, as seen in Figure 7). However, comparisons are difficult as very different approaches were taken in making these measurements. If the methods were directly comparable they indicate that none of the biofilms in DFR tests became fully saturated with Ag^+.

The similarity in suspended cell and resuspended biofilm titration curves suggests that proteins of *N. europaea*, and not polysaccharides or other polymers associated with EPS, are responsible for binding Ag^+. This agrees with the results of previous titrations involving *N. europaea*, BSA, and alginate (Ostermeyer et al., 2013), which found that free Ag^+ decreased with increasing *N. europaea* cell protein or increasing BSA, but not with increasing alginate. The lack of Ag^+ binding by EPS supports the findings in Section 4.2.1 that found no protection from inhibition in resuspended biofilms. If biofilm protection from inhibition resulted from binding of Ag^+ to EPS, then some residual protection would be expected in resuspended biofilms. However, no such effect was observed.

4.5 Comparison to other biofilm studies with Ag^+ and AgNP

Inhibition

This study confirmed previous findings (Bjarnsholt et al., 2007; Giska, 2013) that substantially higher concentrations of Ag^+ are required to inhibit biofilms compared to suspended cells (Figure 1, Figure 14). None of the *N. europaea* biofilms were completely inhibited after 48 hours of exposure to up to 1.5 ppm Ag^+. Bjarnsholt et al. (2007) found that *Pseudomonas aeruginosa* biofilms were inhibited but not eradicated after 24 hours of exposure to 2.2 ppm Ag^+; the researchers estimated that concentrations required to eliminate biofilms would be in excess of 5 ppm Ag^+. AgNP-induced inhibition was minimal in this study, even after 48 hours of 1.5 ppm AgNP exposure (Figure 6). Wirth et al. (2012) found that biofilms of *Pseudomonas fluorescens* maintained some activity after 18 hours of exposure to AgNP at concentrations up to 100 ppm.

AgNP sorption

Standard biofilms of *N. europeaea* adsorbed between 2.4% and 13.9% of the mass of Ag^+ to which they were exposed after 48 hours, and between 6.6% and 14.8% of AgNP (Table 2). This range is slightly higher than that measured by Fabrega et al. (2009), who found that a maximum of 10% of AgNP mass was retained by *Pseudomonas putida* biofilms after 24 hours of exposure. The current study found markedly higher adsorption by mature *N. europaea* biofilms, however, with approximately 50% of influent Ag^+ adsorbed. Due to the slow growth of *N. europaea*, standard biofilms in this study were grown for a minimum of 3 weeks (mature biofilms, 8 weeks), compared to the 3 days in Fabrega's study.

Ag^+ titration tests showed that *N. europaea* biofilms adsorbed Ag^+ on the same protein basis as suspended cells, indicating that EPS does not play an important role in binding Ag^+ (Figure 24). It was unclear from these results whether EPS might

interact differently with AgNP. Previous work suggests that EPS does not act as a physical barrier to AgNP transport. Gaidhani et al. (2013) studied a range of bacterial species and found that AgNP were able to penetrate thick layers of biofilms without becoming adsorbed to EPS. Fabrega et al. (2009) found AgNP located within the EPS matrix of *P. putida* biofilms as well as attached to bacterial cells.

Sloughing

Results from this study suggest that Ag^+ and AgNP may induce sloughing in *N. europaea* biofilms, contributing to loss of nitrifying activity. AgNP-induced biofilm sloughing has been documented in previous work with other bacterial species. Fabrega et al. (2009) reported an 8% loss of biomass in 3-day-old *P. putida* biofilms exposed to 0.2-2 ppm citrate-capped AgNP in a flow cell reactor. This sloughing was greatest during the first 4 hours of AgNP exposure. Kalishwaralal et al. (2010) found that biosynthesized AgNP induced rapid detachment of 24-hour-old *P. aeruginosa* and *S. epidermidis* biofilm cells grown in microtiter plate wells. At 50 nM, 50% detachment was seen after 2 hours, and at 100 nM, 95-98% detachment was observed.

Viability

Live/Dead staining of cells detached from intact biofilms after exposure to 1.5 ppm Ag^+ found a higher percentage of cell death in intact biofilms exposed to Ag^+ than in controls (Figure 20). Resuspended biofilms exposed to 0.5 ppm – 0.10 ppm Ag^+ showed no significant difference in cell death compared to controls (Figure 22), consistent with these low concentrations in suspended cells (Figure 18). No Live/Dead staining was performed on cells exposed to AgNP. Previous studies differ on whether AgNP affects the viability of biofilm cells. Kalishwaralal et al. (2010) found that AgNP concentration affected cell viability in *P. aeruginosa* and *S. epidermidis* biofilms. Biofilms exposed to 50 nM AgNP continued to grow, but slowed EPS production by 90%. Biofilms exposed to 100 nM AgNP ceased growth.

Fabrega et al. (2009) monitored *P. putida* biofilm cell viability using the Live/Dead *Bac*Light staining kit (as in this study). Instead of harvesting biofilms for analysis , however, Fabrega used a confocal laser scanning microscope to study biofilms in situ and found that cell viability was independent of AgNP concentration in solution (the maximum AgNP concentration studied was 2 ppm). Wirth et al. (2012) used the Live/Dead *Bac*Light staining kit and measured fluorescence intensity of *P. fluorescens* biofilms in 96-well plates exposed to PVP-capped AgNP. Loss of viability was slight up to 10 ppm exposure; biofilms exposed to 100 ppm experienced a significant decrease in viability. As noted previously, some of the cell death observed in this study may have resulted from the resuspension of harvested biofilms prior to staining and flow cytometry. Measuring cell viability of intact biofilms, as done by Fabrega and Wirth, may yield different results from those obtained via flow cytometry. It is also possible that AgNP may affect viability to a lesser extent than Ag^{+}. Results may also differ significantly between species.

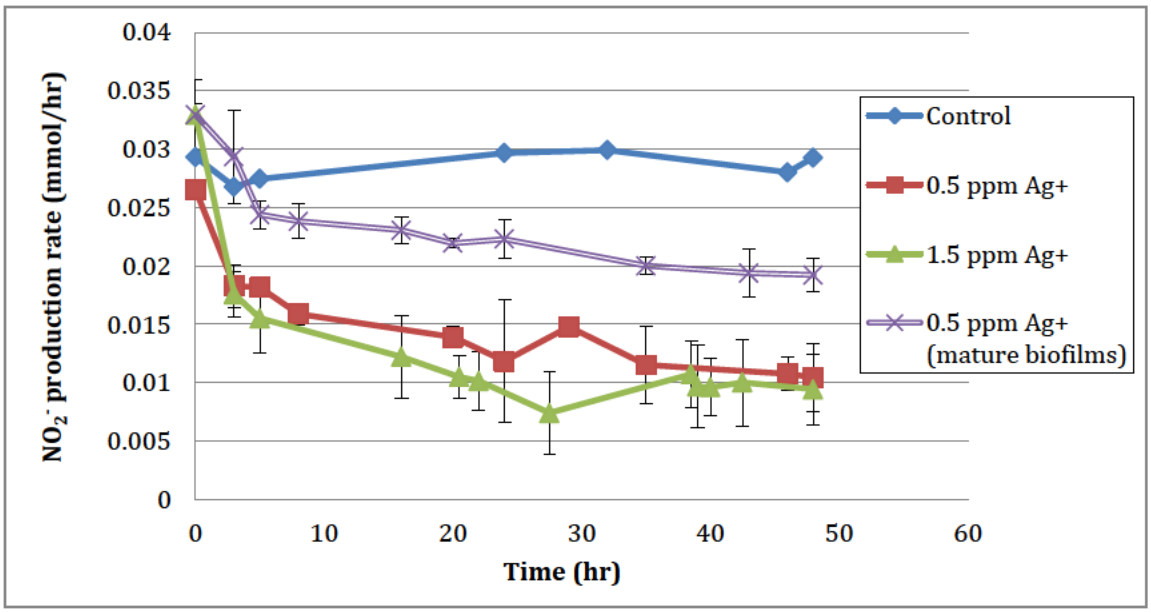

(a)

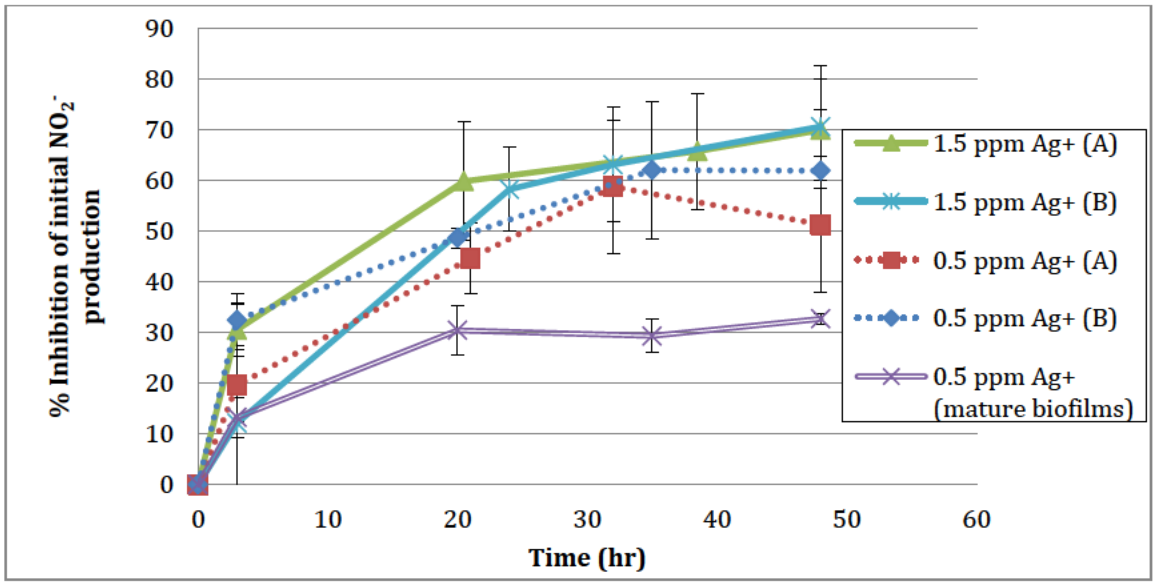

(b)

Figure 1. (a) Nitrite production rates of *N. europaea* biofilms during 48-hour Ag^+ exposure experiments. One control is shown for comparison; other controls showed the same constant activity. Lines (except for control) represent the average of two lanes (one experiment). In order to more clearly demonstrate trends, only one experiment is shown for each treatment condition. (b) Percent inhibition or loss of initial nitrification. Lines represent the average of two lanes (one experiment); all experiments are included. Error bars represent 95% confidence intervals.

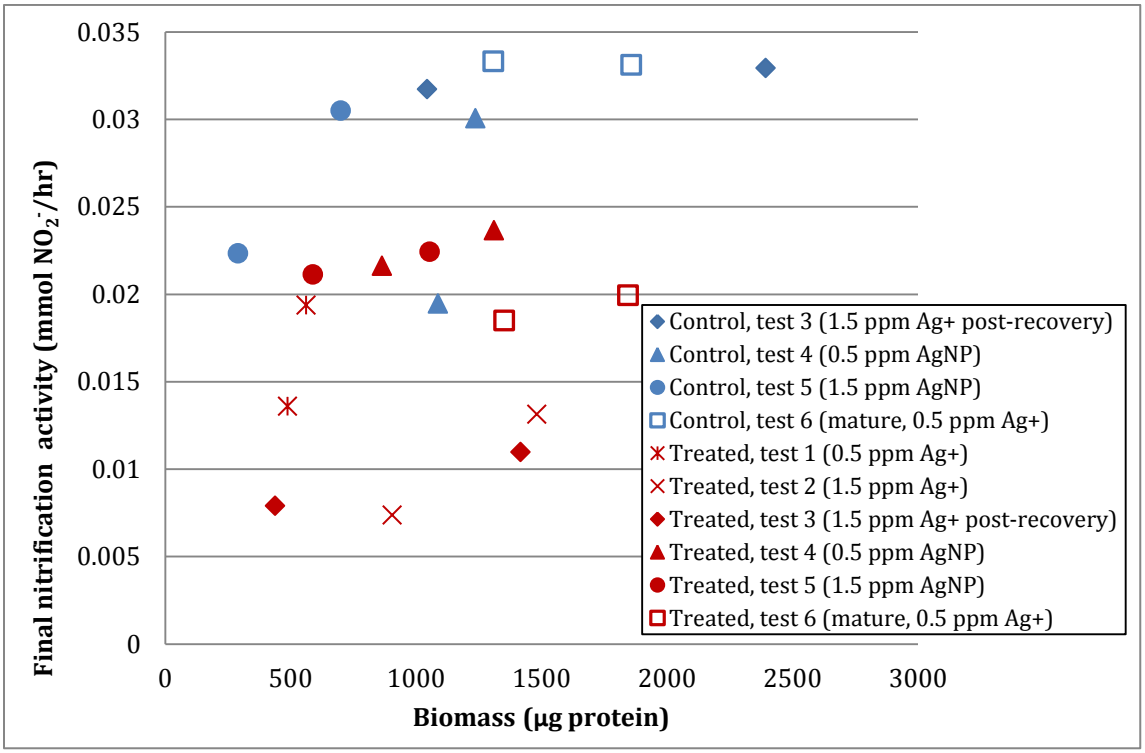

Figure 2. Final nitrification rates of biofilms versus harvested biomass. Control biofilms are shown in blue, and biofilms exposed to Ag^+ or AgNP are shown in red. Protein content was not measured for all control biofilms, as some were used for further experiments.

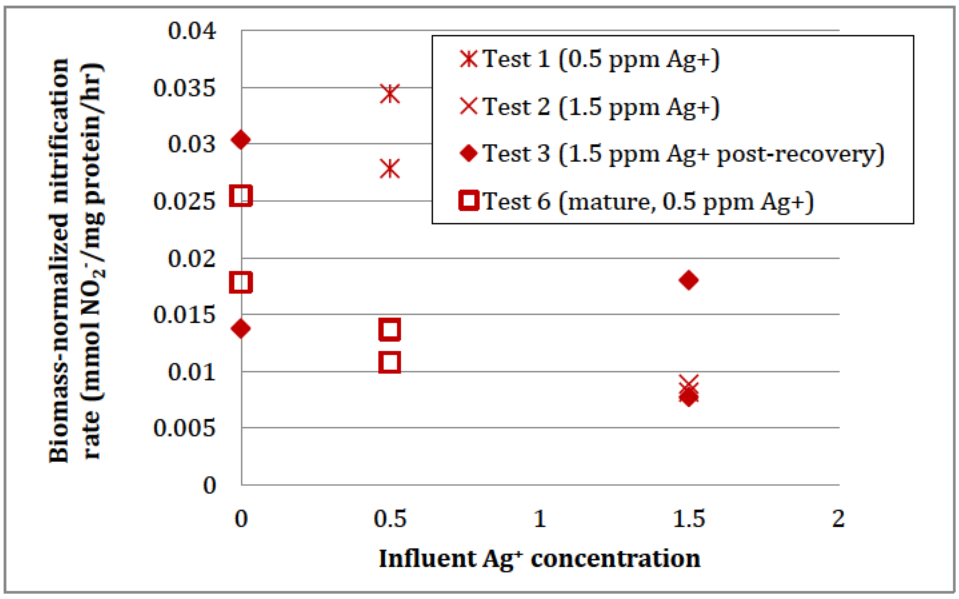

(a)

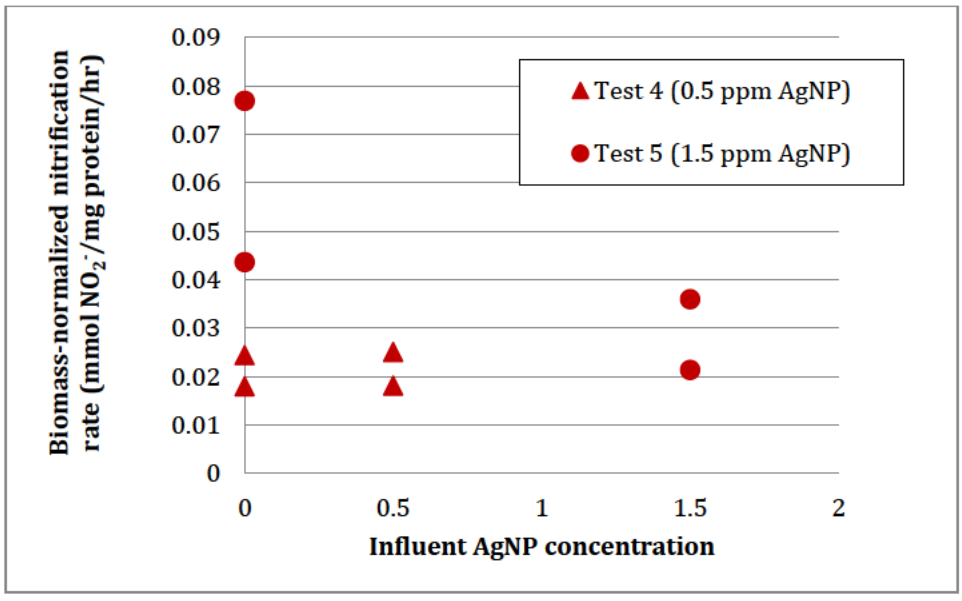

(b)

Figure 3. Final biomass-normalized nitrification rates versus influent Ag^+ (a) or AgNP (b) concentrations. Control data are not available for Test 1 or Test 2.

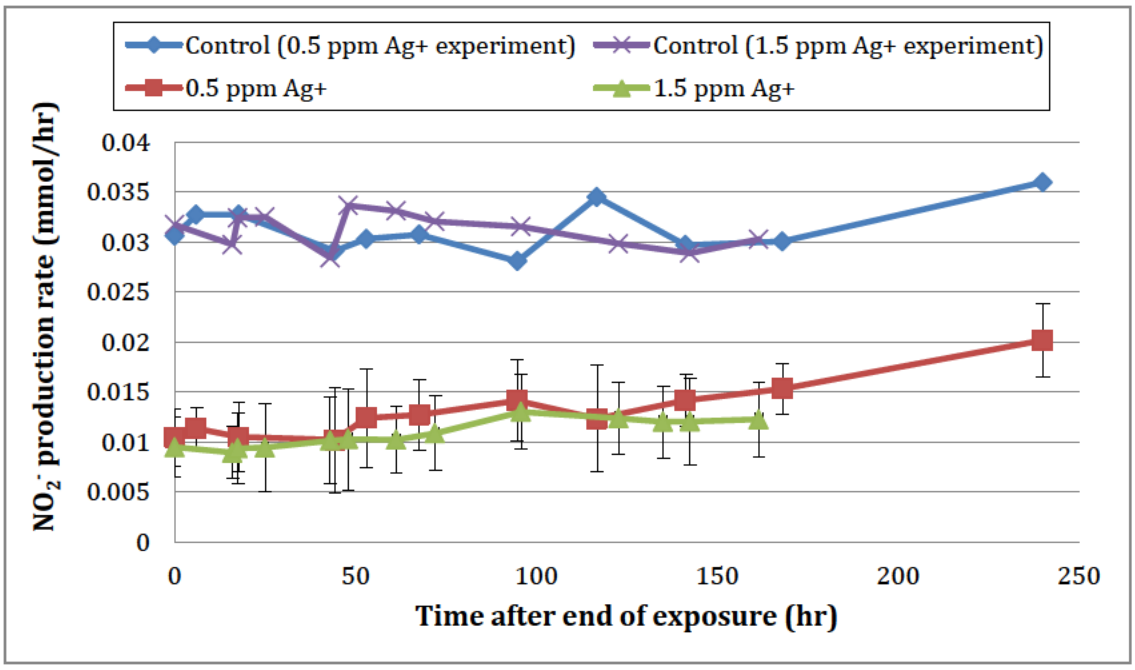

(a)

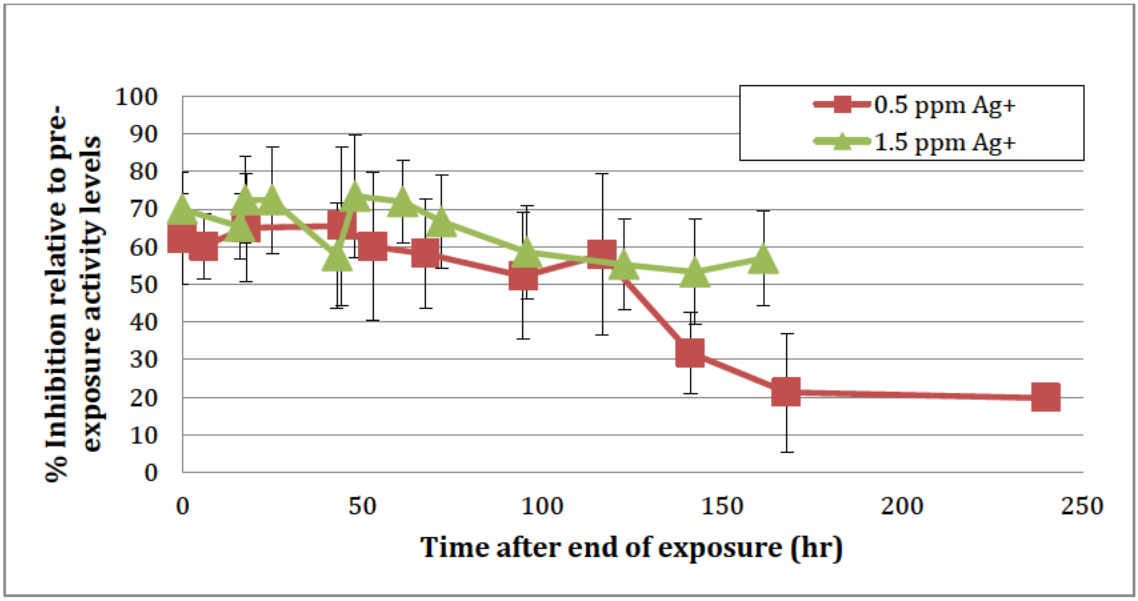

(b)

Figure 4. (a) Nitrite production and (b) percent nitrification inhibition (relative to pre-exposure activity levels) of Ag^+-exposed biofilms following end of exposure period. Percent inhibition was normalized to inhibition of controls in order to account for system-wide fluctuations. The 1.5 ppm Ag^+ test was stopped when no recovery was seen after one week. A media change immediately following the 240-hour sampling resulted in death of biofilms in the 0.5 ppm Ag^+ recovery test. Error bars represent 95% confidence intervals (two lanes).

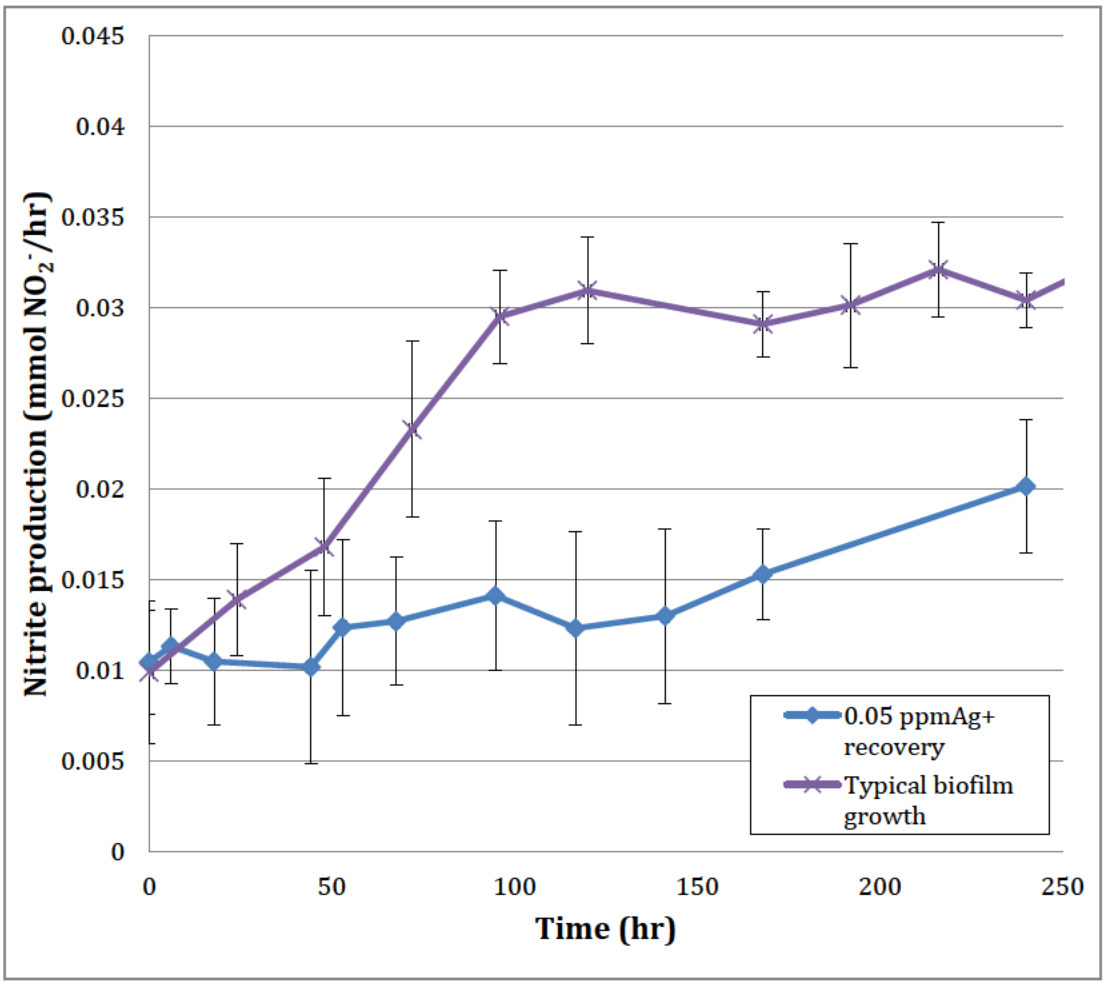

Figure 5. Increasing nitrite production during recovery of 0.5 ppm Ag^+-exposed biofilms (average of 2 lanes) versus during typical biofilm growth (average of 8 lanes from 2 separate DFRs) when both types of biofilms start from a baseline rate of ~0.01 mmol NO_2^-/hr. Error bars represent 95% confidence intervals. Regular (unexposed) biofilms increase their nitrification activity at a significantly higher rate than recovering Ag^+-exposed biofilms. The mean time for regular biofilms to achieve production rates of 0.01 mmol NO_2^-/hr (the starting point in this graph) is 168 hours after start of media flow.

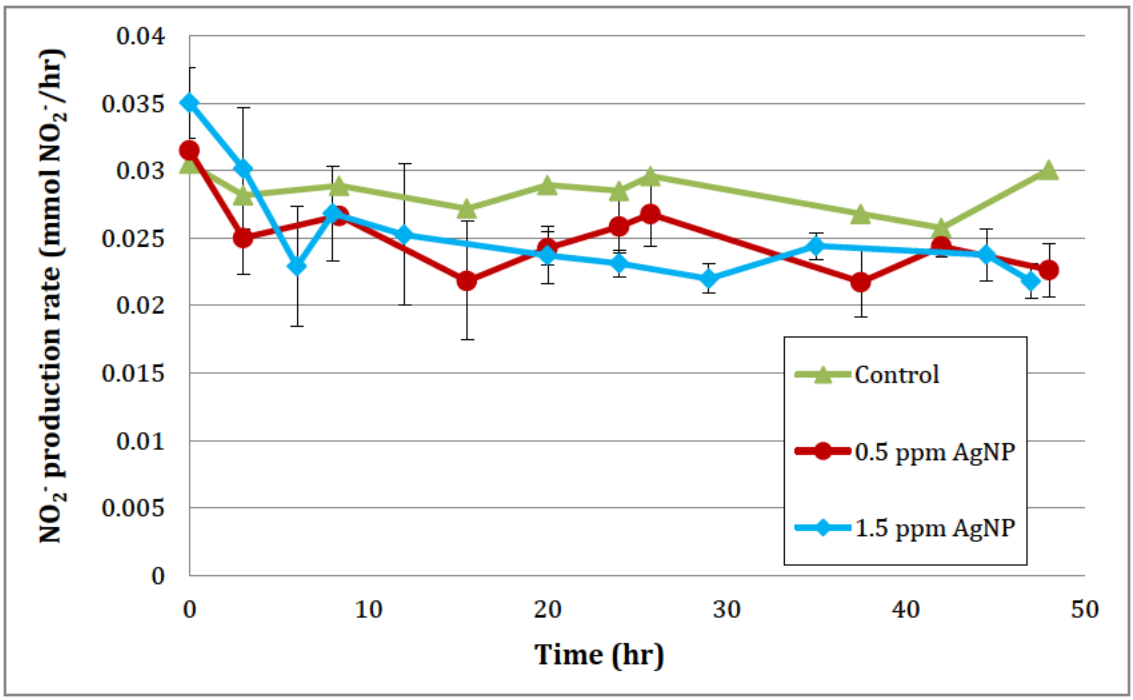

(a)

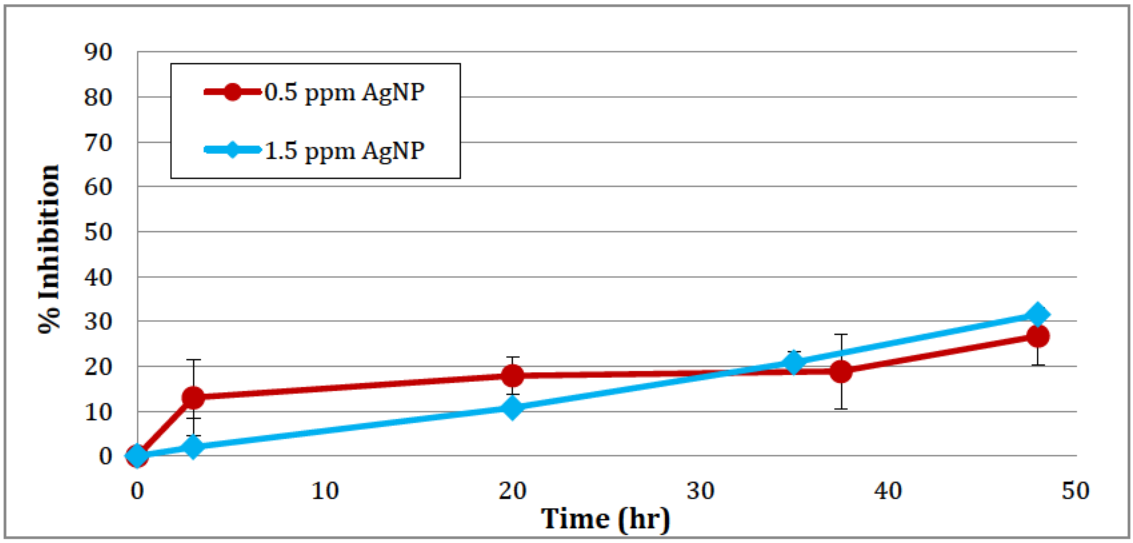

(b)

Figure 6. (a) Nitrite production rates of *N. europaea* biofilms during 48-hour silver nanoparticle exposure experiments. One control lane is shown for comparison; other controls had similarly constant rates. (b) Percent nitrification inhibition during exposure to AgNP. Lines represent average measurements of two lanes. Error bars represent 95% confidence intervals.

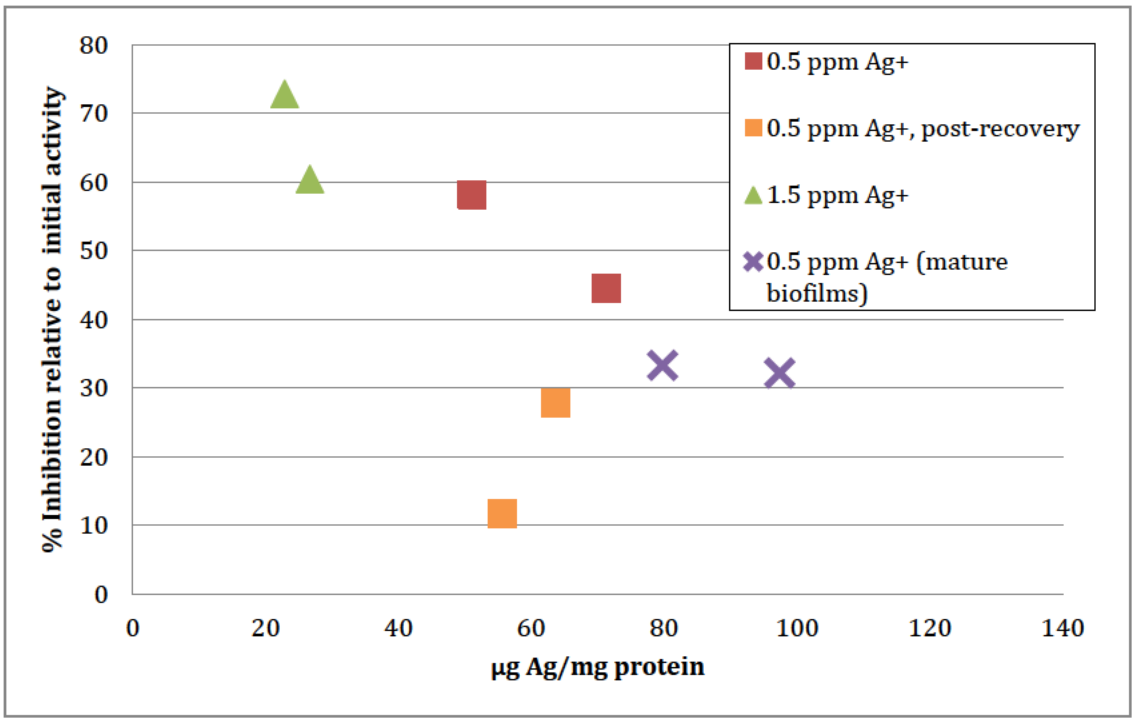

(a)

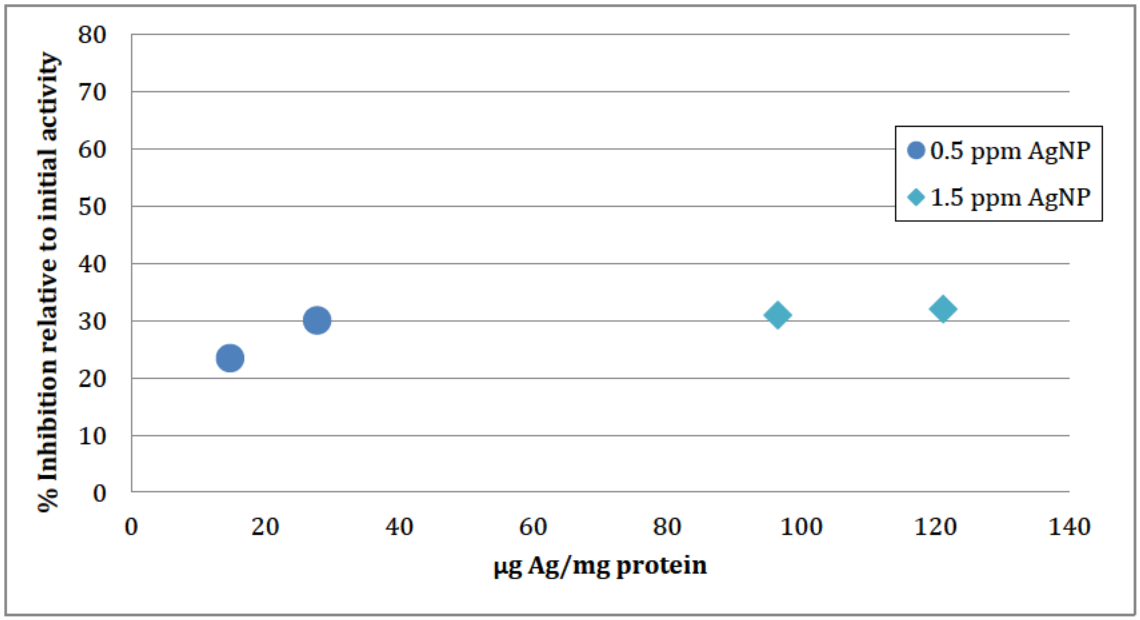

(b)

Figure 7. Percent inhibition after 48 hours versus bound silver in biofilms. (a) Ag^+ exposure experiments. (b) AgNP exposure experiments. Data for 1.5 ppm Ag^+ post-recovery biofilms are not included (samples decayed during prolonged storage).

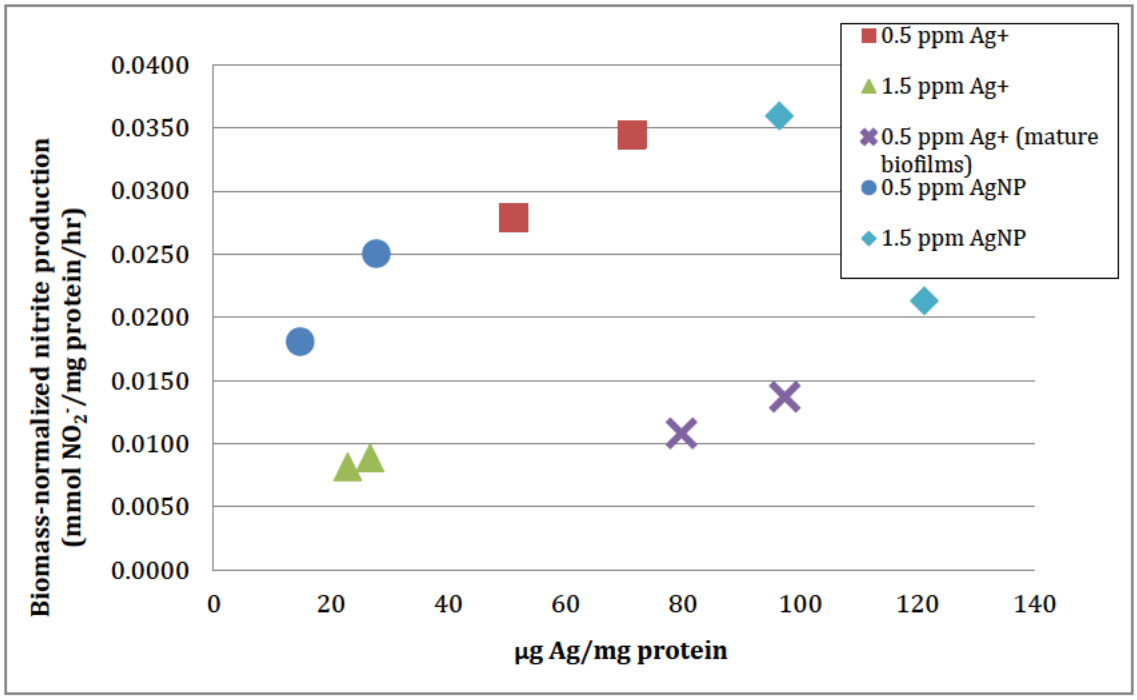

Figure 8. Biomass-normalized nitrite production rates versus bound silver in DFR biofilms.

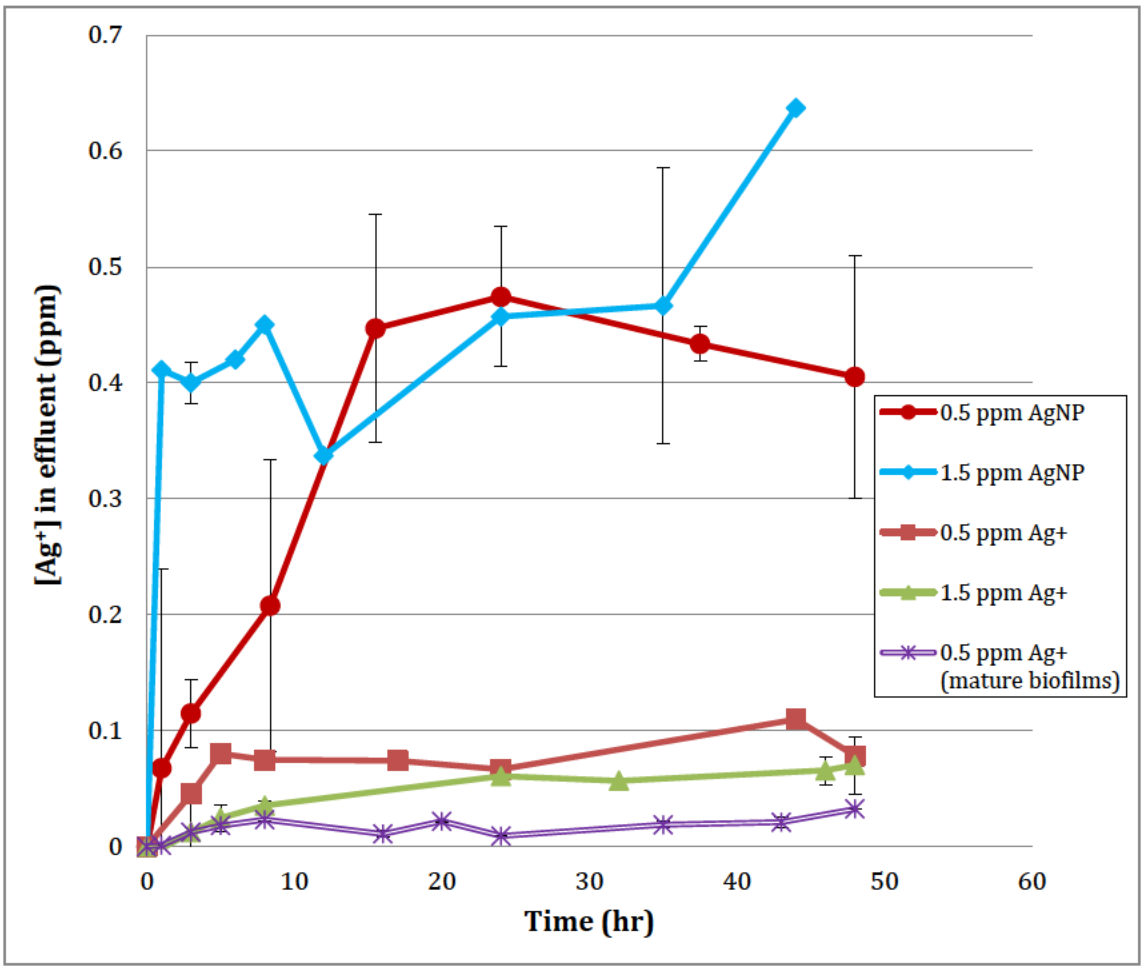

Figure 9. Concentrations of silver in DFR effluent during 48-hour Ag^+ and AgNP exposures. Error bars represent 95% confidence intervals. Only one sample was available (no replicates) for the 0.5 ppm Ag^+ effluent measurements. Other lines represent averages of two lanes.

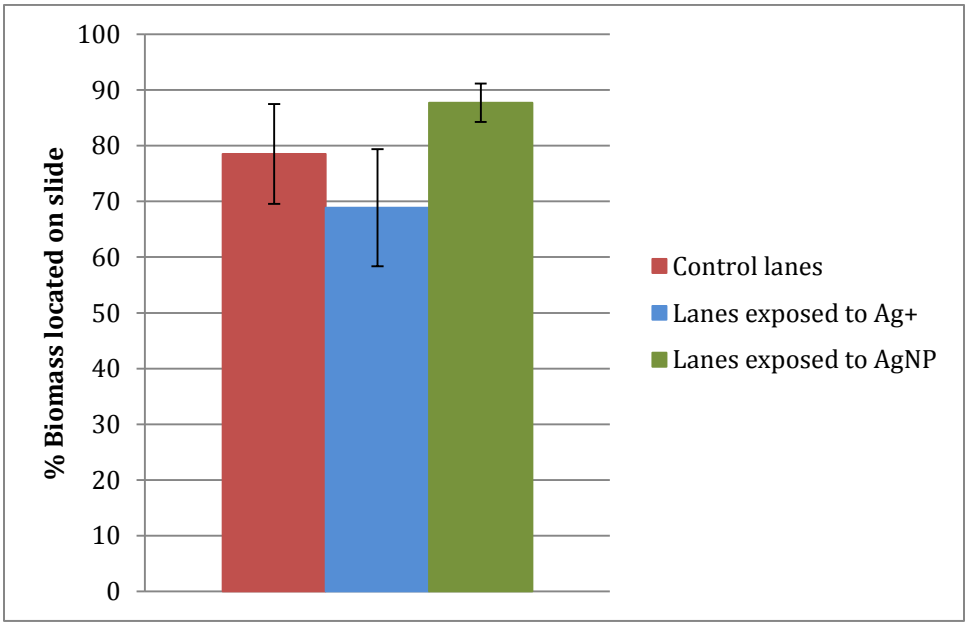

(a)

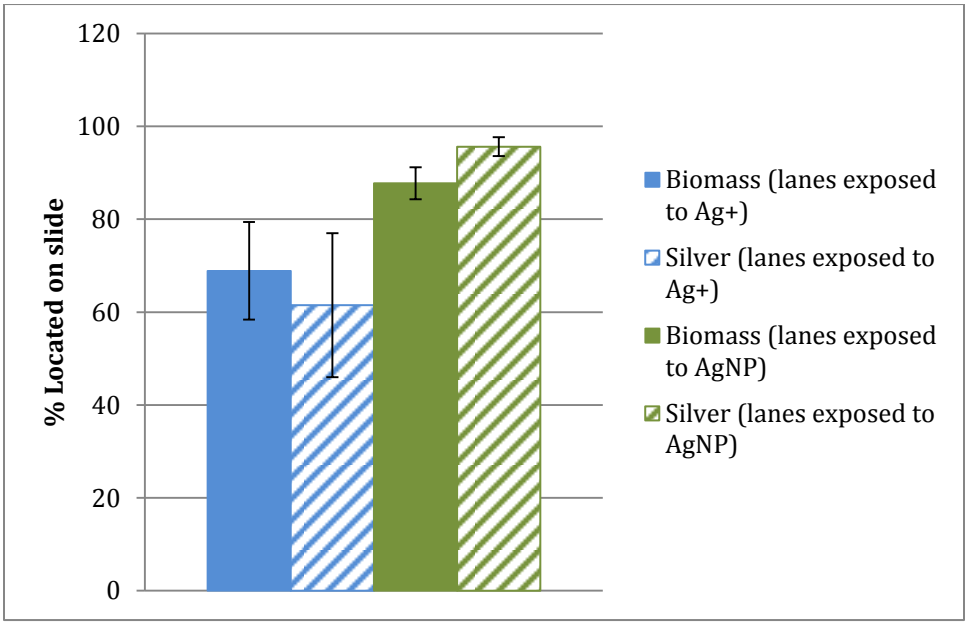

(b)

Figure 10. Spatial distributions of biomass and silver in control and exposed lanes. The percentage of biomass in each lane located on the glass slide (as opposed to the well) is shown in (a). Percentages of biomass and silver located on slides exposed to silver are shown in (b). Error bars represent 95% confidence intervals.

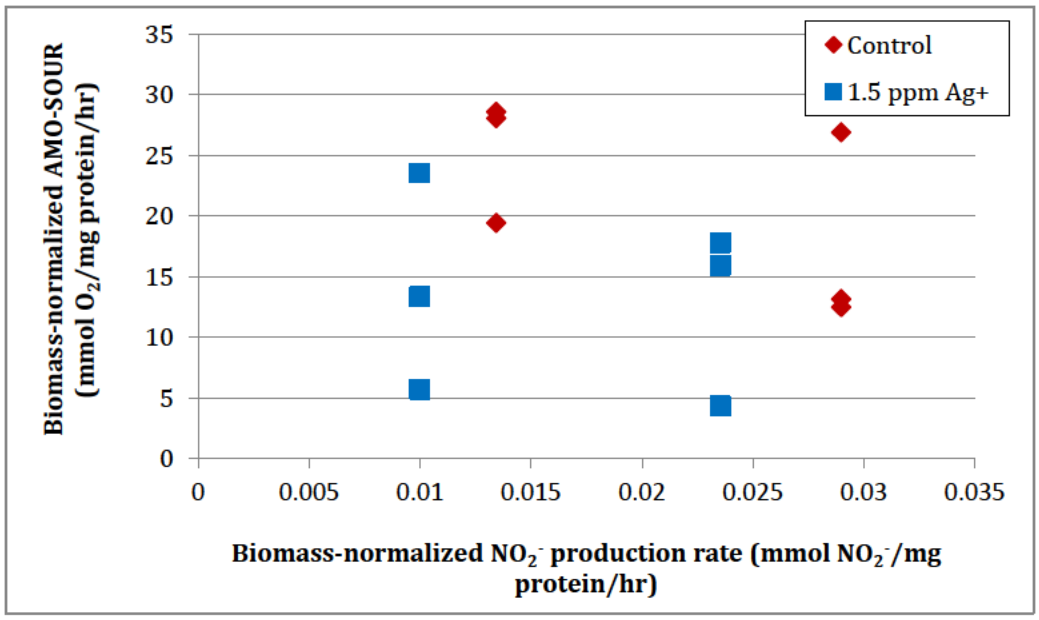

(a)

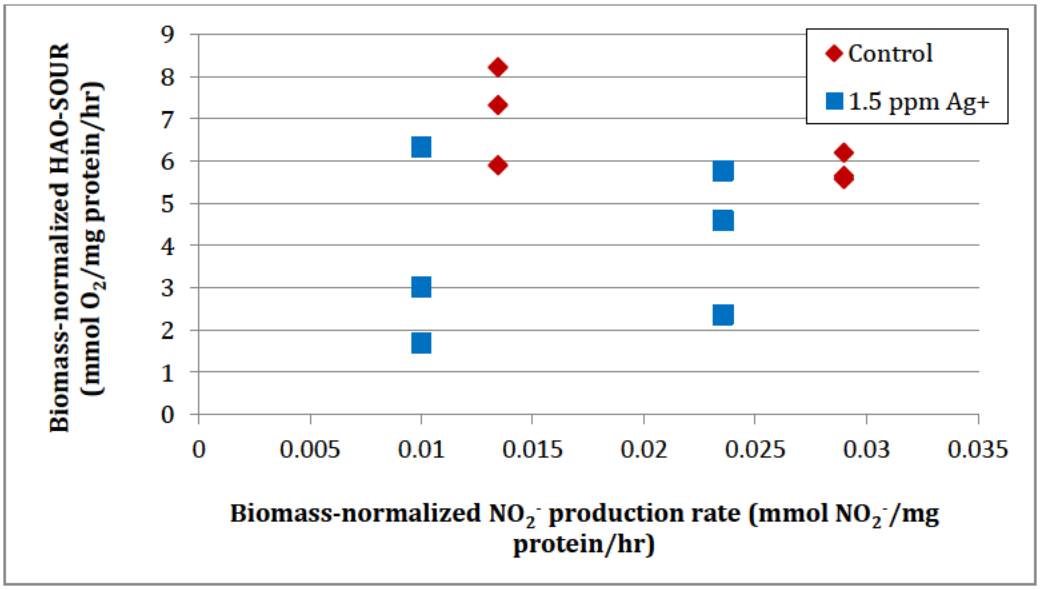

(b)

Figure 11. Biomass-normalized SOURs for (a) AMO and (b) HAO versus biomass-normalized NO_2^- production rates. All data points are from biofilms harvested following DFR Test 3 (1.5 ppm Ag^+ with recovery). 3 AMO-SOURs (one each for upper slide, lower slide, and well) and 3 HAO-SOURs (upper slide, lower slide, and well) were performed on biomass harvested from each lane. NO_2^- production rates were calculated from final effluent samples of intact biofilms taken immediately prior to harvesting (hence only one measured NO_2^- production rate per lane).

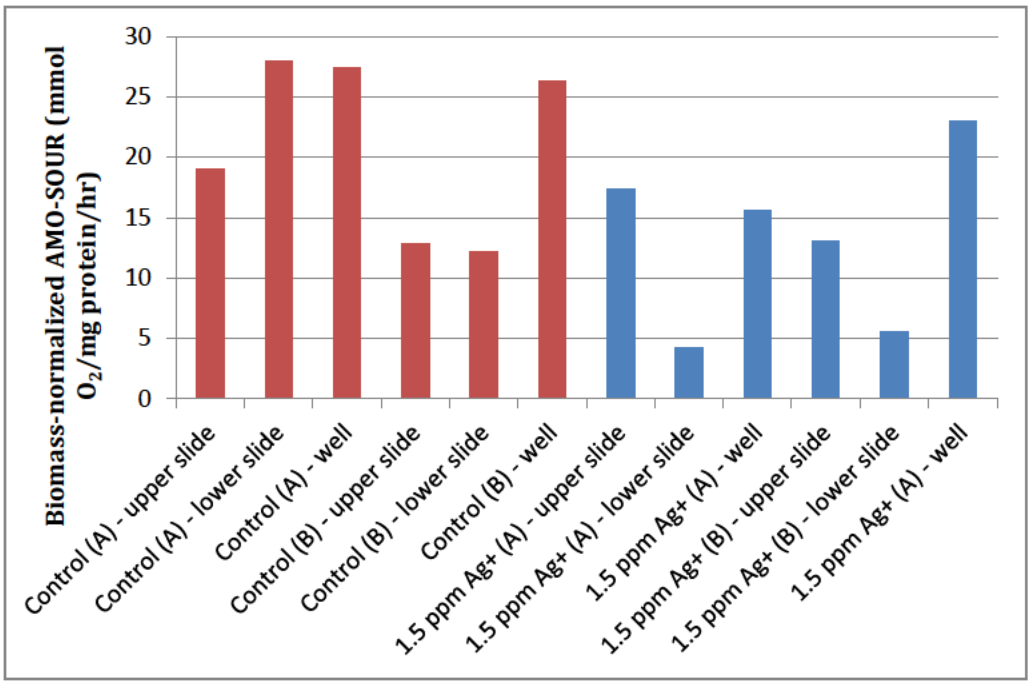

(a)

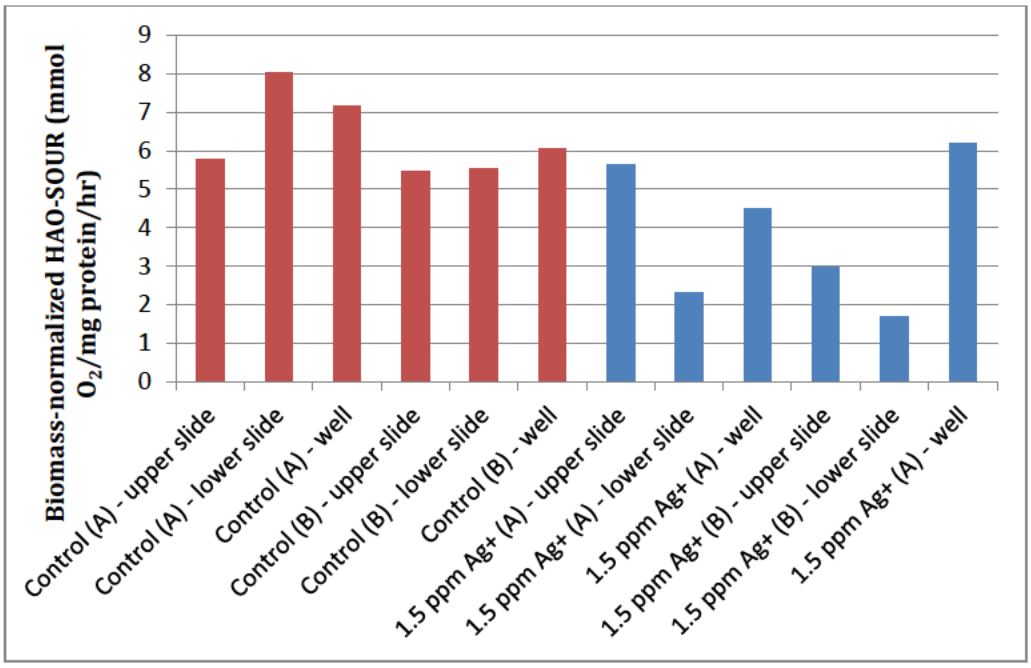

(b)

Figure 12. Biomass-normalized AMO-SOURs (a) and HAO-SOURs (b) for slide and well samples. Control samples are in red and treated samples are in blue. All measurements are from biofilms harvested after DFR Test 3 (1.5 ppm Ag^{+} with recovery).

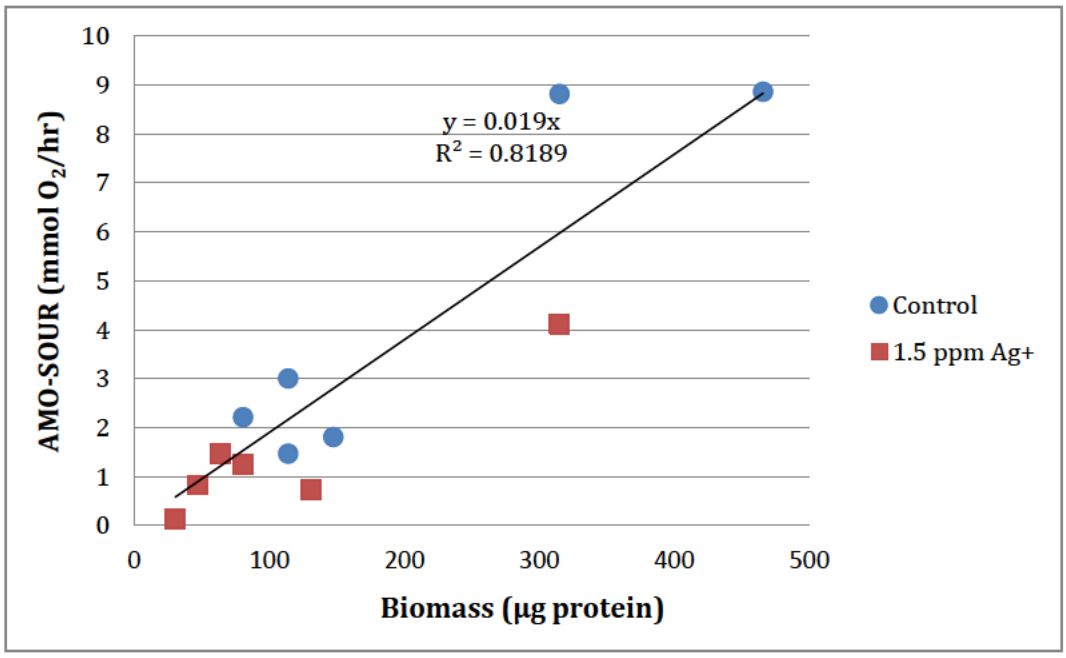

(a)

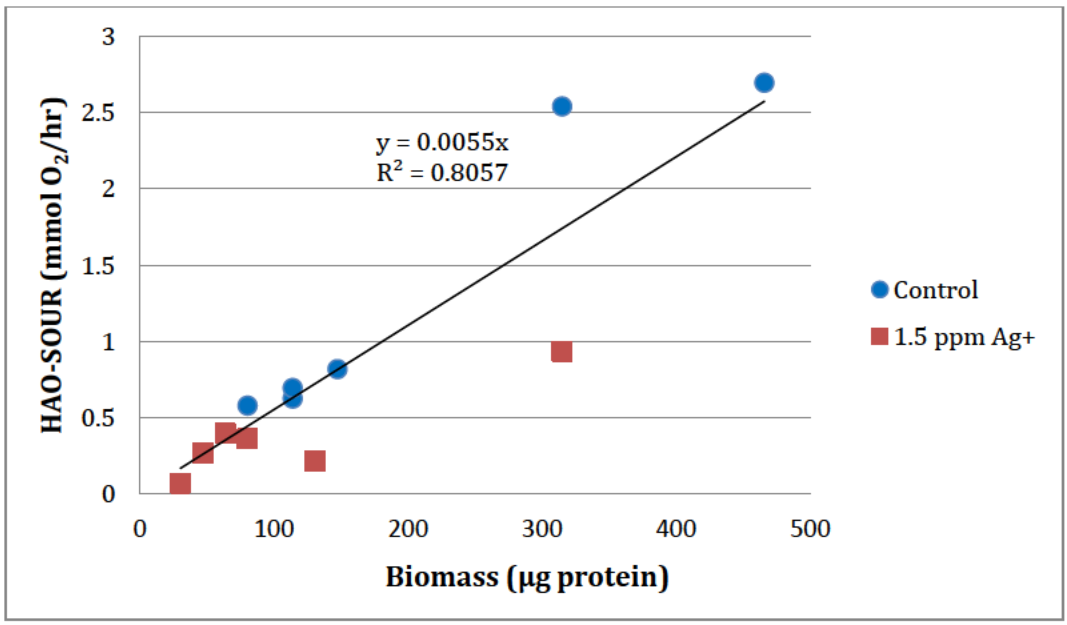

(b)

Figure 13. AMO-SOURs (a) and HAO-SOURs (b) graphed against protein content of samples. All samples are from biofilms harvested following DFR Test 3 (1.5 ppm Ag^+ inhibition with recovery).

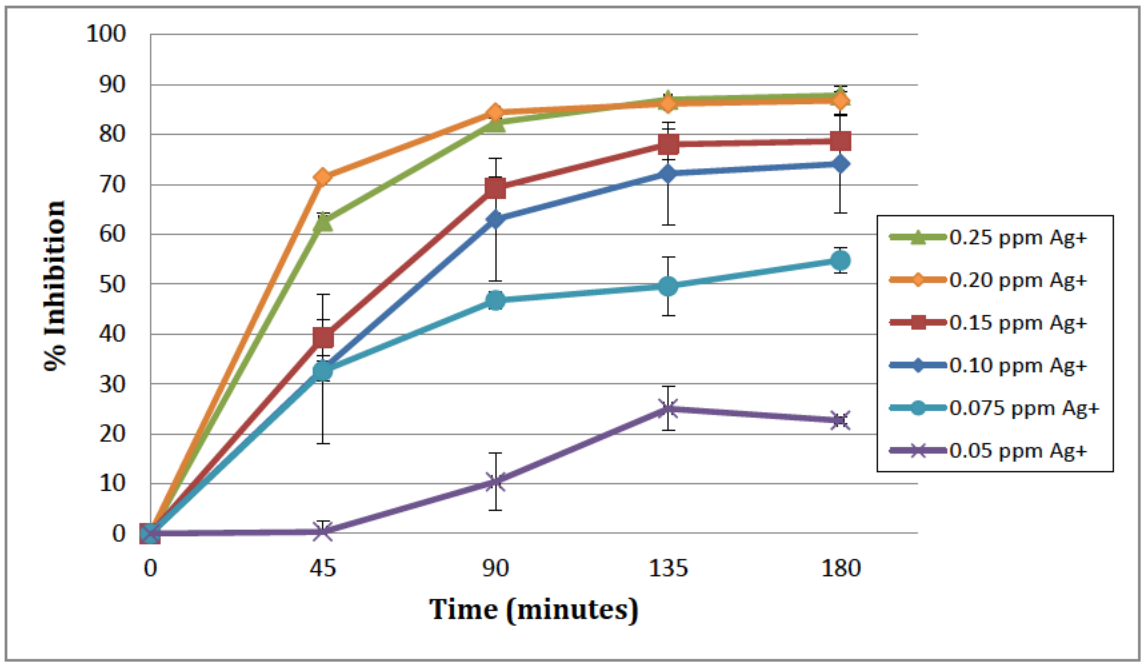

(a)

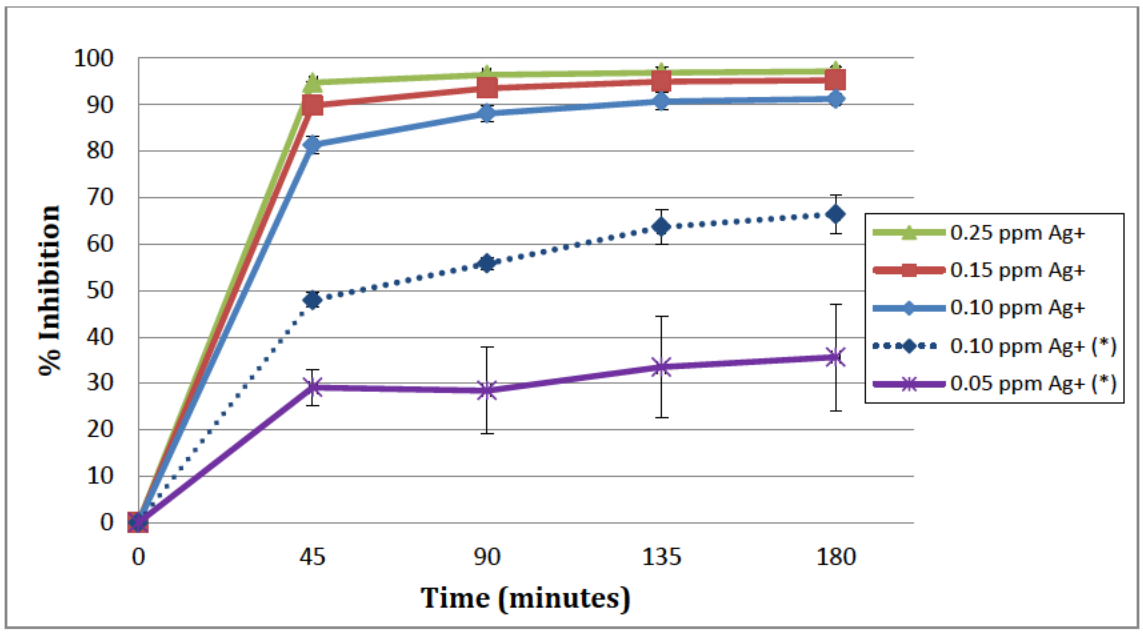

(b)

Figure 14. Nitrification inhibition of (a) suspended cells and (b) resuspended biofilms during 3-hour batch silver ion inhibition tests. Error bars represent 95% confidence intervals. The second set of resuspended biofilm experiments (denoted with an asterisk (*)) was performed with minimal agitation and washing of biofilm cells in order to minimize shearing and potential loss of EPS.

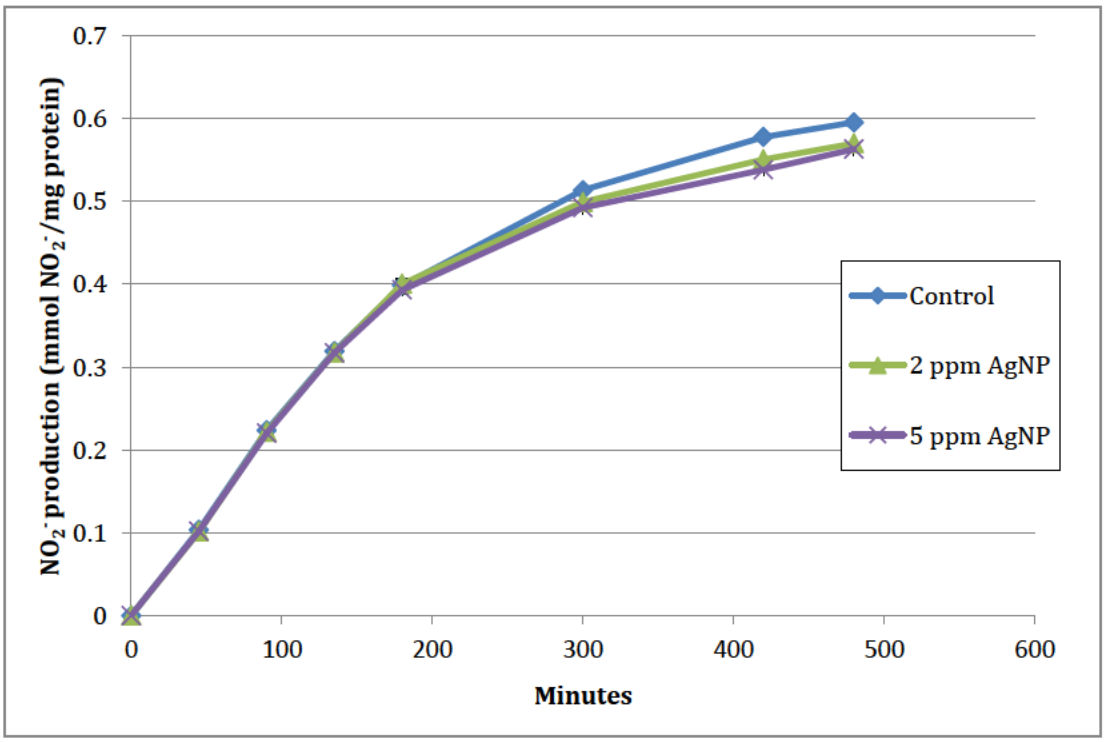

Figure 15. NO_2^- production by suspended cells in extended (8-hr) batch AgNP inhibition tests. Error bars (representing 95% confidence intervals) are present but not visible due to the high consistency of replicates.

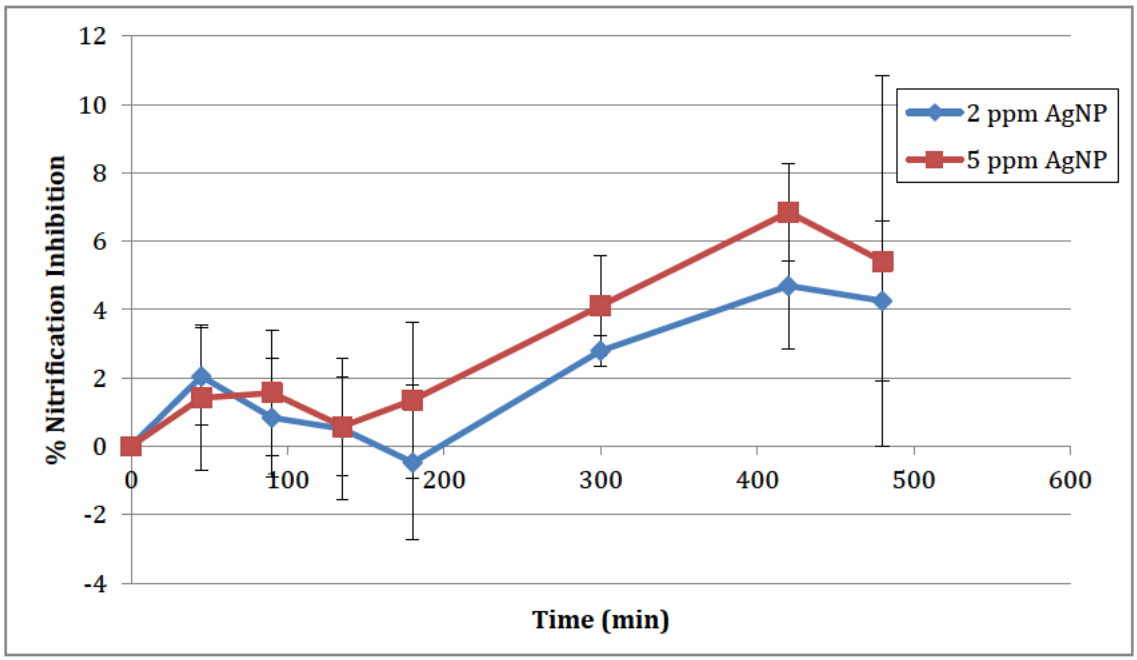

Figure 16. Inhibition of suspended cells exposed to AgNP over the course of 8-hour batch tests.

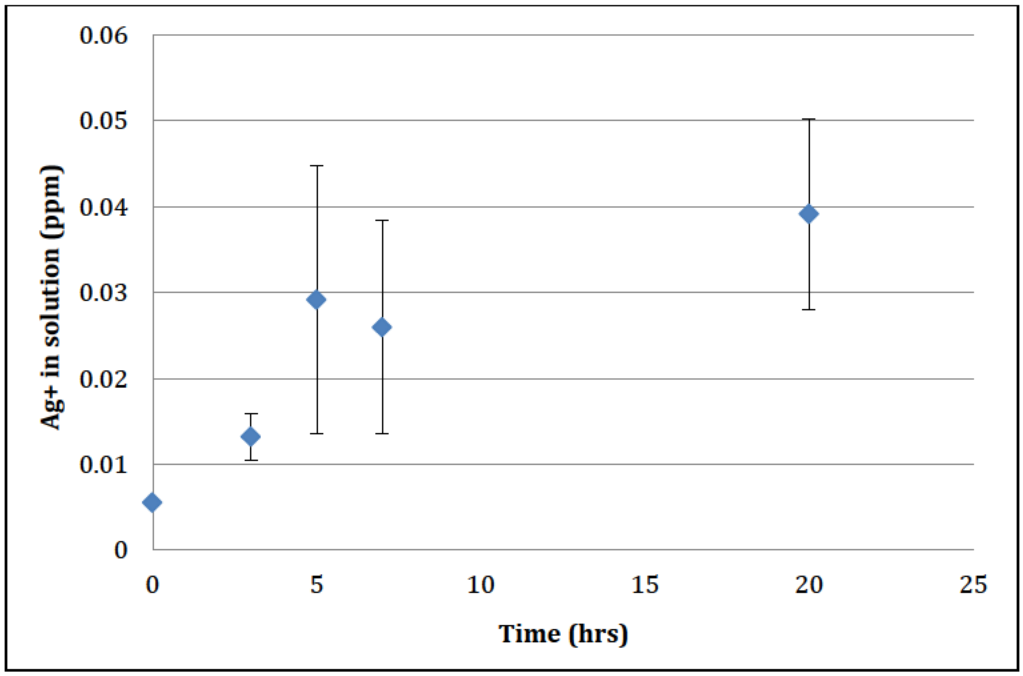

Figure 17. Free Ag^+ released into test media in bottles containing 2 ppm AgNP. Error bars represent 95% confidence intervals.

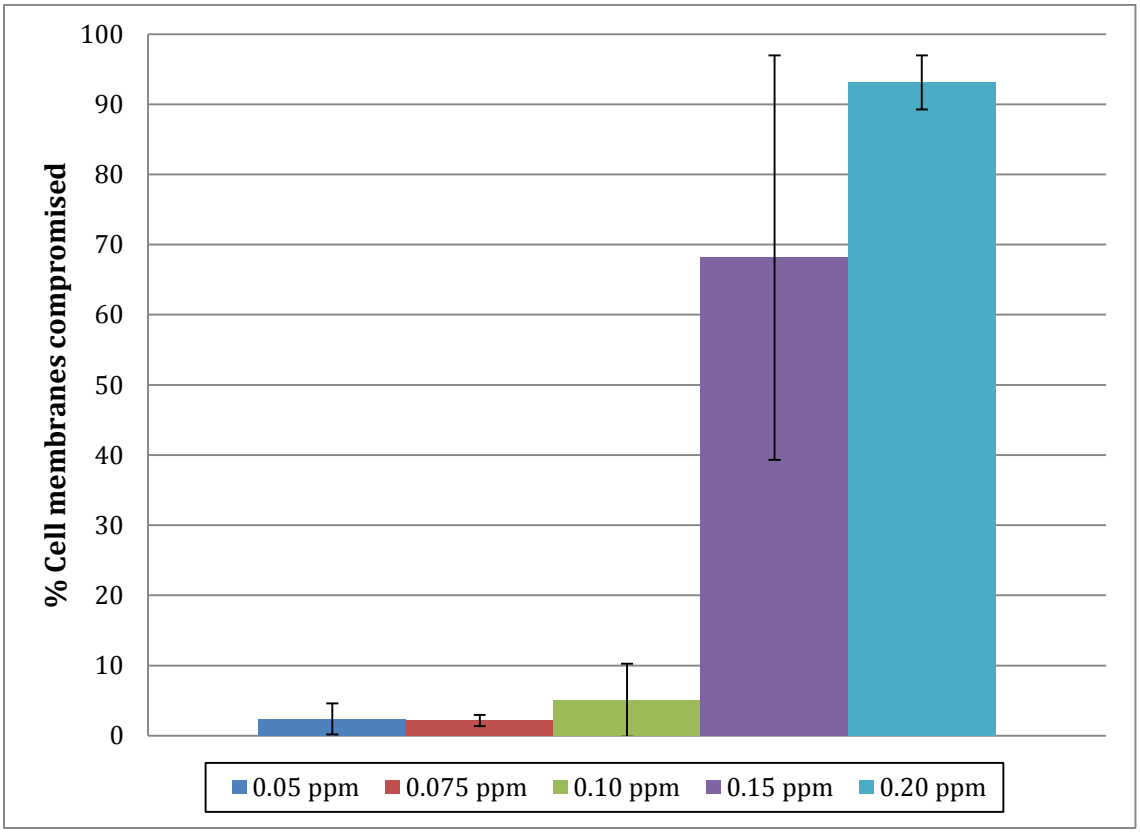

Figure 18. Percent of cell membranes compromised after 3-hour Ag^{+} batch inhibition tests on batch-grown suspended cells (compared to control bottles). Error bars represent 95% confidence intervals. Values are calculated by subtracting percentages of dead cells in control bottles. Dead cells in control bottles varied between batches of cells, typically ranging from 5-8%.

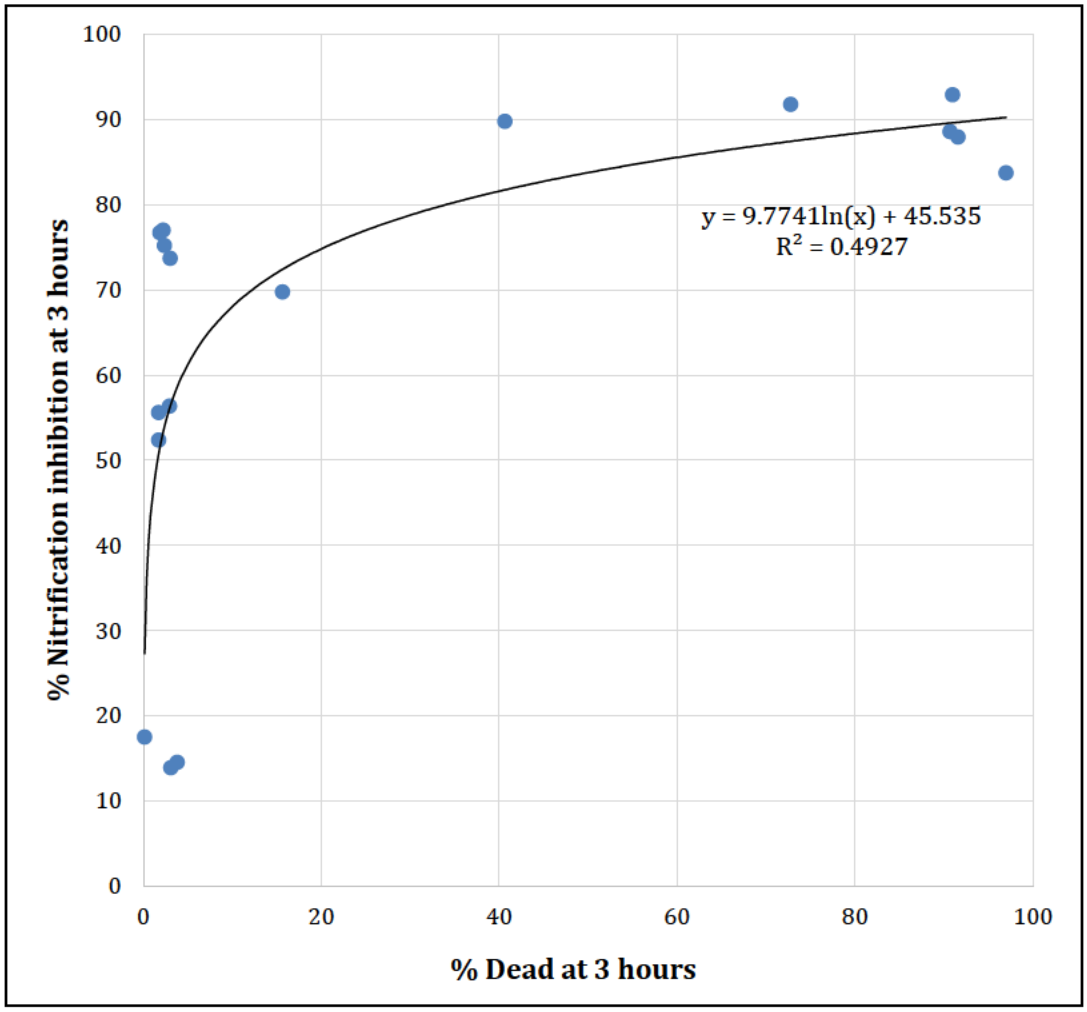

Figure 19. Percent nitrification inhibition of suspended cells after 3-hour batch exposures to Ag^{+}, graphed against the percentage of dead cells (defined as those with compromised membranes).

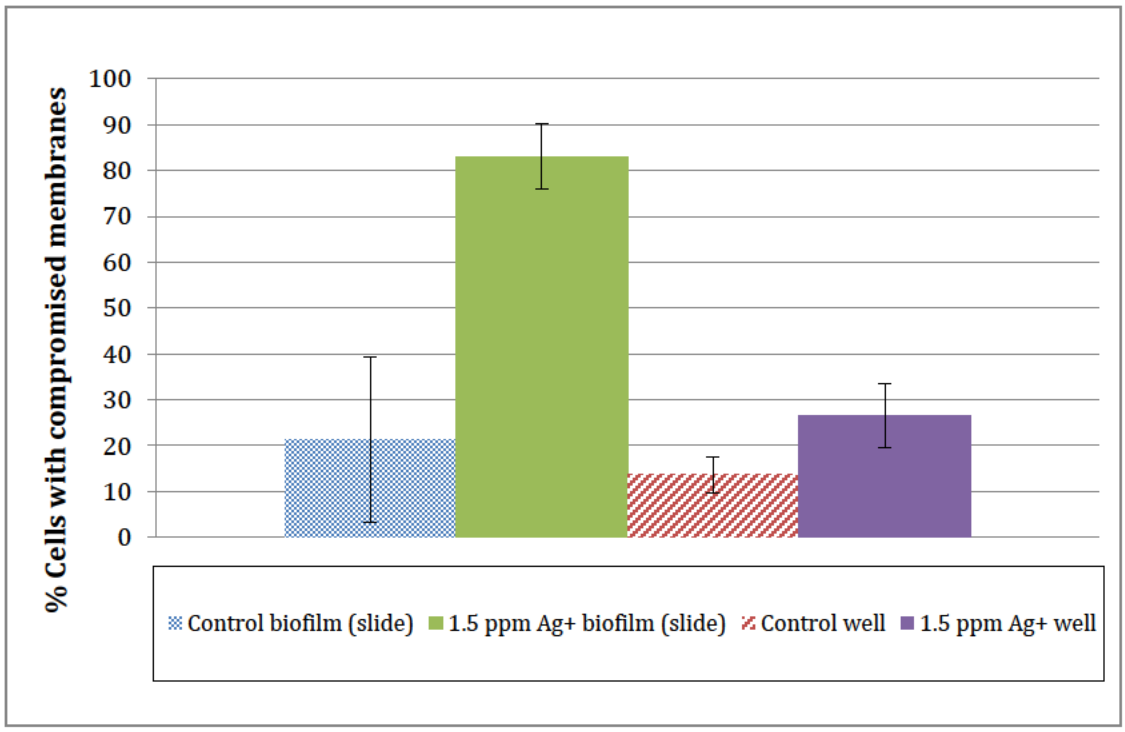

Figure 20. Percentage of dead cells in biofilms (cells attached to slides) and wells (downstream of slides) following a 48-hour exposure experiment using 1.5 ppm Ag^+. Error bars represent 95% confidence intervals. Inhibition data for this experiment are shown in Figure 1b and reproduced below.

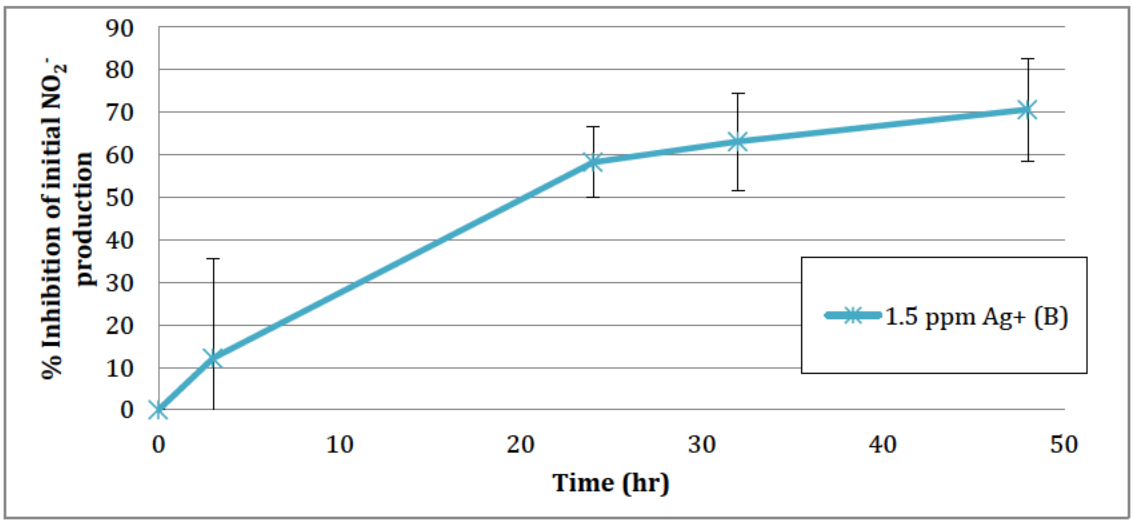

Figure 21. Inhibition versus time for intact biofilms exposed to 1.5 ppm Ag^+ (excerpted from Figure 1b). Biofilms averaged 70% inhibition after 48 hours, roughly equivalent to the inhibition seen in suspended cells exposed to 0.10 ppm Ag^+ in batch tests for 3 hours.

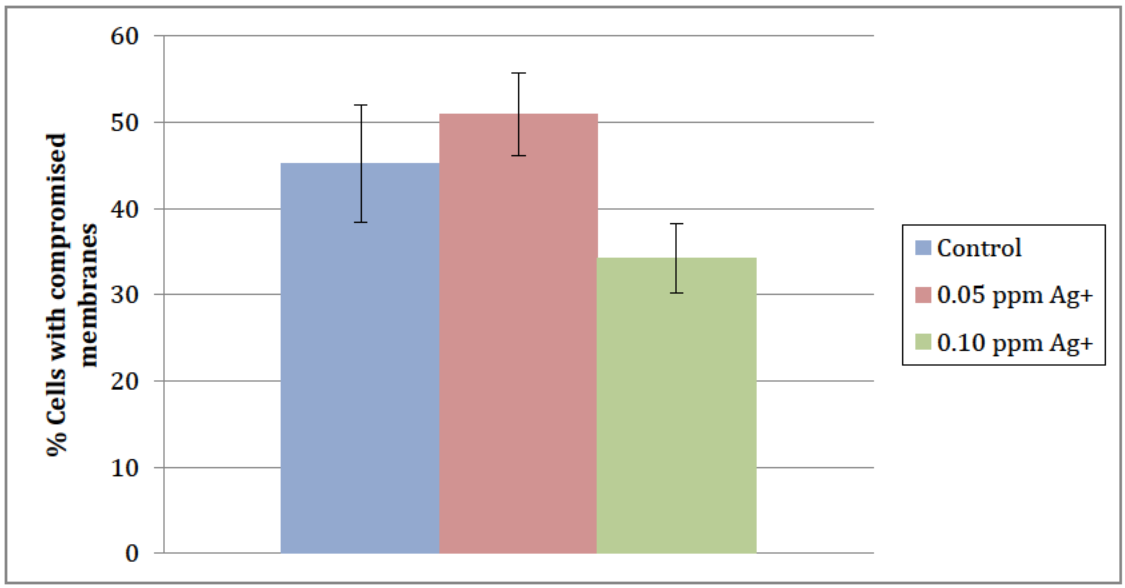

Figure 22. Percentage of dead cells in resuspended biofilms following 3-hour batch Ag^+ inhibition experiments. Error bars represent 95% confidence intervals (3 replicates, each sampled twice). Inhibition data for these experiments are shown in Figure 14b and reproduced below.

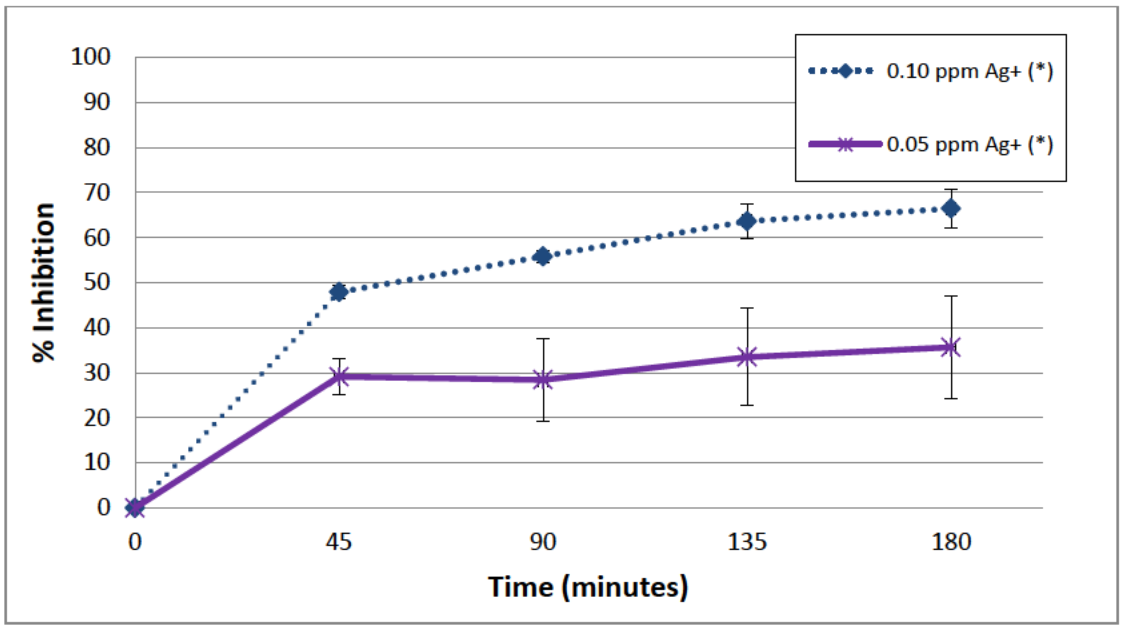

Figure 23. Inhibition data for 3-hour batch Ag^+ inhibition tests on resuspended biofilms corresponding to the Live/Dead results shown in Figure 22. These data are excerpted from Figure 14b.

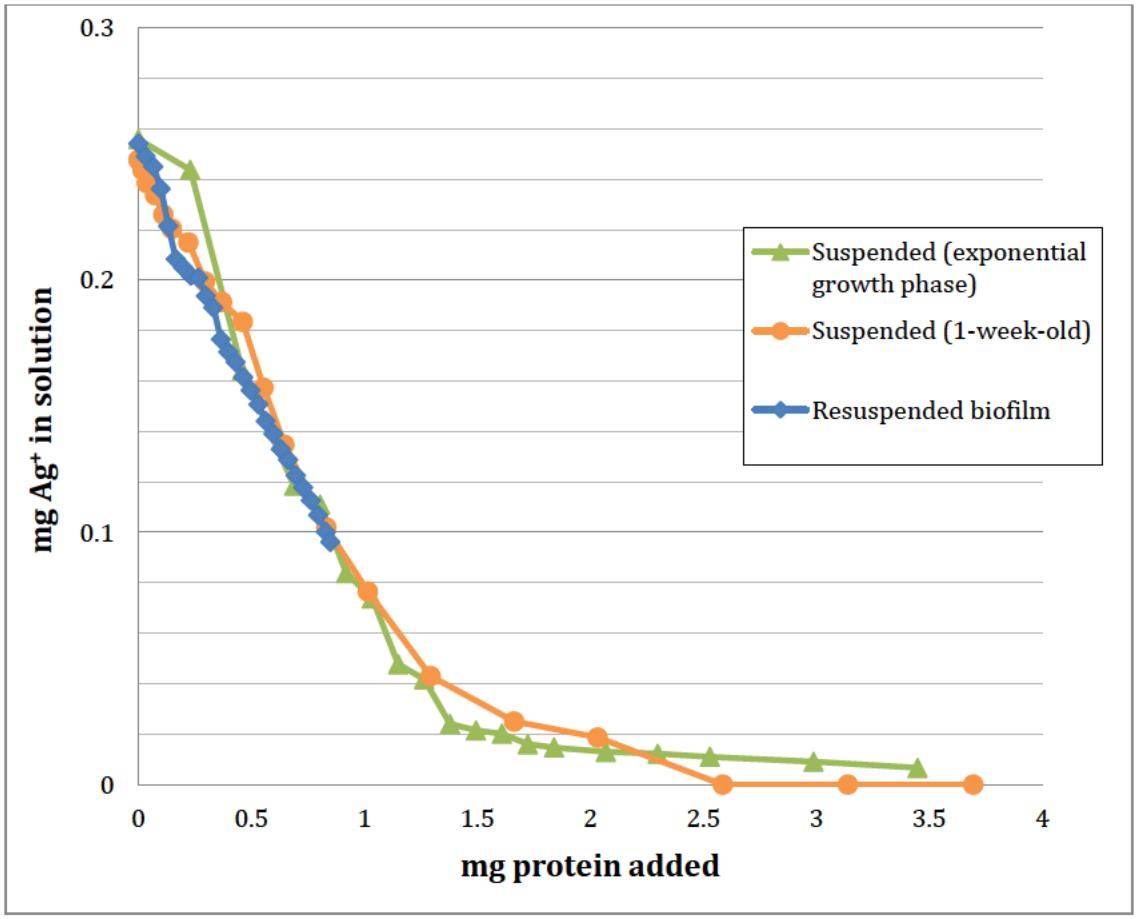

Figure 24. Ag^+ remaining in solution graphed against biomass titrated into solution. Insufficient biofilm was available to further extend the curve.

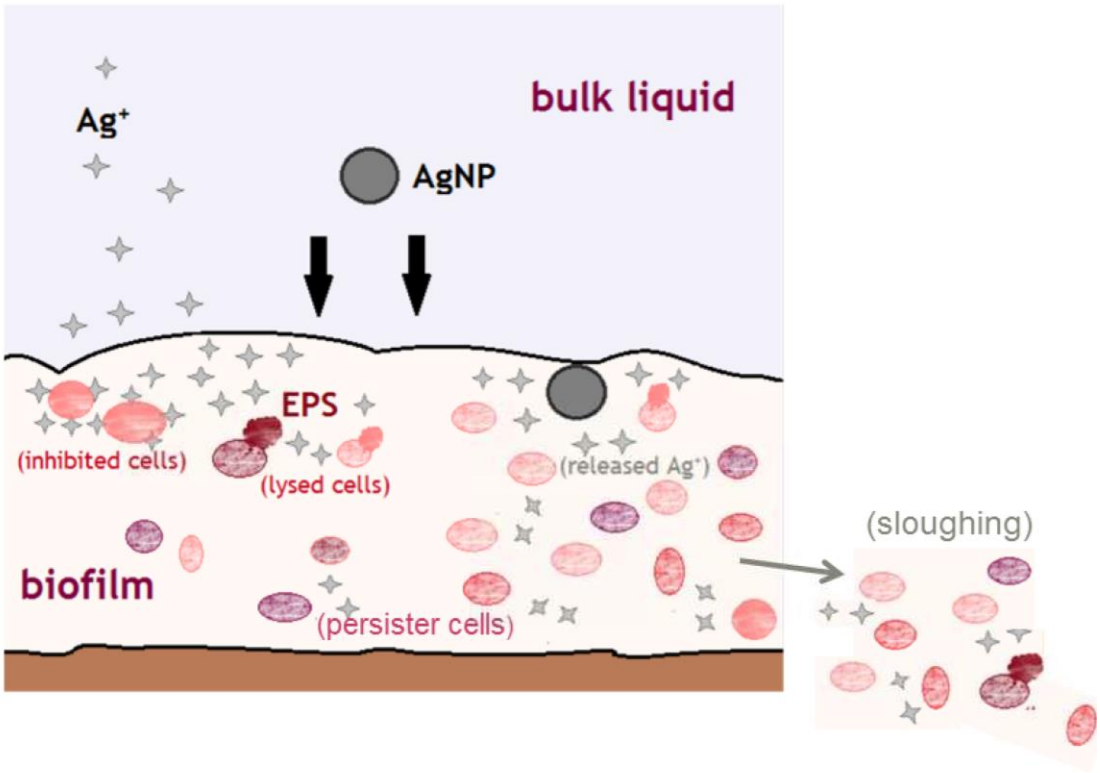

Figure 25. Conceptual model of *N. europaea* biofilm exposure to Ag^+ and AgNP.

		Test #	Influent silver	Biomass (µg protein)	Final nitrite production rate (mmol NO_2^-/hr)	Final specific nitrite production rate (mmol NO_2^-/mg protein/hr)	Average biomass (µg protein)	Average specific rate (mmol NO_2^-/mg protein/hr)
Standard biofilms	Control	3	0 ppm	2393	0.0329	0.0138	1125 ± 50%	0.0345 ± 54%
		3	0 ppm	1044	0.0317	0.0304		
		4	0 ppm	1237	0.0301	0.0243		
		4	0 ppm	1088	0.0195	0.0179		
		5	0 ppm	700	0.0305	0.0435		
		5	0 ppm	291	0.0223	0.0768		
	Exposed	1	0.5 ppm Ag+	563	0.0194	0.0344	911 ± 27%	0.0254 ± 31%
		1	0.5 ppm Ag+	488	0.0136	0.0279		
		2	1.5 ppm Ag+	1482	0.0131	0.0089		
		2	1.5 ppm Ag+	905	0.0074	0.0082		
		3	1.5 ppm Ag+ (post-recovery)	439	0.0079	0.0180		
		3	1.5 ppm Ag+ (post-recovery)	1416	0.0110	0.0078		
		4	0.5 ppm AgNP	1311	0.0237	0.0180		
		4	0.5 ppm AgNP	864	0.0216	0.0250		
		5	1.5 ppm AgNP	1054	0.0224	0.0213		
		5	1.5 ppm AgNP	589	0.0211	0.0359		
Mature biofilms	Control	6	0 ppm	1309	0.0333	0.0255	1583 ± 34%	0.0216 ± 35%
		6	0 ppm	1858	0.0331	0.0178		
	Exposed	6	0.5 ppm Ag+	1352	0.0185	0.0137	1598 ± 30%	0.0122 ± 23%
		6	0.5 ppm Ag+	1845	0.0199	0.0108		

Table 1. Final biomass measurements and nitrite production rates of control biofilms and biofilms exposed to Ag^+ or AgNP. Final nitrite production rates were calculated from effluent immediately prior to harvest. Biomass was measured immediately after biofilms were harvested. Specific nitrite production rates were calculated by dividing final nitrite production rates by measured biomass. Data are not available for the 0.5 ppm Ag^+ recovery test.

Table 2. Theoretical silver mass loadings and measured silver mass in *N. europaea* biofilms. Results from duplicate lanes are shown. Results for recovery experiments are not available due to post-experiment biofilm death (0.5 ppm Ag^+) or silver loss during prolonged storage (1.5 ppm Ag^+). Measured Ag mass for each biofilm includes silver from both the slide and the DFR well. Separate numbers for slide and well Ag are presented in Table 3.

Experiment	Test #	Influent Ag concentration (ppm)	Theoretical Ag mass loading (µg)	Measured Ag mass in biofilm (µg)	Measured / theoretical
0.5 ppm Ag^+	1	0.5	288	40.1	**0.139**
	1	0.5	288	25.0	**0.0867**
0.5 ppm Ag^+, mature biofilms	6	0.5	288	132	**0.457**
	6	0.5	288	147	**0.511**
1.5 ppm Ag^+	2	1.5	864	39.6	**0.0458**
	2	1.5	864	20.7	**0.0240**
0.5 ppm AgNP	4	0.5	288	19.4	**0.0674**
	4	0.5	288	24.1	**0.0836**
1.5 ppm AgNP	5	1.5	864	128	**0.148**
	5	1.5	864	56.8	**0.0657**

Table 3. Spatial distribution (between slide and well) of biomass and silver in control lanes and lanes exposed to Ag^+ or AgNP. *Results for the 0.5 ppm Ag^+ post-recovery experiment are shown but were not incorporated into averages because all biofilms in this experiment were killed by contaminated media immediately prior to harvest; consequently, their protein and bound silver values are suspect. **Silver measurements are not available for the 1.5 ppm Ag^+ + recovery experiment.

Treatment	Test #	Biomass on slide (µg)	Biomass in well (µg)	Ag on slide (µg)	Ag in well (µg)	% Biomass on slide	% Silver on slide
Control lanes:	4	1110	127	0	0	89.7	n/a
	4	644	443	0	0	59.3	n/a
	5	555	145	0	0	79.2	n/a
	5	183	108	0	0	62.8	n/a
	3	2170	224	0	0	90.6	n/a
	3	727	317	0	0	69.6	n/a
Average, control lanes:		**898 ± 553**	**227 ± 105**			**75.2 ± 10.8**	**n/a**
*0.5 ppm Ag+, post-recovery ****	*7*	*145*	*34*	*5.4*	*6.0*	*81.2*	*47.7*
	7	*127*	*52*	*4.1*	*5.9*	*70.8*	*40.9*
0.5 Ag+	1	358	205	24.2	15.9	63.6	60.4
	1	330	158	12.6	12.4	67.5	50.5
Mature, 0.5 Ag+	6	1132	220	126.4	5.3	83.7	96.0
	6	1560	285	144.2	3.0	84.6	98.0
1.5 ppm Ag+, post-recovery	3	215	224	n/a**	n/a**	49.0	n/a**
	3	1239	177	n/a**	n/a**	87.5	n/a**
1.5 Ag+	2	704	778	35.8	3.8	47.5	90.4
	2	760	145	16.3	4.4	83.9	78.9
Average, lanes exposed to Ag+ (excluding mature biofilms):		**601 ± 305**	**281 ± 196**			**66.5 ± 13.1**	**70.0 ± 17.6**
0.5 AgNP	4	1203	108	18.9	0.6	91.7	97.1
	4	719	145	23.3	0.8	83.2	96.8
1.5 ppm AgNP	5	927	127	124.2	5.2	88.0	96.0
	5	518	71	54.2	4.3	87.9	92.6
Average, lanes exposed to AgNP:		**842 ± 287**	**113 ± 31**			**87.7 ± 3.4**	**95.6 ± 2.0**
Average, all exposed lanes (excluding mature biofilms):		**697 ± 219**	**214 ± 126**			**75.0 ± 10.4**	**82.8 ± 12.5**

Sample Name	AMO SOUR (mmol O_2/hr)	HAO SOUR (mmol O_2/hr)	AMO/HAO	Biomass in sample (μg)	Biomass-normalized AMO-SOUR (mmol O_2/mg protein/hr)	Biomass-normalized HAO-SOUR (mmol O_2/mg protein/hr)	Biomass-normalized nitrite production rate (mmol NO_2^-/mg protein/hr)
(++) Control - upper slide	8.86	2.69	3.29	466	19.0	5.8	0.0134
(++) Control - lower slide	8.82	2.54	3.48	315	28.0	8.0	0.0134
(++) Control - well	2.21	0.578	3.83	81	27.5	7.2	0.0134
(+) Control - upper slide	1.47	0.623	2.35	114	12.9	5.5	0.0290
(+) Control - lower slide	1.80	0.816	2.21	148	12.2	5.5	0.0290
(+) Control - well	3.00	0.692	4.34	114	26.3	6.1	0.0290
Average (control)	4.36	1.32	3.25	206	21.0	6.34	0.0212
1.5 ppm Ag+ (A) - upper slide	0.821	0.266	3.08	47	17.4	5.7	0.0235
1.5 ppm Ag+ (A) - lower slide	0.128	0.071	1.82	30	4.2	2.3	0.0235
1.5 ppm Ag+ (A) - well	1.26	0.362	3.47	81	15.6	4.5	0.0235
1.5 ppm Ag+ (B) - upper slide	4.12	0.935	4.40	315	13.1	3.0	0.0100
1.5 ppm Ag+ (B) - lower slide	0.731	0.219	3.34	131	5.6	1.7	0.0100
1.5 ppm Ag+ (B) - well	1.47	0.396	3.72	64	23.1	6.2	0.0100
Average (1.5 ppm Ag+)	1.42	0.375	3.31	111	13.2	3.9	0.0168

Table 4. AMO- and HAO-SOURs of control biofilms and biofilms exposed to 1.5 ppm Ag^+.

5. Conclusion

This research confirmed earlier findings that intact biofilms of *N. europaea* are more resistant than suspended cells to Ag^+, and that sensitivity to Ag^+ is higher than to AgNP. It extended these findings to longer exposures and found that biofilms maintain their nitrifying ability even after 48-hour exposures to Ag^+ and AgNP. These results suggest that long-term exposure to low levels of Ag^+ and AgNP are less toxic than equivalent mass loadings distributed over a shorter time frame. This, coupled with the lack of correlation between bound silver and final percent nitrification activity, may indicate that mass loading alone cannot be used to predict nitrification inhibition in intact biofilms.

Figure 25 presents a conceptual model of biofilm exposure to Ag^+ and AgNP illustrating theorized sources of inhibition and protection. In brief, results indicate that AgNP toxicity in this study resulted from released Ag^+; Ag^+ diffuses into the biofilm, causing enzymatic inhibition at lower concentrations, and leading to death and lysis at longer exposures or higher concentrations. Some loss of activity may result from sloughing of viable biomass in response to Ag^+ or AgNP exposure. Ag^+ does not bind to EPS, but cells deep within the biofilm may be protected by a diffusion gradient that limits contact with Ag^+. Persister cells may be protected by virtue of their low activity.

The mechanisms by which biofilms are protected from contaminants are a continuing source of debate. The results of this experiment suggest that the structure of the *N. europaea* biofilm is key, insofar as separation from the growth surface and resuspension in media results in a loss of protection from inhibition. Inhibition and titration experiments with resuspended biofilms do not support the hypothesis that the extracellular matrix binds Ag^+, thereby preserving cells from harm. Instead, results support a model in which cells far from the biofilm surface are protected from inhibition due to mass transfer limitations; some protection may

also be attributable to low activity levels in some biofilm cells. The diffusion gradient produced by the biofilm structure may protect cells deep within the biofilm from contact with Ag^+. Future experiments could expose resuspended biofilms to AgNP to determine if EPS stabilizes AgNP or provides another form of protection from inhibition.

This study found that cell death is responsible for some, but not all, Ag^+-induced nitrification inhibition observed in suspended cells. For intact biofilms to experience equivalent inhibition, substantially higher Ag^+ concentrations were required. In those biofilms, cell death was higher than in suspended cells with equivalent nitrification inhibition. However, the exposure time was much longer in the biofilms. Live/Dead staining of intact biofilms points to a general loss of metabolic activity and cell membrane integrity, rather than a loss of nitrification-specific enzymatic activity, though this may differ with shorter exposures. This may have implications for biofilm recovery in the wake of Ag^+or AgNP exposure; recovery tests indicated that exposed biofilms increased activity slower than regular growing biofilms.

Sloughing is likely responsible for some of the loss of nitrifying activity observed in DFR biofilms, but the lack of a strong correlation between biomass and NO_2^- production complicates analysis. The lower biomass-normalized NO_2^- production rates of Ag-exposed biofilms versus control biofilms confirm that death or other nonspecific inhibition mechanisms play a key role in loss of activity. Quantification of the protein content, nitrifying activity, and amount of silver bound to sloughed biomass could provide insight into whether sloughed biofilm cells are more or less vulnerable than attached biomass to Ag^+ and AgNP, and what the implications of sloughing are for real-world systems.

This study did not find any evidence of nanoparticle-specific toxicity. No detectable inhibition occurred during the regular time frame in suspended cell batch AgNP inhibition experiments, likely as a result of AgNP aggregation. The slow onset of inhibition during AgNP exposures in both DFR and suspended cell experiments

suggests Ag^+ release as the toxic mechanism in these systems. Given the higher concentrations of natural organic matter and divalent cations in wastewater, higher aggregation of AgNP and lower Ag^+ release are likely. As a result, AgNP are unlikely to significantly disrupt biological wastewater treatment. However, substantial accumulations of silver in WWTP sludge may be of concern in determining how it may be used or disposed of in future.

Future work could build on the results of this study by extending some Ag^+ tests to AgNP. These include batch tests on resuspended biofilms, including inhibition and Live/Dead quantification, as well as Live/Dead staining following experiments on intact biofilms exposed to AgNP and tests to study recovery of biofilms exposed to AgNP. Shorter DFR exposures (of intact biofilms) and longer batch exposures (of suspended cells and resuspended biofilms) could also be performed to explore the connection between length of exposure and frequency of cell death. Locations of live and dead cells in intact biofilms could be studied in order to confirm or disprove the role of a diffusion gradient in protecting biofilm cells from inhibition. Techniques could include using 3D confocal microscopy to visualize cells and probing oxygen activity at different depths within the biofilm. Research could also examine the role of biofilm sloughing through quantification of sloughed biofilm protein, as well as measuring the NO_2^- production and bound silver concentrations of sloughed biomass.

APPENDIX

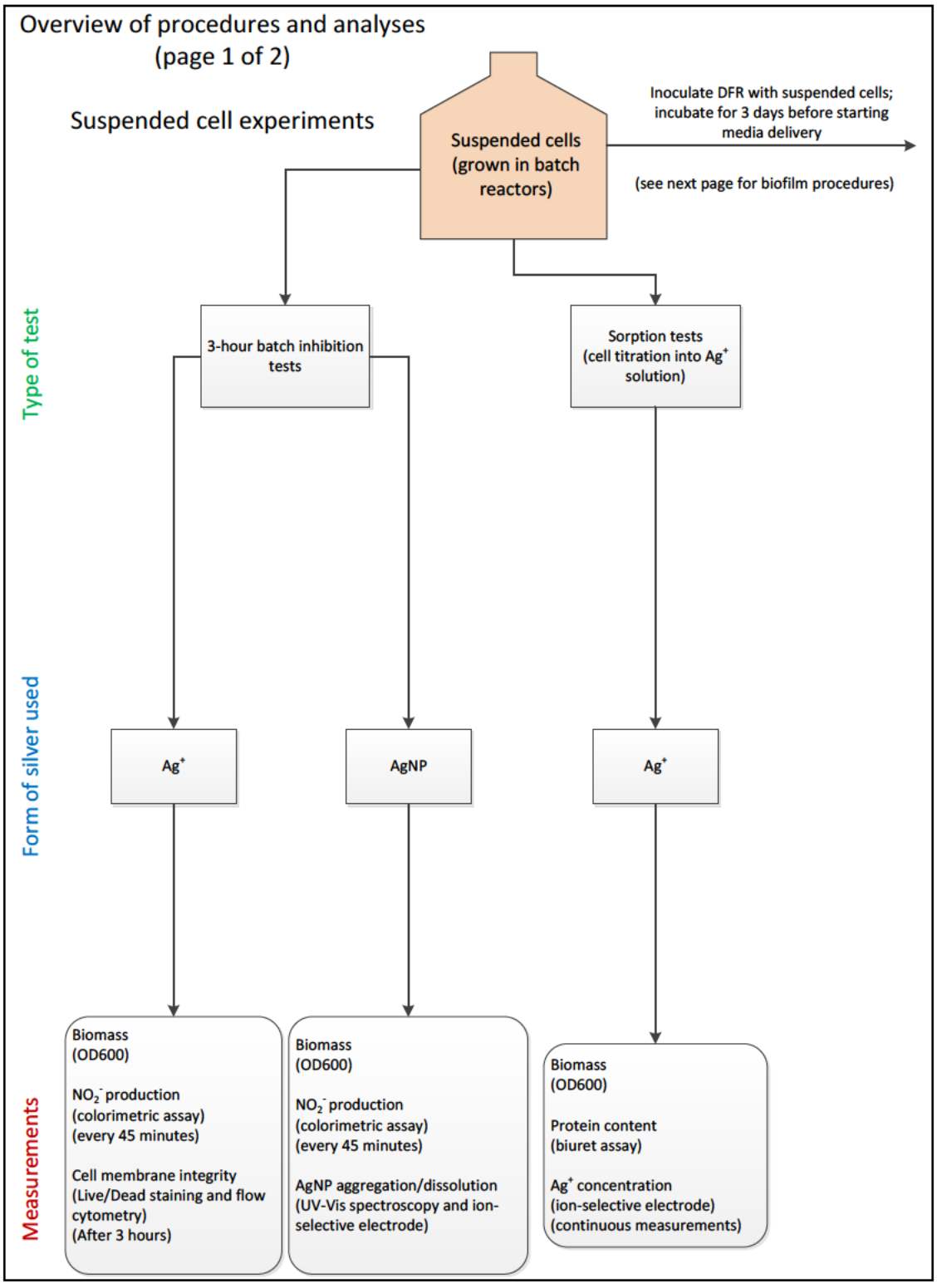

Figure 26. Overview of procedures and analyses performed in this study. Page 1: suspended cell experiments.

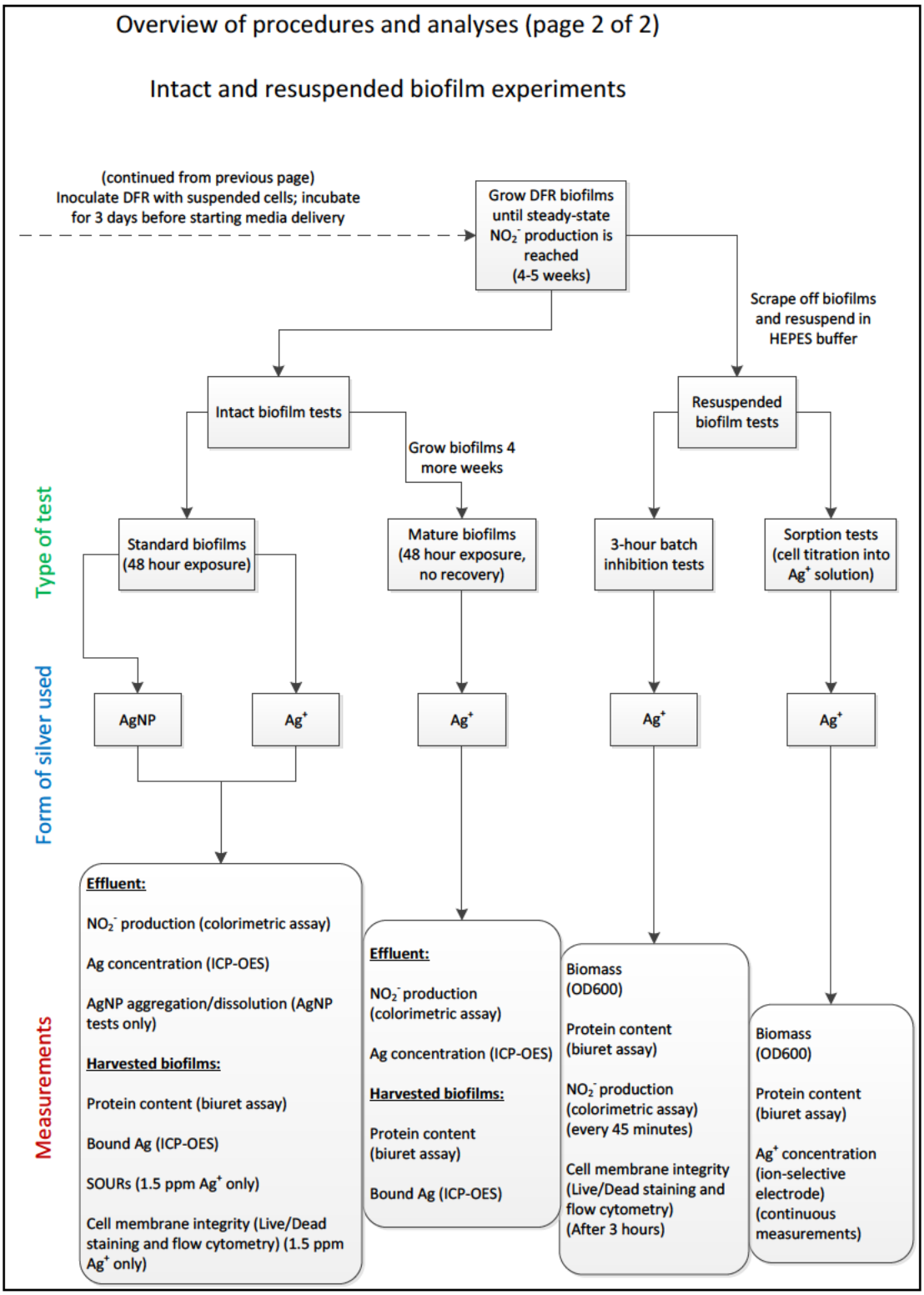

Figure 27. Overview of procedures and analyses performed in this study. Page 2: intact and resuspended biofilm experiments.

Notes on sudden death of DFR biofilms immediately following media changes:

On several occasions in this study, a change of media led to the sudden death of all biofilms in the DFR. Biofilms were killed within minutes following addition of new media. This recurred with multiple DFRs over the course of one month; the only experiment affected was Test 7 (0.5 ppm Ag^{+} with recovery), in which the media change occurred after more than 240 hours of post-exposure recovery. The cause was not identified. One suspected cause was dissociation of HEPES in the presence of ambient light, resulting in the production of hydrogen peroxide. This phototoxicity has been previously reported (Lepe-Zuniga, Zigler, & Gery, 1987). Because of these suspicions, we covered media bottles in aluminum foil to limit light exposure during storage and removed the foil once the media was hooked up to the DFR (the constant-temperature room containing the DFR was kept in the dark). Biofilm death following media changes was not observed after this change in protocol was made.

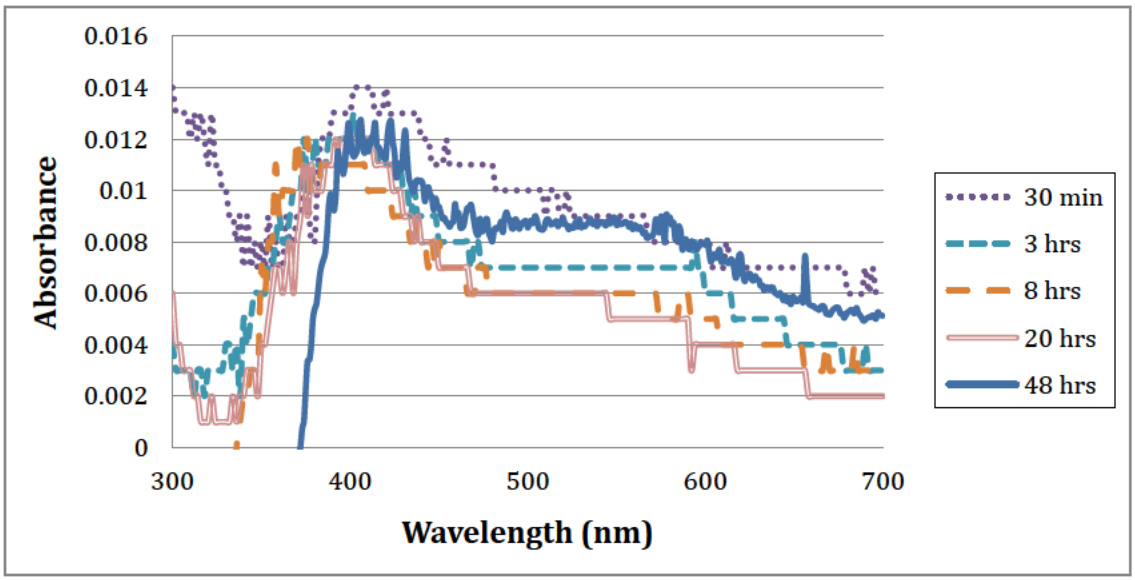

Figure 28. Scans of effluent from lanes exposed to 0.5 ppm AgNP. An attempt was made to quantify AgNP aggregation/dissolution via UV-Vis spectroscopy.

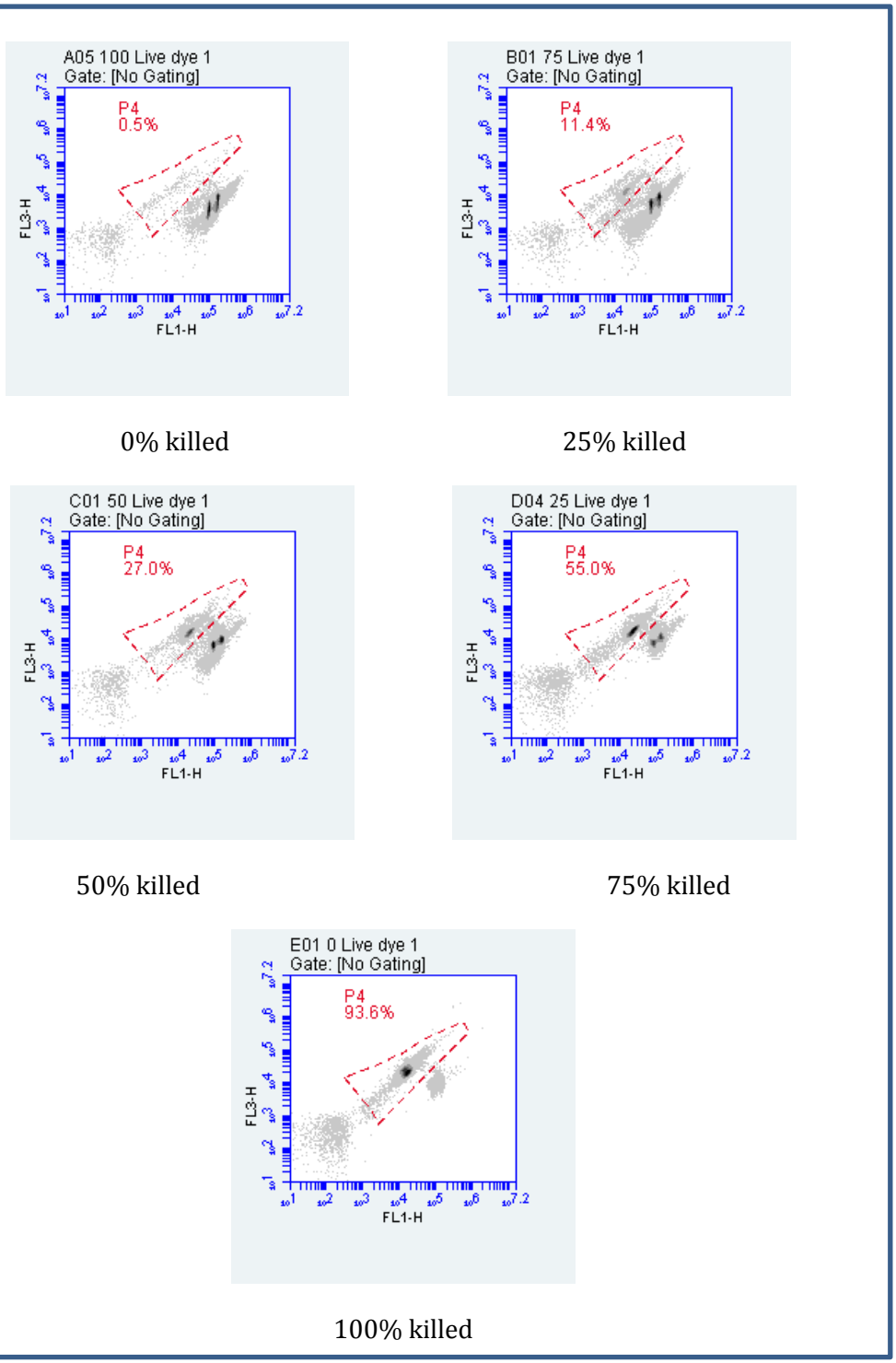

Figure 29. Sample two-dimensional flow cytometer scatter plots of live/dead standards. The manually-generated gate (dashed red line) encompasses the region associated with compromised cell membranes.

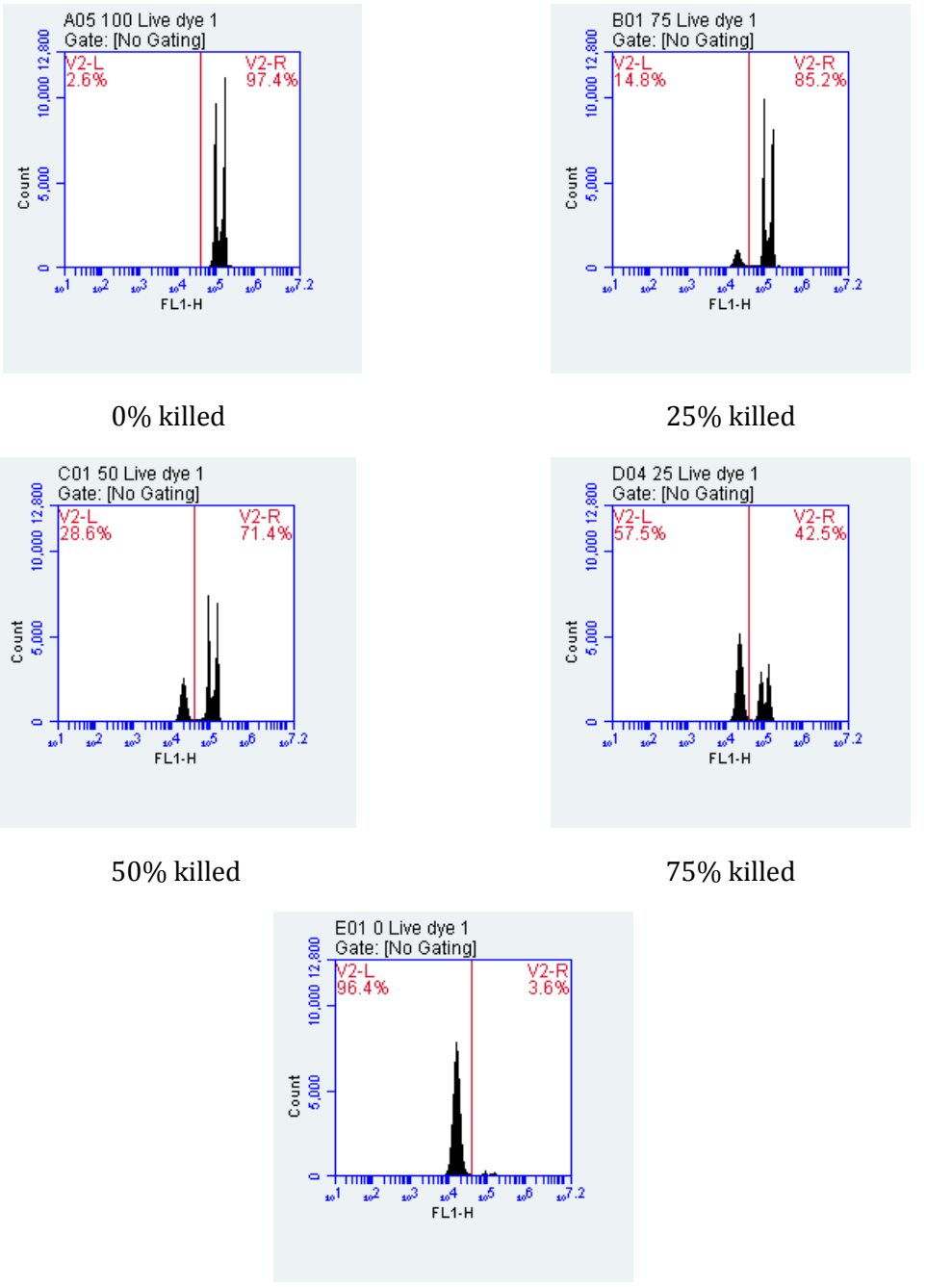

Figure 30. Sample one-dimensional flow cytometer output for live/dead standards. The vertical red line was positioned manually and divides frequencies associated with intact cell membranes from those associated with compromised cell membranes. The two-dimensional scatter plot (Figure 29) was found to give more consistent output, and data from the 2D plots was used to produce the standard curve used in later live/dead analysis.

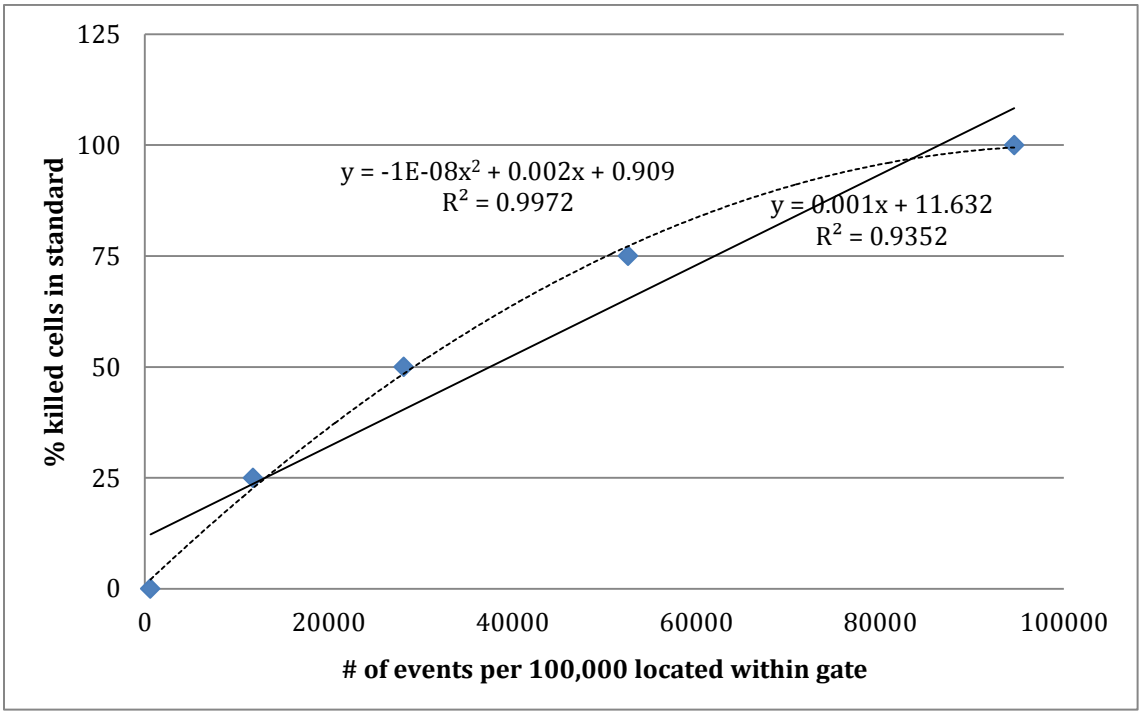

Figure 31. Live/Dead standard curve produced using *N. europaea* cells harvested in late-exponential phase. Cells were killed using ethanol and combined in five different ratios with live cells to produce standards.

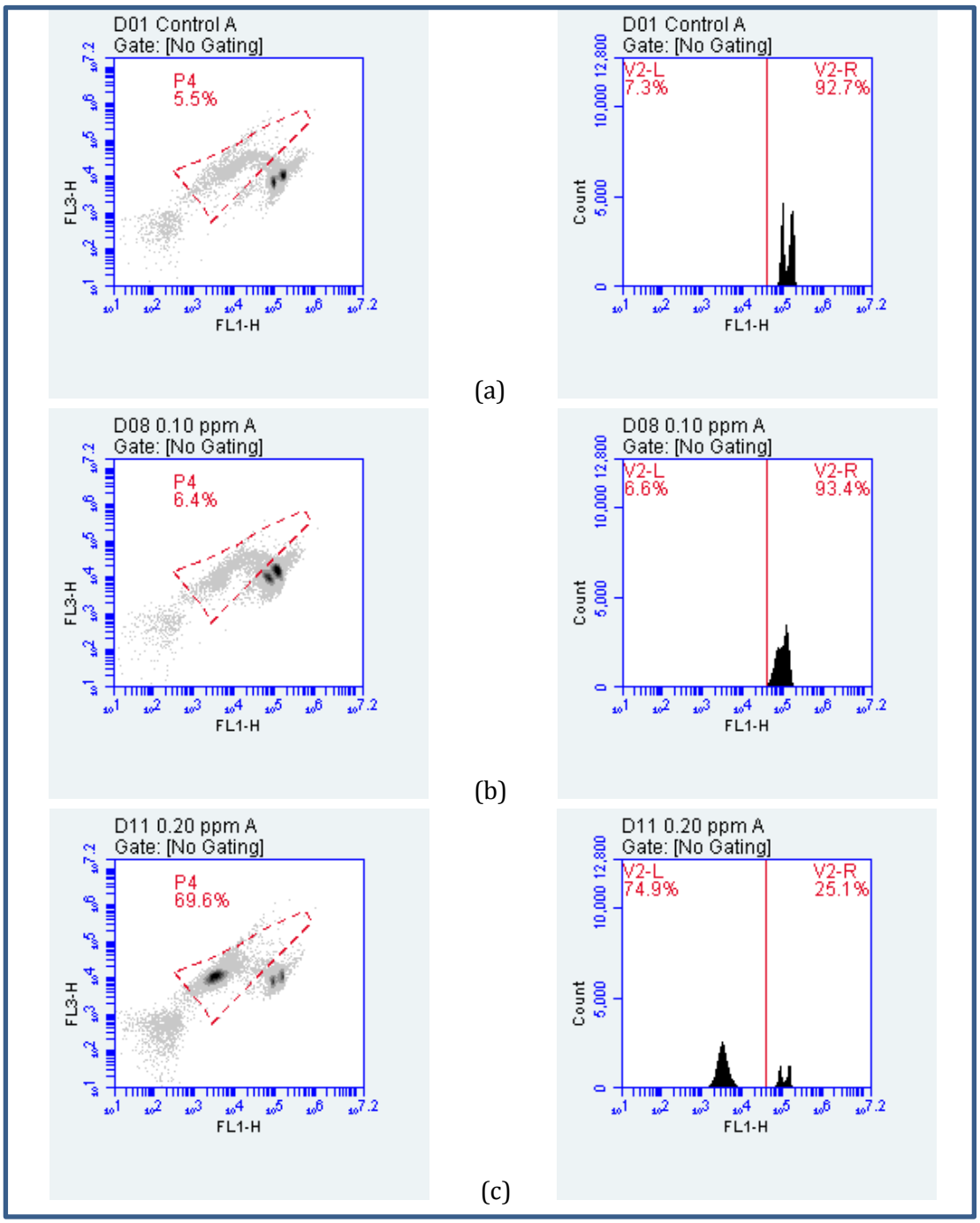

Figure 32. Sample raw flow cytometry data from batch tests of suspended cells. Shown are event plots for (a) control cells, (b) cells exposed to 0.10 ppm Ag^+, and (c) cells exposed to 0.20 ppm Ag^+. The high percentage of dead cells in the 0.20 ppm Ag^+ treatment can be clearly seen in the concentration of events within the two-dimensional plot gate (c, at left) and to the left of the gate line in the one-dimensional plot (c, at right). Standard curves and live/dead percentages of test samples were calculated using the two-dimensional plot and gate, which were deemed slightly more consistent.

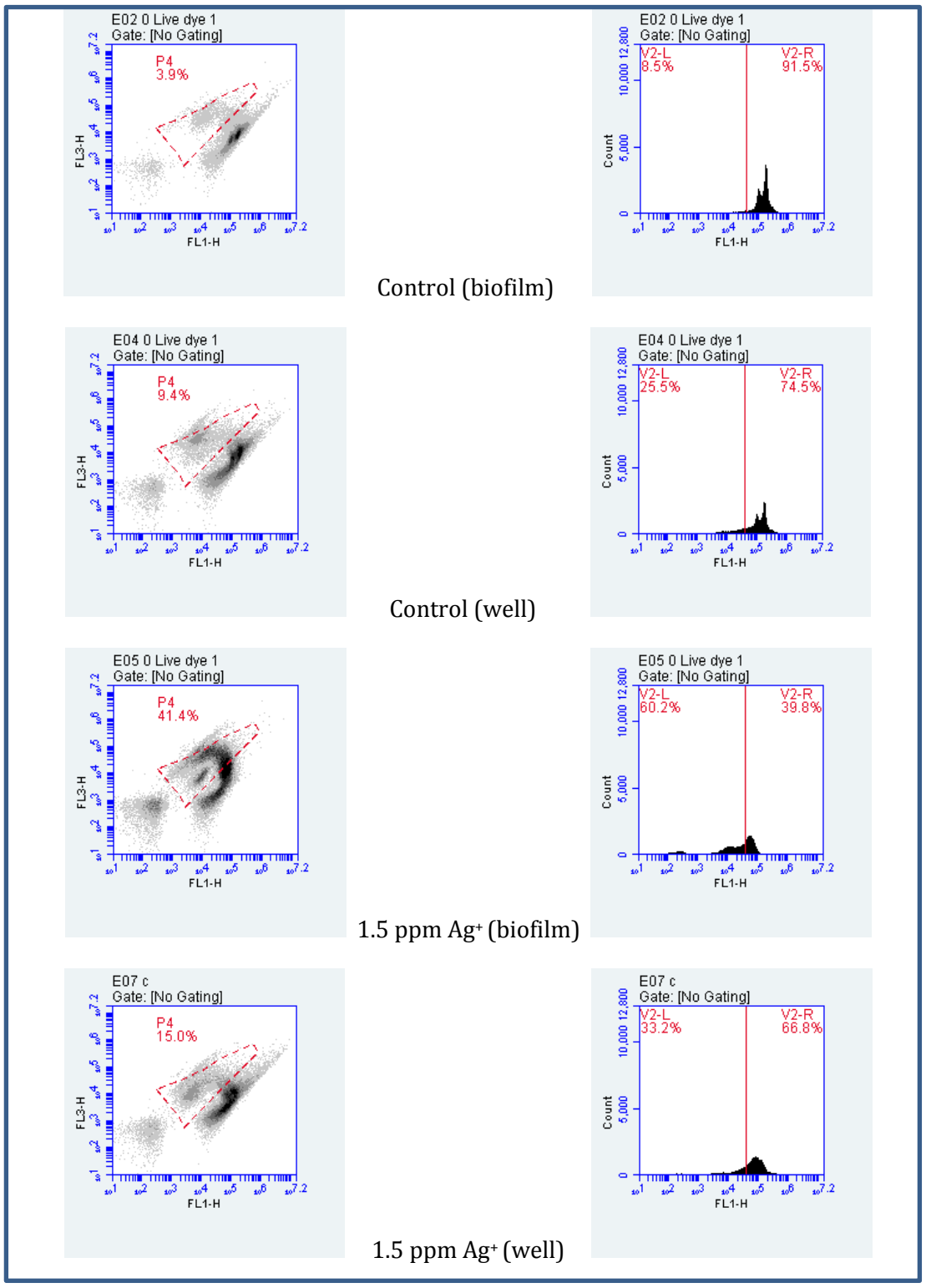

Figure 33. Sample flow cytometer output from tests on intact DFR biofilms exposed to 1.5 ppm Ag^+ for 48 hours. Gating is less clear-cut than in suspended cell experiments; this is particularly notable in the one-dimensional plots (right).

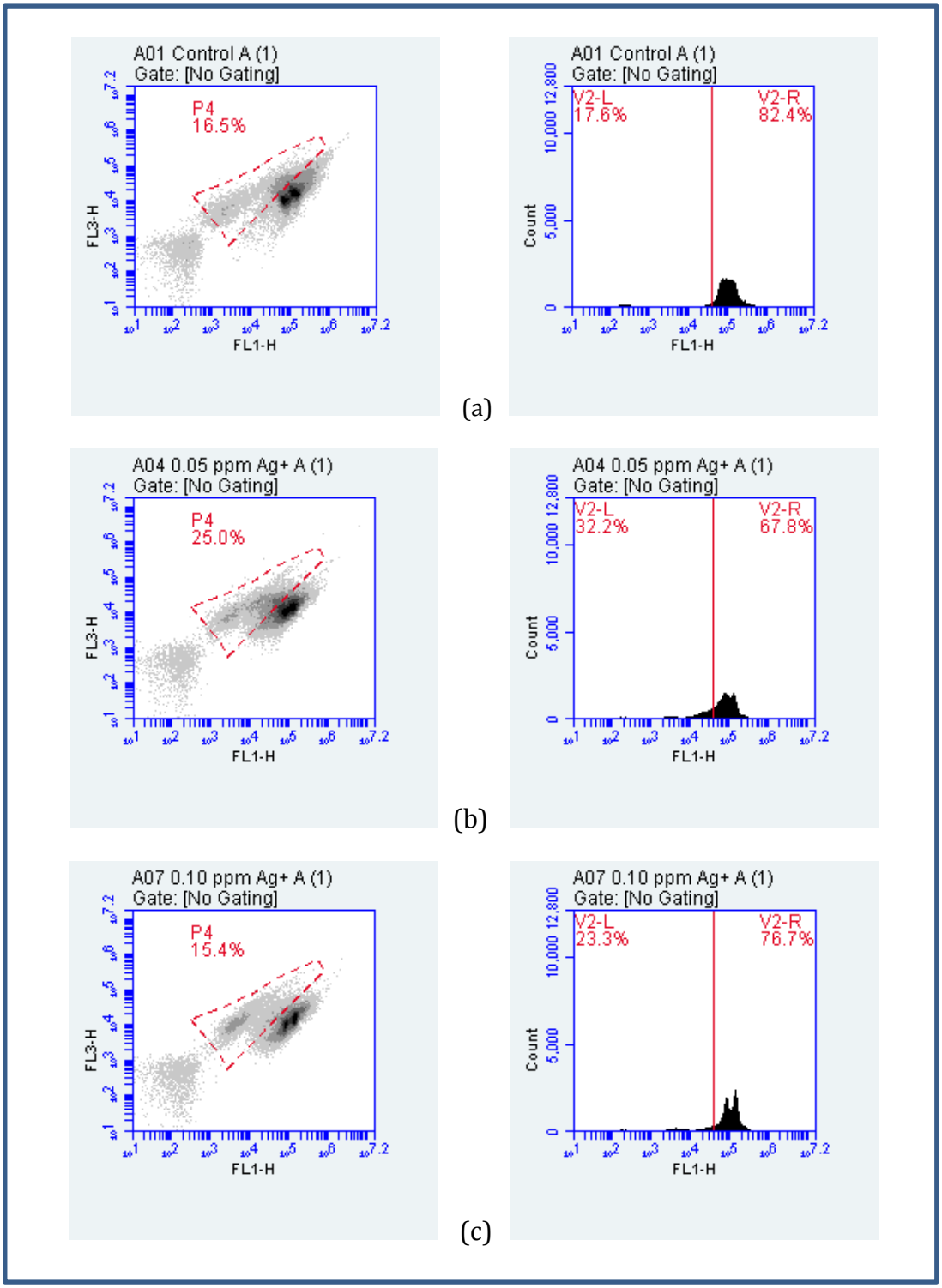

Figure 34. Sample flow cytometer output from 3-hour batch Ag^+ inhibition tests on resuspended biofilms. (a) control; (b) 0.05 ppm Ag^+; (c) 0.10 ppm Ag^+.

Table 5. Nitrite production in DFR biofilms prior to start of AgNP exposure tests (-48hr ≤ t ≤ 0 hr) compared with nitrite production during final 24 hours of exposure (24 hr < t ≤ 48 hr). An independent samples t-test was performed to determine if the two sets of measurements differed significantly. Both treated biofilms experienced significant decreases in nitrite production. Both controls showed no significant change.

	(++) Control		(+) Control		0.5 ppm AgNP (A)		0.5 ppm AgNP (B)	
Nitrite production 0-48 hours before test (mmol NO_2^-/hr)	0.028145 0.026859 0.031558 0.031608 0.030509		0.021976 0.024848 0.029487 0.03054 0.019933		0.029048 0.029904 0.026641 0.032185 0.031498		0.030084 0.030502 0.031364 0.030909 0.031551	
	Mean	SD	Mean	SD	Mean	SD	Mean	SD
	0.029736	0.002135	0.025357	0.004611	0.029855	0.002186	0.030882	0.000605
Nitrite production 24 hr < t ≤ 48 hr (mmol NO_2^- /hr)	0.029594 0.026791 0.025755 0.030062		0.026899 0.02397 0.026405 0.019476		0.025581 0.020402 0.024798 0.023661		0.027996 0.023083 0.023979 0.021622	
	Mean	SD	Mean	SD	Mean	SD	Mean	SD
	0.028051	0.002104	0.024188	0.003392	0.02361	0.00228	0.02417	0.00273
Outcome of t-test	p = 0.27644		p = 0.67469		p = 0.00512		p = 0.01423	
Significant?	No		No		Yes		Yes	

Table 6. Nitrite production in DFR biofilms prior to start of AgNP exposure tests (-48hr ≤ t ≤ 0 hr) compared with nitrite production during final 24 hours of exposure (24 hr < t ≤ 48 hr). An independent samples t-test was performed to determine if the two sets of measurements differed significantly. All treated biofilms (0.5 ppm AgNP and 1.5 ppm AgNP) experienced significant decreases in nitrite production. *One control biofilm in the 1.5 ppm AgNP test showed a significant loss of nitrite production (likely due to temporary loss of media flow in that lane's influent tubing); treated biofilm inhibition (Figure 6b) was normalized for the slight loss in the control. Treated biofilms still exhibited significantly greater loss of nitrification than this control (Figure 35). The other control showed no loss of nitrification activity.

	(++) Control		(+) Control		1.5 ppm AgNP (A)		1.5 ppm AgNP (B)	
Nitrite production 0-48 hours before test (mmol NO_2^- /hr)	0.037051 0.03094 0.031506 0.035208		0.028392 0.026483 0.027788 0.023846		0.037252 0.034191 0.033973 0.036382		0.034726 0.033887 0.032883 0.033701	
	Mean	SD	Mean	SD	Mean	SD	Mean	SD
	0.033676	0.00294	0.026627	0.002018	0.035449	0.001621	0.033799	0.000756
Nitrite production 24 hr < t ≤ 48 hr (mmol NO_2^-/hr)	0.031226 0.029127 0.030761 0.030492		0.02101 0.021599 0.02265 0.022346		0.021422 0.024922 0.024755 0.02244		0.022549 0.023914 0.022774 0.021143	
	Mean	SD	Mean	SD	Mean	SD	Mean	SD
	0.030402	0.000902	0.021901	0.00074	0.023385	0.001731	0.022595	0.001138
Outcome of t-test	p = 0.10874		p = 0.01319		p = 0.00005		p = 0.00001	
Significant?	No		Yes*		Yes		Yes	

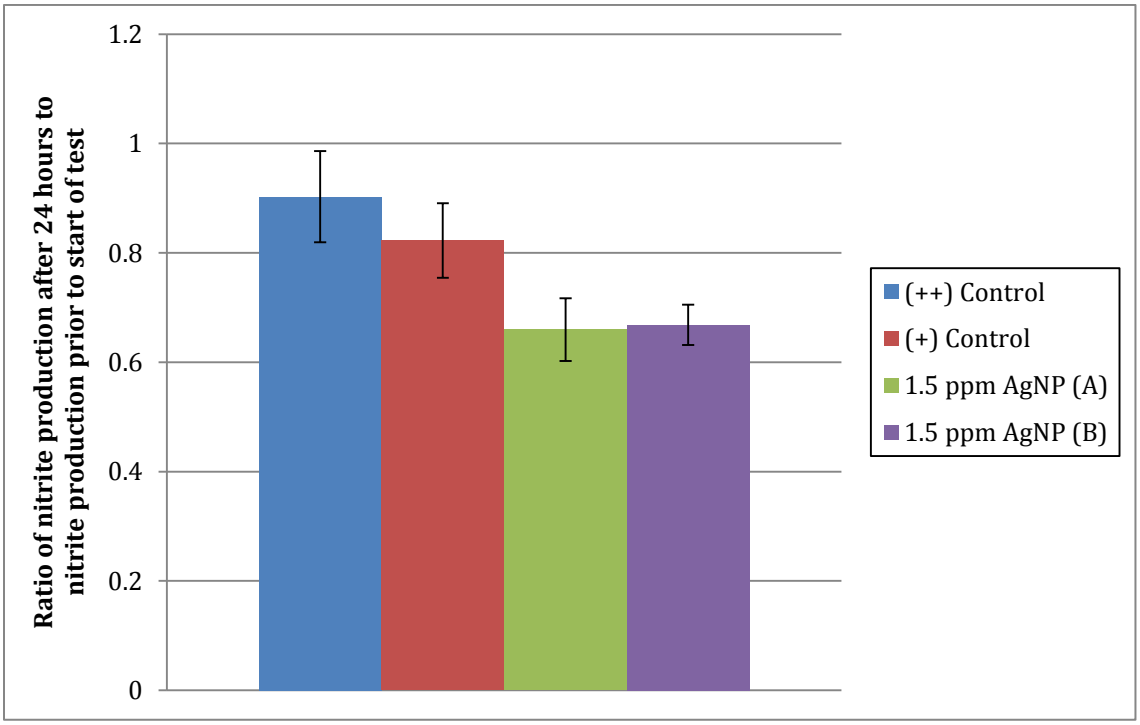

Figure 35. Nitrite production during 1.5 ppm AgNP DFR exposure test (24 hr < t ≤ 48 hr) divided by nitrite production prior to start of test (-48 hr ≤ t ≤ 0 hr). Error bars represent standard deviations. Treated biofilms show significantly lower ratios of post-test:pre-test activity than controls.

7. Bibliography

Adams, N. W. H., & Kramer, J. R. (1999). Silver speciation in wastewater effluent, surface waters, and pore waters. *ENVIRONMENTAL TOXICOLOGY AND CHEMISTRY, 18*(12), 2667-2673.

Ahrland, S., Chatt, J., Davies, N. R., & Williams, A. A. (1958a). 54. The relative affinities of co-ordinating atoms for silver ion. Part I. Oxygen, sulphur, and selenium. [10.1039/JR9580000264]. *Journal of the Chemical Society (Resumed)*(0), 264-276.

Ahrland, S., Chatt, J., Davies, N. R., & Williams, A. A. (1958b). 55. The relative affinities of co-ordinating atoms for silver ion. Part II. Nitrogen, phosphorus, and arsenic. [10.1039/JR9580000276]. *Journal of the Chemical Society (Resumed)*(0), 276-288.

Alexander, J. W. (2009). History of the Medical Use of Silver. *Surgical Infections, 10*(3), 4.

An, Y. H. F. R. J. (2000). *Handbook of bacterial adhesion : principles, methods, and applications*. Totowa, NJ: Humana Press.

Anderson, G. G., & O'Toole, G. A. (2008). Innate and induced resistance mechanisms of bacterial biofilms (Vol. 322, pp. 85-105). BERLIN: SPRINGER-VERLAG BERLIN.

Anderson, J. W., Semprini, L., & Radniecki, T. S. (2014). Influence of Water Hardness on Silver Ion and Silver Nanoparticle Fate and Toxicity Toward *Nitrosomonas europaea*. *Environmental Engineering Science, 31*(7), 7.

Arnaout, C. L. (2012). *Assessing the Impacts of Silver Nanoparticles on the Growth, Diversity, and Function of Wastewater Bacteria.* Duke University.

Arnaout, C. L., & Gunsch, C. K. (2012). Impacts of Silver Nanoparticle Coating on the Nitrification Potential of Nitrosomonas europaea. *Environmental Science & Technology, 46*(10), 5387-5395.

Arp, D. J., Sayavedra-Soto, L. A., & Hommes, N. G. (2002). Molecular biology and biochemistry of ammonia oxidation by *Nitrosomonas europaea*. *Archives of Microbiology, 178*(4), 250-255.

Berne, C., Kysela, D. T., & Brun, Y. V. (2010). A bacterial extracellular DNA inhibits settling of motile progeny cells within a biofilm. [Article]. *Molecular Microbiology, 77*(4), 815-829.

Bjarnsholt, T., Kirketerp-Møller, K., Kristiansen, S., Phipps, R., Nielsen, A. K., Jensen, P. Ø., et al. (2007). Silver against Pseudomonas aeruginosa biofilms. [Article]. *APMIS, 115*(8), 921-928.

Blaser, S. A., Scheringer, M., Mcleod, M., & Hungerbuhler, K. (2008). Estimation of cumulative aquatic exposure and risk due to silver: Contribution of nano-functionalized plastics and textiles. *Science of The Total Environment, 390*(2–3), 396 - 409.

Burton, E. O., Read, H. W., Pellitteri, M. C., & Hickey, W. J. (2005). Identification of Acyl-Homoserine Lactone Signal Molecules Produced by *Nitrosomonas europaea* Strain Schmidt. *Applied and Environmental Microbiology, 71*(8), 4906-4909.

Chain, P., Lamerdine, J., Larimer, F., Regala, W., Lao, V., Land, M., et al. (2003). Complete Genome Sequence of the Ammonia-Oxidizing Bacterium and Obligate Chemolithoautotroph *Nitrosomonas europaea*. *Journal of Bacteriology, 185*(9), 2759-2773.

Chinnapongse, S. L., MacCuspie, R. I., & Hackley, V. A. (2011). Persistence of singly dispersed silver nanoparticles in natural freshwaters, synthetic seawater, and simulated estuarine waters. *Science of The Total Environment, 409*(12), 2443-2450.

Choi, O., & Hu, Z. (2008). Size Dependent and Reactive Oxygen Species Related Nanosilver Toxicity to Nitrifying Bacteria. *Environmental Science & Technology, 42*(12), 4583-4588.

Eisler, R. (1996). *Silver hazards to fish, wildlife, and invertebrates: A synoptic review*.

Ely, R. L., Williamson, K. J., Guenther, R. B., Hyman, M. R., & Arp, D. J. (1995). A COMETABOLIC KINETICS MODEL INCORPORATING ENZYME-INHIBITION, INACTIVATION, AND RECOVERY .1. MODEL DEVELOPMENT, ANALYSIS, AND TESTING. *Biotechnology and bioengineering, 46*(3), 218-231.

Ensign, S. A., Hyman, M. R., & Arp, D. J. (1993). In Vitro Activation of Ammonia Monooxygenase from *Nitrosomonas Europaea* by Copper. *Journal of Bacteriology, 175*(7), 1971-1980.

Fabrega, J., Renshaw, J., & Lead, J. R. (2009). Interactions of Silver Nanoparticles with *Pseudomonas putida* Biofilms. *Environmental Science & Technology, 43*(23), 9004-9009.

Farré, M., Gajda-Schrantz, K., Kantiani, L., & Barceló, D. (2009). Ecotoxicity and analysis of nanomaterials in the aquatic environment. *Analytical and Bioanalytical Chemistry, 393*(1), 81-95.

Frattini, A., Pellegri, N., Nicastro, D., & Sanctis, O. d. (2005). Effect of amine groups in the synthesis of Ag nanoparticles using aminosilanes. *Materials Chemistry and Physics, 94*(1), 148-152.

Gaidhani, S., Singh, R., Singh, D., Patel, U., Shevade, K., Yeshvekar, R., et al. (2013). Biofilm disruption activity of silver nanoparticles synthesized by Acinetobacter calcoaceticus PUCM 1005. *Materials Letters, 108*, 324-327.

Giska, J. R. (2013). *The Effects of Silver Ions and Nanoparticles.* Oregon State University, Corvallis, OR.

Guo, Z., & Tan, L. (2009). *Fundamentals and Applications of Nanomaterials* (1 ed.). Norwood, MA: Artech House.

Hageman, R. H., & Hucklesby, D. P. (1971). Nitrate reductase from higher plants. *Methods in Enzymology, 45*(23), 491-503.

Hall-Stoodley, L., & Stoodley, P. (2009). Evolving concepts in biofilm infections. [Article]. *Cellular Microbiology, 11*(7), 1034-1043.

Holt, K. B., & Bard, A. J. (2005). Interaction of Silver(I) Ions with the Respiratory Chain of *Escherichia coli*: An Electrochemical and Scanning Electrochemical Microscopy Study of the Antimicrobial Mechanism of Micromolar Ag+. *Biochemistry, 44*(39), 13214-13223.

Hyman, M. R., & Arp, D. J. (1995). Effects of ammonia on the de novo synthesis of polypeptides in cells of Nitrosomonas europaea denied ammonia as an energy source. *Journal of Bacteriology [H.W.Wilson - GS], 177*(17), 4974.

Kalishwaralal, K., BarathManiKanth, S., Pandian, S. R. K., Deepak, V., & Gurunathan, S. (2010). Silver nanoparticles impede the biofilm formation by Pseudomonas aeruginosa and Staphylococcus epidermidis. *Colloids and surfaces.B, Biointerfaces, 79*(2), 340-344.

Karatan, E., & Watnick, P. (2009). Signals, Regulatory Networks, and Materials That Build and Break Bacterial Biofilms. *Microbiology and Molecular Biology Reviews, 73*(2), 310-310.

Kittler, S., Greulich, C., Diendorf, J., Koller, M., & Epple, M. (2010). Toxicity of Silver Nanoparticles Increases during Storage Because of Slow Dissolution under Release of Silver Ions. *CHEMISTRY OF MATERIALS, 22*(16), 4548-4554.

Kostigen Mumper, C., Ostermeyer, A.-K., Semprini, L., & Radniecki, T. S. (2013). Influence of ammonia on silver nanoparticle dissolution and toxicity to Nitrosomonas europaea. *Chemosphere, 93*(10), 2493-2498.

Lauchnor, E. G., Radniecki, T. S., & Semprini, L. (2011). Inhibition and gene expression of Nitrosomonas europaea biofilms exposed to phenol and toluene. *Biotechnology and Bioengineering, 108*(4), 750-757.

Lea, M. C. (1889). ART. L.--On Allotropic Forms of Silver: Properties possessed by all the varieties in common and distinguishing them all from normal silver. A. Soluble Allotropic Silver. C. Gold-Yellow and Copper-colored Silver. *American Journal of Science, 37*(222), 476.

Lepe-Zuniga, J., Zigler, J., & Gery, I. (1987). Toxicity of light-exposed Hepes media. *Journal of Immunological Methods, 103*(1), 145.

Lewis, K. (2005). Persister cells and the riddle of biofilm survival. *Biochemistry (Moscow), 70*(2), 267-267.

Lin, J.-J., Lin, W.-C., Dong, R.-X., & Hsu, S.-h. (2012). The cellular responses and antibacterial activities of silver nanoparticles stabilized by different polymers. *Nanotechnology, 23*(6), 065102-065102.

Liu, J., & Hurt, R. H. (2010). Ion release kinetics and particle persistence in aqueous nano-silver colloids. *Environmental science & technology, 44*(6), 2169-2175.

Liu, J., Sonshine, D. A., Shervani, S., & Hurt, R. H. (2010). Controlled release of biologically active silver from nanosilver surfaces. *ACS nano, 4*(11), 6903-6913.

Lok, C.-N., Ho, C.-M., Chen, R., He, Q.-Y., Yu, W.-Y., Sun, H., et al. (2007). Silver nanoparticles: partial oxidation and antibacterial activities. *Journal of Biological Inorganic Chemistry : JBIC : a publication of the Society of Biological Inorganic Chemistry, 12*(4), 527-534.

Lopez, D., Vlamakis, H., & Kolter, R. (2010). Biofilms. *Cold Springs Harbor Perspectives in Biology, 2*(7), 1-11.

Lubick, N. (2008). Nanosilver toxicity: ions, nanoparticlesor both? *Environmental science & technology, 42*(23), 8617-8617.

Luoma, S. (2008). *Silver Nanotechnologies and the Environment: Old Problems or New Challenges?* Washington, D.C.: Woodrow Wilson International Center for Scholars.

MacCuspie, R. I. (2011). Colloidal stability of silver nanoparticles in biologically relevant conditions. *Journal of Nanoparticle Research, 13*(7), 2893-2908.

Manes, M. (1968). USA Patent No.: U. S. P. Office.

McDonnell, G., & Russell, A. D. (1999). Antiseptics and Disinfectants: Activity, Action, and Resistance. *Clinical Microbiology Reviews, 12*(1), 147-179.

McDougald, D., Rice, S. A., Barraud, N., Steinberg, P. D., & Kjelleberg, S. (2011). Should we stay or should we go: mechanisms and ecological consequences for biofilm dispersal. *Nature Reviews Microbiology, 10*, 39-50.

Metcalf & Eddy. (1979). *Wastewater Engineering: Treatment, Disposal, Reuse* (2 ed.). Boston: McGraw-Hill.

Montanaro, L., Poggi, A., Visai, L., Ravaioli, S., Campoccia, D., Speziale, P., et al. (2011). Extracellular DNA in biofilms. *INTERNATIONAL JOURNAL OF ARTIFICIAL ORGANS, 34*(9), 824-831.

Morones, J. R., Elechiguerra, J. L., Camacho, A., Holt, K., Kouri, J. B., Ramírez, J. T., et al. (2005). The bactericidal effect of silver nanoparticles. *Nanotechnology, 16*(10), 2346-2353.

Moudry, Z. V. (1960). USA Patent No.: U. S. P. Office.

nanoComposix. (2014). Silver Nanoparticles: Physical Properties. Retrieved 8/5/2014, 2014

Nowack, B., Krug, H. F., & Height, M. (2011). 120 years of nanosilver history: implications for policy makers. *Environmental science & technology, 45*(4), 1177-1183.

Ostermeyer, A.-K., Kostigen Mumper, C., Semprini, L., & Radniecki, T. S. (2013). Influence of Bovine Serum Albumin and Alginate on Silver Nanoparticle Dissolution and Toxicity to Nitrosomonas europaea. *Environmental Science & Technology*.

Pal, S., Tak, Y. K., & Song, J. M. (2007). Does the Antibacterial Activity of Silver Nanoparticles Depend on the Shape of the Nanoparticle? A Study of the Gram-Negative Bacterium Escherichia coli. *Applied and Environmental Microbiology, 73*(6), 1712-1720.

Project on Emerging Nanotechnologies. (2014). Consumer Products Inventory. Retrieved 19 February, 2014

Purcell, T. W., & Peters, J. J. (1998). Sources of silver in the environment. *ENVIRONMENTAL TOXICOLOGY AND CHEMISTRY, 17*(4), 539-546.

Radniecki, T. S., Dolan, M. E., & Semprini, L. (2008). Physiological and Transcriptional Responses of Nitrosomonas europaea to Toluene and Benzene Inhibition. *Environmental Science & Technology, 42*(11), 4093-4098.

Radniecki, T. S., Semprini, L., & Dolan, M. E. (2009). Expression of merA, trxA, amoA, and hao in continuously cultured Nitrosomonas europaea cells exposed to cadmium sulfate additions. *Biotechnology and bioengineering, 104*(5), 1004-1011.

Radniecki, T. S., Stankus, D. P., Neigh, A., Nason, J. A., & Semprini, L. (2011). Influence of liberated silver from silver nanoparticles on nitrification inhibition of Nitrosomonas europaea. *Chemosphere, 85*(1), 43-49.

Rani, S. A., Pitts, B., Beyenal, H., Veluchamy, R. A., Lewandowski, Z., Davison, W. M., et al. (2007). Spatial patterns of DNA replication, protein synthesis, and oxygen concentration within bacterial biofilms reveal diverse physiological states. [Article]. *Journal of Bacteriology, 189*(11), 4223-4233.

Royal Society and Royal Academy of Engineering (2004). *Nanoscience and nanotechnologies: opportunities and uncertainties*.

Russell, A. D., & Hugo, W. B. (1994). Antimicrobial Activity and Action of Silver. In G. P. Ellis & D. K. Luscombe (Eds.), *Progress in Medicinal Chemistry* (Vol. 31, pp. 351-370): Elsevier Science B.V.

Sheng, Z., & Liu, Y. (2011). Effects of silver nanoparticles on wastewater biofilms. *Water Research, 45*(18), 6039-6050.

Sondi, I., & Salopek-Sondi, B. (2004). Silver nanoparticles as antimicrobial agent: a case study on E. coli as a model for Gram-negative bacteria. *Journal of Colloid and Interface Science, 275*(1), 177 - 182.

Stark, G. (2005). Functional Consequences of Oxidative Membrane Damage. *Journal of Membrane Biology, 205*(1), 1-16.

Clean Water Act of 1977 423 (1977).

U.S.EPA. (1993). *Process Design Manual: Nitrogen Control*.

Watson, S., Valois, F., & Waterbury, J. (1981). The Family Nitrobacteraceae. In M. P. Starr, H. Stolp, H. Truper, A. Balows & H. Schlegel (Eds.), *The prokaryotes: A Handbook on Habitats, Isolation, and Identification of Bacteria* (pp. 1005-1022). New York: Springer-Verlag.

Whitchurch, C. B., Tolker-Nielsen, T., Ragas, P. C., & Mattick, J. S. (2002). Extracellular DNA Required for Bacterial Biofilm Formation. *Science, 295*(5559), 1487.

Wirth, S. M., Lowry, G. V., & Tilton, R. D. (2012). Natural Organic Matter Alters Biofilm Tolerance to Silver Nanoparticles and Dissolved Silver. *Environmental Science & Technology, 46*(22), 12687-12696.

Zook, J. M., Long, S. E., Cleveland, D., Geronimo, C. L. A., & MacCuspie, R. I. (2011). Measuring silver nanoparticle dissolution in complex biological and environmental matrices using UV–visible absorbance. *Analytical and Bioanalytical Chemistry, 401*(6), 1993-2002.